PCT / CA 98 / 00908 09/509462

13 OCTOBER 1998 (13·10·98)

OPIC
OFFICE DE LA PROPRIÉTÉ INTELLECTUELLE DU CANADA

CIPO
CANADIAN INTELLECTUAL PROPERTY OFFICE

Bureau canadien des brevets

Certification

Canadian Patent Office

Certification

REC'D 27 OCT 1998
WIPO PCT

La présente atteste que les documents ci-joints, dont la liste figure ci-dessous, sont des copies authentiques des documents déposés au Bureau des brevets.

This is to certify that the documents attached hereto and identified below are true copies of the documents on file in the Patent Office.

Specification and Drawings, as originally filed, with Application for Patent Serial No: **2,217,088**, on September 30, 1997, by **UNIVERSITE DE SHERBROOKE**, assignee of Ghassan Bkaily, Pedro D'Orléans-Juste, Joao B. Calixto and Rosendo Yunes, for "New Mandevilla Derivatives as Steady-State R-Type CA^{2+} Channel Blockers, Method of Making and Use Thereof".

PRIORITY DOCUMENT
SUBMITTED OR TRANSMITTED IN COMPLIANCE WITH RULE 17.1(a) OR (b)

BEST AVAILABLE COPY

S. Gregoire
Agent certificateur/Certifying Officer

October 13, 1998
Date

Industrie Canada Industry Canada

(CIPO 68)

Canada

TITLE:

New *Mandevilla velutina* and *Mandevilla illustris* derivatives as steady-state R-type Ca^{2-} channel blockers, method of making and use thereof.

FIELD OF THE INVENTION

The present invention relates to the R-type Ca^{2+} channel blockers activity of *Mandevilla velutina* and *Mandevilla illustris* (MV08 and MV12) and their related compounds. The present invention also relates to the treatment of several pathologies that involve the nifedipine-insensitive but isradipine sensitive steady-state R-type Ca^{2+} channel and the use of steady-state R-type Ca^{2+} channel blockers in the treatment of these pathologies.

Background of the invention

Sustained increase of intracellular Ca^{2+} or sustained Ca^{2+} overload (cytosolic, nuclear and mitochondrial) is known to be associated with many abnormal cell function including hypertension, artherosclerosis, hyperinsulinemia, diabetes Melitus type II, abnormal cell proliferation, cell-cell interactions, necrosis, ischemia/reperfusion, arrythmias, platelets activation and aggregation as well as inflammation and Asthma (Bkaily 1994a,b, Sowers et al., 1993, 1994; Hurwitz *et al.*, 1991, Nagano *et al.*, 1992, Anand *et al.*, 1989, Dhalla *et al.*, 1996; Karmazyn, 1996; Curtis, 1993; De Brum *et al.*, 1996; Foreman, 1993; Furberg *et al.*, 1993; Holgate *et al.*, 1993, Jacobs *et al.*, 1993; Johnson *et al.*, 1993; Levy *et al.*, 1994; Ramon *et al.*, 1995; Sperelakis and Caulfield, 1984; Standley *et al.*, 1993; Wray *et al.*, 1989). A wide variety of drugs has been tested against different types of Ca^{2+} channels (P, N, T and L) and the development of Ca^{2+}

blockers was concentrated on the L-type Ca^{2+} channel which was never been shown to undergo any abnormal function in many diseases implicating sustained increase of intracellular Ca^{2+} ($[Ca]_i$) or Ca^{2+} overload. Also, these drugs with the exception of isradipine (PN200-110, Lomir/Dynacirc), failed to block or prevent the sustained increase of $[Ca]_i$, Ca^{2+} overload and necrosis. Recently, the inventors reported the presence of a steady-state nifedipine (L-type blocker)-insensitive but isradipine (dual L and R-type blocker) R-type (resting-type) Ca^{2+} channel that is voltage and Ligand-G protein-dependent (Bkaily *et al.*, 1991, 1992, 1993, 1995, 1996, Bkaily, 1994a). This channel was responsible for maintaining the resting cytosolic and nuclear Ca^{2+} levels and its stimulation levels by sustained depolarization or by permanent presence of some hormones such as insulin, ET-1, PAF, TNFα, PDGF, Bradykinin, or IL-1 induced sustained increase of $[Ca]_c$ and $[Ca]_n$. (Bkaily *et al.*, 1991-1993, 1995-1996-96e, Bkaily G. 1994a, 1994b; Taoudi *et al.*, 1995). The important features that distinguish this channel from other Ca^{2+} channels are the sustained activity(as long as the depolarization or the agonist is present) and the large number of disparate agonists that indirectly (via receptor-G proteins coupling) stimulate the channel. For example, the sustained activation of the R-type channel by insulin may explain in part " syndrome X ", the hypertension, hyperglycemia, dyslipidemia, vascular smooth muscle proliferation and end organ damage associated with non-insulin-dependent diabetes mellitus (NIDDM) and obesity-induced hypertension. Also, the sustained increase in $[Ca]_c$ and mainly $[Ca]_n$ mediated by the stimulation of the R-type Ca^{2+} channel would contribute to the expression

of oncogenes and to the proliferation of malignant cells. The finding that Lomir/Dynacirc (but none of the other L-type Ca^{2+} antagonists) is unique in blocking the R-type Ca^{2+} channel permits the identification and characterization of this type of Ca^{2+} channel. Non published results in two human osteoblast cancer lines (MG63 and FAOS-2) clearly showed that Lomir/Dynacirc (10^{-8}M) reduced spontaneous cell proliferation. In contrast, an L-type Ca^{2+} blocker, nifedipine (10^{-6}M) had no effect. A role for the R-type Ca^{2+} channel and Lomir/Dynacirc in human cancer is suggested by the above findings and supported by the finding of reduced cancer rates in the Lomir/Dynacirc treated group of the MIDAS study. The identification of a potent and specific antagonists may hold the possibility of a new therapeutic target for novel medications. The novel R-type Ca^{2+} channel may prove important in dissecting differential signalling pathways in immune cells. The evaluation of these mechanisms leads to R-type blockade as a therapeutic tool for specific intervention in graft rejection, autoimmune diseases and asthma. Unpublished results from the inventors showed in organ transplant in the rabbit that there are an increase of circulating ET-1 and a decrease of blood flow that were not prevented by cyclosporin-A and by the pure L-type blocker nifedipine. In contrast to dual R- and L-type Ca^{2+} blocker Lomir/Dynacirc restored ET-1 and blood flow levels in cyclosporin-A treated and transplanted animals. A recent report in patients with type I and type II Raynaud's phenomenon (pain and numbness in the fingers, which in some subjects can be complicated by skin ulcers) showed that Lomir/Dynacirc significantly reduced the elevated plasma concentration of ET-1 level, frequency, severity, and disabling nature of

acute attacks of Renaud's phenomenon (La Civita *et al.*, 1996). The decrease of the elevated ET-1 circulating level by Lomir/Dynacirc is due to the blockade of the R-type Ca^{2+} channel which reverses the sustained increase of $[Ca]_c$ and $[Ca]_n$, thus, reducing the autocrine and self perpetuating secretion of mitogenic factors such as ET-1. A blockade of the elevated autocrine and self perpetuating secretion of mitogenic factors by cancer cells may in turn contribute to reduction and even blockade of expression of oncogenes and proliferation of these cells. Work of the inventors is investigating several other types of human cancer cell lines to determine if the proliferative effect of the R-type Ca^{2+} channel is a common mechanism in cancer and tumor cells; preliminary results seem to highly suggest that this hypothesis to be true. Also, a role for the R-type Ca^{2+} channel and its blockade by Lomir/Dynacirc in human cancer is suggested by the reduction of cancer rates in the Lomir/Dynacirc treated group of the MIDAS cohort.

Also, the use of Sandimmune is known to produce potentially serious side of renal impairment and hypertension. These side effects will restrict Sandiummune's use in autoimmune indications such as psoriasis and rheumatoid arthritis and a combination use with R-type Ca^{2+} channel blocker is suggested to block these side effects.

The renal impairment and hypertension are attributable to altered renal hemodynamics induced by Sandimmune. The L-type Ca^{2+}-channel blockers have been used successfully to treat hypertension and renal impairment. The benefits of the Ca^{2+}-channel blockers

have been attributed to their effects on renal hemodynamics specifically dilation of the afferent renal arteriole.

Data exists to indicate that the dual R-and L-type Ca^{2+} channel blocker isradipine (but not a pure L-type blocker) may correct the vasoconstriction at both the afferent and efferent renal arterioles. The advantage of dilation of the afferent and efferent arterioles is a correction of renal blood flow and glomerular filtration without an increase in filtration fraction. Filtration fraction is an indicator of filtration pressure. An increase in filtration pressure could increase the likelihood of developing glomerulonephritis and eventual renal failure.

The potential benefit of blockade of the R-type Ca^{2+} channel by Lomir/Dynacirc on filtration pressure is supported by the existing literature. For example Grossman et al. (1991) in a 3-month study with Lomir/Dynacirc showed that filtration fraction remained constant. The filtration fraction remained constant despite the increase in glomerular filtration rate and renal blood flow. Vascular resistance was also reduced by the 3-month treatment with Lomir/Dynacirc.

A favourable effect on filtration fraction has been corroborated in transplant patients (Berg *et al.*, 1991). These investigators showed that filtration fraction was reduced by Lomir/Dynacirc while renal blood flow increased.

At present, we have unpublished data on the rabbit (see example 9) indicating the presence of the R-type Ca^{2+} channel in both the afferent and efferent renal arterioles. The R-type Ca^{2+} channel has also been identified and characterised in vascular smooth muscle cells isolated from human renal arteries (Bkaily *et al.*, 1991). This work could provide a rational for an advantage of R-type Ca^{2+} blocking agent such as Lomir/Dynacirc over other pure L-type Ca^{2+}-channel blockers in the long-term protection of renal function.

An unpublished work of two of the inventors (Drs Bkaily and D'Orléans-Juste) on the contribution of endothelin to the Sandimmune induced side effects of renal impairment and hypertension, highly suggests that blockade of the R-type Ca^{2+} channel by Lomir/Dynacirc blocks the elevated circulating endothelin level induced with the Sandimmune drugs.

From the wide variety of L-type Ca^{2+} channel blockers such as nifedipine, nicardipine, Diltiazem, Clentiazem, Verapamil, D600 and D888 none were found to block the R-type Ca^{2+} with the exception of isradipine (Lomir/Dynacirc) (unpublished results). This later compound was found to block the R-type Ca^{2+} channel with an ED_{50} near (10^{-8}M), the T-type Ca^{2+} channel with an ED_{50} near (10^{-7}M), the L-type Ca^{2+} channel with an ED_{50} near (10^{-6}M) and the fast Na^{+} channel with an ED_{50} near (10^{-5}M) (Bkaily G., unpublished results). Thus, the R-type Ca^{2+} channel blocker isradipine seems to be a potent R-type

Ca^{2+} blocker but not highly specific. This drug on a clinical point of view seems to be more potent and possesses less side effects than other dihydropyridines (DHP) derivitive L-type Ca^{2+} channel blockers. Such a difference between isradipine and other DHPs compounds could be due to the potential of the former, as R-type Ca^{2+} blocker. Recently, we demonstrated that as PAF, insulin and ET-1, bradykinin (BK) also induced sustained increase of $[Ca]_i$ that was mainly nuclear and was due to the stimulation of the R-type Ca^{2+} channel in human aortic endothelial and vascular smooth muscle as well as chick and heart ventricular cells. The stimulation of R-type Ca^{2+} channel by BK was due to the kinin activation of the B_1-receptor. Since 1985, Calixto's group (two of the inventors) has worked on extracts of *Mandevilla velutina* (MV) and claimed that some of the extracts (such as MV8608 and MV8612) had antagonistic properties against the effect of bradykinin (BK). The compound MV8608 has been characterized in 1987 (Calixto et al.,). It has been found to be selective in its ability to inhibit the contraction of rat uterus induced by BK. The previous work made by Calixto's group as well as others on extracts of Mandevilla species have always focused on compounds which have a presumed action at the BK receptor site.

In a review article published after 1990, Calixto's group mentioned that the compounds MV8608 and MV8612 had a pregnane structure. It is further mentioned that MV8608 is an aglycone compound (without any sugar) and that MV8612 is a steroid glycoside. **No specific structure is shown in this review article.** This review is a compendium of

data, characteristics, and properties of MV8608 and MV8612 in numerous systems responding to BK (therefore not limited to the effect of BK on rat uterus). Again, it may be deducted from this publication that this group of researchers have focused their study on the search of a ligand which is a BK receptor antagonist. MV8612 has been retained as a good candidate because this compound best corresponds to established receptor classification criteria (pA2 fairly good, competition curve whose slope does not differ from one and selectivity). At the time of this publication, the Calixto group did not consider that MV8612 may have an action which is not aimed at the receptor directly. Even though on certain systems the effect of MV8612 has been shown to be non-selective, no explanation on this lack of selectivity toward BK has been provided. Therefore, this publication does not teach any role of MV8608 and MV8612 as a calcium channel blockers.

Other compounds isolated from *Mandevilla Pentlandia* which also have been claimed an anti-BK activity have been the object of a patent application filled by Proctor and Gamble Co. (EP no=0.359310). Furthermore, other Mandevilla extracts, particularly from Mandevilla Illustris also have antagonist activity against BK. All the compounds obtained from Mandevilla species are also described as compounds having anti-BK activity without mentioning the specific site of action of these compounds. All these compounds are deemed to be useful for treating pathologies and conditions involving bradykinin (inflammation, smooth muscle contraction, pain, hypotension, etc.), although they lack

selectivity.

The lack of selectivity may suggest that Mandevilla extracts bind to a non-specific feature of " related " receptors or that these extracts bind to entity which is not a receptor site and that the apparent BK-antagonist action reported for MV8608 and MV8612 is due to the blockade of the R-type Ca^{2+} channel that is indirectly stimulated by the kinin activation of B_1 and/or B_2-receptors. The properties of the MV compounds towards the calcium channel type R (which has been discovered by the present inventors) are not presented in earlier publication and should be novel and non-obvious.

The publications from the inventors show that an inhibitor of a calcium channel such as isradipine, which has an effect on calcium channel types L and R, reduces or abolishes the effect of hormones like insulin and PAF (platelet-activating factor), ET-1 and BK which effect is absent when using nifedipine (a L-channel blocker). These publications are indicative of the contribution of the R-type calcium channel in the effect of insulin, PAF, ET-1 and BK. The results obtained with isradipine, when compared to the reported effects of MV8608 and MV8612 may have led the inventors to verify the activity of these compounds on the calcium R-type Ca^{2+} channel, as well as T, L Ca^{2+} channels and the fast Na^+ and delayed outward K^+ channels.

In spite of the recent discovery of the R-type Ca^{2+} channel, there is a definite need of a

new generation of class of drugs to treat R-type Ca^{2+} channel-associated diseases for the following reasons :

1. There is no drug approved for the treatment related to sustained elevation of $[Ca]_c$, $[Ca]_n$ or R-type Ca^{2+} blocking.

2. There is a definite need for better drugs for the treatment of hypertension, artherosclerosis, inflammation, arthritis, asthma, cancer, pain, diabetes type II and ischemia-reperfusion, hyperventilation and high circulating ET-1 level.

Summary of the invention

Invention concerning the new saponin-like isolated from *Mandevilla velutina* with R-type calcium channel blocking properties.

Mandevilla velutina is a native Brazilian plant used in folk medicine to treat snake bites and as an anti-inflammatory agent. Some non-peptidic compounds extracted from this plant blocks bradykinin and related kinins action. It shows potent analgesic and anti-inflammatory activities (Calixto *et al.*, 1987). The freshly collected rhizomes of *Mandevilla velutina* were extracted with ethyl acetate and then fractionated by column

chromatrography on silica gel with methylene chloride and ethyl acetate as solvents giving 20 components. Two of these fractions showed indirect bradykinin blocking action. One of them named Velutinol (MV8608) shows that the structure comprises a pregnane skeleton. Structure of Velutinol A was determined (Yunes *et al.,1993*) as : 3-ß-hydroxipregna-5-one derivatives see Figure 1.

For comparison structure of 5-pregnane-3ß-ol-20 one is shown in Figure 2.

We discovered that compound MV8608 has an inhibitory activity on the R-type calcium channel.

Isolated from the same *Mandevilla velutina* rhizomes an other compound MV8612 has very specific inhibitory activity on calcium channel type R. The invention relates to structure of MV8612 compound and its saponin-like derivatives with the inhibitory activity of the R-type calcium channel. Primary structure of mentioned saponin is shown in Figure 3,

It is important that the invented molecule consists of a classical saponin oligosugar (ET) part and steroid (S) one. Structure of steroid (S) component of the molecule is based on 5 pregnane-3ß-ol derivative with tricyclic oxygenated ring system as shown in Figure 3,

however similar compounds can possess inhibitory activity on the Ca^{2+} influx into the cytosol, the nucleus, the mitochondria as well as the SR and ER, in the combination ETS as in Fig. 3. Structure of S part of the molecule is preferably 5-pregnane-3ß-ol oxytricyclo 15-ol as shown in Fig. 3, but also 5-pregnane-3ß-ol-20-one, cholesterol, cholic acid, ergosterol, stigmasterol, androstenon, digitoxygenin, ß-sitostenol, uvaol, ursolic acid, sarsasapogenin, 18, ß-glycyrrhetinic acid, betulin, betulinic acid, oleanoic acid, podocarpic acid.

In the above formula ETS, T is preferably α(1-4) (2-deoxy, 3-methoxy) -L-lyxotetrose, α(1-4) (2-deoxy, 3-methoxy) L-xylotetrose, α(1-4) (2-deoxy, 3-methoxy)-L-arabinotetrose, α(1-4) (2-deoxy, 3-methoxy)-L-xylotetrose, α(1-4) (2-deoxy, 3-methoxy-L-ribopyranotetrose, α(1-4) (2-deoxy, 3 methoxy-L-sorbotetrose, α(1-4)-L-lyxotetrose, α(1-4)-L-xylotetrose, α(1-4)-L-arabinotetrose, α(1-4)-L-xylotetrose, α(1-4)-3,4 methoxy-L-lyxotetrose, α(1-4)-3, 4 methoxy-L-xylotetrose, α(1-4)-3,4 methoxy-L-arabinotetrose, α(1-4)-3,4 methoxy-L-xylotetrose, α(1-4)-3,4 methoxy-L-ribopyranotetrose, α(1-4)-3,4 methoxy-L-sorbopyranotetrose, α(1-4)-L-lyxotetrose, α(1-4)-L-xylotetrose,α(1-4)-L-arabinotetrose,α(1-4)-L-ribopyranotetrose,α(1-4)-L-sorbotetrose.

T has preferably tetra sugar derivative but also monomeric to aligomeric of mentioned sugar derivatives. The terminal E part is preferably 4-acetoxy-3 methoxy-L-α-lyxose, 4-acetoxy-3-methoxy-L-α-xylose, 4-acetoxy-3-methoxy-L-α-arabinose, 4-acetoxy-3-

methoxy-L-α-xylose,4-acetoxy-3-methoxy-L-α-ribopyranose,4-acetoxy-3-methoxy-L-α-sorbose-acetoxy.

The compound of formula (I) and (III) could be if wanted submitted to a deprotection reaction of amines functions in peptidic syntheses (acid treatment or catalytic hydrogenation depending of the T nature) in order to obtain compounds of formula I or vice versa compounds of formula (III). The compounds of formula (I) and (II) could be, if necessary purified using classical technique such as crystallisation and/or silice column chromatography.

They can be also ionized with an acceptable pharmaceutical acid, or if it is possible and if we desire with an acceptable pharmaceutical base.

The necessary crude materials used in the processes described are :

- or commercials
- or easy accessible to a knowledgeable person in accordance to procedures available in the literature.

In comparison with the dual L and R-type Ca^{2+} channel blocker, israpidine (PN200-110), the compounds of the present invention, presents a highly superior *in vivo* as well as *in vitro* specificity and potency as well as protective and therapeutics cellular activities

against Ca^{2+} overload in all cell types including heart, vascular smooth muscle, vascular and non vascular endothelial cells, bone cells, T lymphocytes, monocytes, smooth muscle cells, nerve cells, cerebral cells, and non-differentiated cell of anaplasic or neoplasic origins.

The tests realized *in vitro* on VSMC, VEC, bone cells, blood immune cells and heart cells in culture, placed in several pathological, electrical and hormonal conditions showed that the compounds of the present invention protected and blocked in a remarkable way and more potently than isradipine, cell integrity and Ca^{2+} overload as well as Ca^{2+}-dependent over stimulation of hormone secretion and abnormal excitation-contraction coupling and conduction. Other tests were done *in vitro* using abnormal proliferation of T-lymphocytes as well as VSM, VEC and osteoblast cells demonstrated that the compounds under invention significantly and remarkably protected the cell from proliferation as well as largely decreased their undergoing spontaneous proliferative process and retained their normal integrity and function. These effects of the compounds of the present invention were largely superior to that of isradipine.

The tests *in vivo*, using rats and rabbits as well as guinea pigs demonstrated that the compounds of invention prevented and blocked in a significant way and largely superior to that of isradipine, vasoconstriction, hypotension and airways hypereactivity induced by PAF, ET-1 and organ transplantation without any side effect which was not the case of

the dual L-and R-type channels blocker isradipine.

The remarkable properties of the compounds of the present invention make them valuable in treatment of diseases of cerebral, cardiac and vascular systems as well as at the level of the immune system for the treatment and prevention of cerebral and cardiac ischemia, vascular contraction, oedema, post-surgery and post-transplantation hyper-immune activities and related pathologies.

In general, the protective effects of the compounds under the present invention and mainly MV8612 give them a sure interest in the treatment of cardiac, vascular and cerebrovascular accidents of different origin, post-surgical traumas, encephalopathy, neuro-degenerative pathology, hypertrophy, cancer, diabetes type II, hyperthyroidism, osteoporosis, arrythmia, fibrillation as well as osteoporosis.

The capacity of the compounds of the invention to protect the cells during hypoxia and ischemia as well as remodelling permits also their use in the treatment and prevention of ischemia of peripheral tissues, mainly in cardiology for myocardial ischemia and coronary ischemia and their different clinical expressions : angina, myocardial infarct, arrhythmias, vasopasms, heart failure, fibrillation, as well as in ophthalmology and in oto-rhino-laryngology during chorio-retinial vascular damage, vertigo of vascular origin, vertigo de Meuniere or d'acouphenes as well as digitalis intoxication.

The invention concerns also the addition of salts to the compounds of formula (I) and (III) obtained with a mineral or organic salts pharmaceutically acceptable.

Among the pharmaceutically acceptable acids that we can use to obtain a salt by addition to the compounds of inventions, we could cite, as an example, chlorhydric acid, phosphoric acid, tartaric acid, malic acid, fumaric acid, oxalic acid, methanesulfonic acid, ethanesulfonic acid, camphoric acid, citric acid, etc.

As acceptable pharmaceutical bases that can saltify the compounds of formula (I) and (III), we can use sodium, potassium, calcium, aluminium hydroxyl, the carbonates of acaly metals or alkalinoterrus or organic bases such as triethylamine, benzylamine, diethanolamin, tertbutylamin, dicyclohexylamin, arginine, etc.

The invention covers also the pharmaceutical compositions including as an active principle, a compound of formula (I) and (III) or their salt by addition with a mineral or organic base or acid with association with one or several inert excipients, non toxic covenants for pharmaceutical use and/or an agent attaching an aromatic agent, a delitement agent, edulcorant agent, lubrificant agent as well as a liquid and semi-liquid vehicle adapted for intravenous administration such as sterile epirogenic water.

Among the pharmaceutical compositions according to the invention, we could cite, in

particular, those that fit well for the oral, parental, ocular, per or transcutan, nasal, rectal, perlingual administrations as well as ocular or nasal drops, pills, sublingus pills, capsules, tablets, suppositories, cremes, pomades, gels, etc.

The compositions obtained were generally presented in a dose form and can contain dependent on the patient treated, age and sex of the patient, from 0.1 to 500 mg of the active principle.

It can, depending on the route of administration (orally, rectally or parenterally) be delivered at a dose of 0.1 to 500 mg of one or several times a day.

The invention is further illustrated with reference to the following examples and accompanying figures of the figures :

Figure 1 shows the structure of compound of Ia and Ib of MV8608.

Figure 2 shows the structure of 5-pregnane-3ß-ol-20 (compound II).

Figure 3 shows the structure of MV8612 (compound III).

Figure 4 shows the absence of the effect of (10^{-7}M) of MV8608 on the TTX-sensitive fast

Na^+ current in single heart cell.

Figure 5 shows the relative weak depressing effect of (10^{-9}M) and (10^{-7}M) of MV8608 on the T-type Ca^{2+} current in heart cells.

Figure 6 shows the relative weak depressing effect of (10^{-9}M) and 5 x (10^{-7}M) of MV8608 on the L-type Ca^{2+} current in heart cells.

Figure 7A shows that intra patch pipette application of (10^{-7}M) of MV8608 decreased the R-type Ca^{2+} channel amplitude and probability of opening and Fig. 7B shows that extra patch pipette application of MV8608 (10^{-7}M) increased the time of opening duration followed by transient decrease of the amplitude of the R-type Ca^{2+} channel.

Figure 8 shows the blockade by MV8608 (10^{-9}M) of the sustained depolarization induced sustained increase of total $[Ca]_i$ via activation of the R-type Ca^{2+} channels in chick and human heart cells.

Figure 9 shows the absence of the effect of nifedipine (10^{-6}M) on ET-1 (10^{-9}M), sustained depolarization (KCl, 30 mM) and PAF (10^{-9}M) induced sustained increase of $[Ca]_i$ via the activation of the R-type Ca^{2+} channel and the blockade of this sustained increase by MV8608 (10^{-9}M) in heart cells.

Figure 10 shows the blockade by MV8608 (10^{-9}M) and the absence of the effect of nifedipine (10^{-6}M) on the sustained depolarization (30 mM), and PAF (10^{-9}M) induced sustained increase of $[Ca]_i$ via activation of the R-type Ca^{2+} channel in human heart cells.

Figure 11 represents histograms showing MV8608 (10^{-9}M) blockade of sustained increase of $[Ca]_i$ (in presence of nifedipine (C+N) induced by sustained depolarization (KCl, 30 mM) and PAF (10^{-9}M) stimulation of the R-type Ca^{2+} channel in human heart cells.

Figure 12 represents histograms illustrating MV8608 (10^{-9}M) blockade of the sustained increase of $[Ca]_i$ induced by sustained depolarization (in presence or absence of nifedipine), PAF and ET-1 stimulation of R-type Ca^{2+} channel in chick heart cells.

Figure 13 shows the blockade by MV8608 (10^{-9}M) of bradykinin (10^{-6}M) induced sustained increase of $[Ca]_i$ (in presence of (10^{-6}M) nifedipine) via activation of the R-type Ca^{2+} channels in chick heart cells, human heart cells and rabbit aortic vascular smooth muscle cells.

Figure 14 represents histograms showing the MV8608 (10^{-9}M) blockade of bradykinin (BK, 10^{-6}M) and PAF (10^{-9}M) induced sustained increase of $[Ca]_i$ via activation of the R-type Ca^{2+} channels in rabbit aortic vascular smooth muscle cells.

Figure 15 shows a typical example of the decrease of basal sustained increase of $[Ca]_i$ by MV8608 (10^{-9}M) in freshly isolated human aortic endothelial cells and the blockade by MV8608 (10^{-9}M) of PAF (10^{-9}M) induced sustained increase of $[Ca]_i$ via activation of the R-type Ca^{2+} channels in freshly isolated human aortic vascular smooth muscle cells.

Figure 16 represents histograms showing that increasing the concentration of PAF (10^{-7}M) required high concentration of MV8608 (10^{-6}M) for blockade of PAF induced sustained increase of $[Ca]_i$ via activation of the R-type Ca^{2+} channels in human aortic vascular smooth muscle cell lines.

Figure 17 represents histograms showing that in double-perfused mesenteric bed of the rat, MV8608 (1 μM) but not Illusteol (1 μM) blocked PAF but not ACh and AngII induced arterial vasodilatation and venconstriction.

Figure 18 shows the time course decreases of the TTX-sensitive fast Na^+ current in chick heart cells by (10^{-8}M) of MV8612.

Figure 19 shows the time course blockade of the L-type Ca^{2+} current by high concentration (10^{-7}M) of MV8612 in human heart cells.

Figure 20 shows graphs and cell attached single R-type Ca^{2+} channel recording (in

presence of (10^{-6}M) nifedipine) showing the decrease of the single channel current amplitude (panel A, current voltage relationship, n=3), probability of opening (panel B, open probability-voltage relationship, n=3) by 10^{-7}M MV8612 application in the patch pipette and panel C, example of single channel current traces. Panels D-E show that application of MV8612 (10^{-9}M) to extrapipette solution only induced a slight decrease of the R-type Ca^{2+} channel amplitude and largely increased the probability of opening of the channel. This demonstrates that MV8612 does penetrate to the cytosol and its effect at the cytosolic side of the channel is different from that at the outer side.

Figure 21 represents graphs showing that both MV8608 (10^{-8}M) and MV8612 (10^{-8}M) but not nifedipine (10^{-7}M) significantly decreased the spontaneous proliferation of human aortic vascular smooth muscle cell line.

Figure 22 represents histograms showing that the L-type Ca^{2+} blocker, nifedipine did not affect basal cytosolic ($[\ ]_c$) and nuclear ($[\ ]_n$) free Ca^{2+} as well as the sustained depolarization and high PAF induced sustained increase of $[Ca]_c$ and $[Ca]_n$. However, MV8608 and MV8612 blocked completely the sustained depolarization induced sustained increase of $[Ca]_c$ and $[Ca]_n$ (panel A) in heart cells. Panel B shows that high concentration of PAF (10^{-7}M) induced sustained increase of $[Ca]_c$ and $[Ca]_n$ is blocked by high concentration of MV8608 (10^{-6}M) but normal concentration of MV8612 (10^{-8}M).

Figure 23 is a 3-dimensional reconstitution showing the absence of effect of nifedipine and the blockade of the sustained increase of $[Ca]_c$ and $[Ca]_n$ induced by sustained depolarization and high PAF (10^{-7}M) in chick heart (A) and human aortic vascular smooth muscle cell line (B).

Figure 24 represents histograms showing the preventive effect by MV8608 and MV8612 of sustained depolarization and high PAF (10^{-7}M) induced sustained increase of $[Ca]_c$ and $[Ca]_n$ via stimulation of the R-type Ca^{2+} channel in chick heart cells and human aortic vascular smooth muscle cell line.

Figure 25 represents histograms showing the preventive effect by MV8612 (10^{-8}M) of sustained depolarization (KCl 30 mM) and high PAF (10^{-7}M) induced a sustained increase of $[Ca]_i$ via activation of the R-type Ca^{2+} channel in human aortic vascular smooth muscle cell line.

Figure 26 represents histograms showing the blockade by MV8612 (10^{-9}M) of sustained depolarization and ET-1 (10^{-9}M) induced sustained increase of $[Ca]_i$ via activation of the R-type Ca^{2+} channels in rabbit aortic vascular smooth muscle.

Figure 27 represents histograms showing the blockade by 10^{-9}M MV8612 of the sustained depolarization, low PAF (10^{-9}M) and ET-1 (10^{-9}M) induced sustained increase of $[Ca]_i$

via the activation of the R-type Ca^{2+} channels in chick heart cells.

Figure 28 shows the marked intrinsic hypotensive properties of the dual L- and R-type Ca^{2+} channel blocker isradipine (panel B) when compared to the pure L-type Ca^{2+} channel blocker, nifedipine (Panel A).

Figure 29 shows that pretreatment with MV8612 (10^{-4}M) abolishes the bronchoconstrictive responses and the hypotensive effect of PAF in the anaesthetized guinea pig model.

The following example illustrate the invention and is not limited by any mean.

Pharmacological study of the compounds of the present invention :

Principle of *in vitro* studies

Single cells from heart, VSM and VEC of human and animals in culture constitute a model of choice for looking at the effect of drugs on different types of ionic channels using whole-cell and single channel patch clamp techniques in normal and stimulated conditions (Bkaily et al., 1988, 1991, 1992, 1992a, 1993a, 1996a-e; Bkaily G. 1994a,b).

Heart cells as well as VSMC possess fast Na^+ current, T, L and R-type Ca^{2+} channels

as well as different types of K^+ channels (Bkaily G., 1991, 1995). However, vascular endothelial cells (VECs) do possess only R-type Ca^{2+} channels and different types of K^+ channels. Thus, the later type of cells constitute a model of choice for studying the effect of drugs on Ca^{2+} influx due to opening of the R-type Ca^{2+} channels (Bkaily G., 1994a; Bkaily *et al.*, 1996a-e). The R-type Ca^{2+} channel was reported by one of the inventors (Bkaily G.) to be responsible for the sustained increase of intracellular calcium and nuclear and cytosolic Ca^{2+} overload that are a result of sustained depolarization of the cell membrane or continual presence of several cardioactive and vasoactive hormones such as ET-1, PAF, bradykinin and insulin (Bkaily G., 1994a, Bkaily *et al.*, 1992, 1993, 1995, 1996a, b, c, d).

A sustained increase of cytosolic, nuclear and mitochondrial Ca^{2+} is pathologicaly visible and measurable aggression in all types of excitable and non excitable cells such as heart cells, VSMC, VEC, osteoblast cells and immune cells (Bkaily *et al.*, 1996a).

The inventors tested the effect of the compounds of invention on the different type of mentioned cells at whole-cell and cell attached patch clamp configurations as well as at $[Ca]_i$, $[Ca]_c$ and $[Ca]_n$ levels using a standard techniques used by the inventors (Bkaily G., 1994a,b, Bkaily *et al.*, 1992, 1993, 1995, 1996a, b, c, d, e).

Methodology

Single cells of different types in culture are prepared from human biopsy, chick and rabbit. Known and accepted methods published by one of the inventors for isolation of fast Na^+ current, T, L and R-type Ca^{2+} channels as well as delayed outward K^+ current are used.

The compounds to be tested are added to the appropriate extracellular solution after recording a stable ionic current or normal steady-state level of $[Ca]_n$ and $[Ca]_n$. The effect of different concentrations compounds are tested on the different type of current and $[Ca]_i$ of the different cell types. The effect of each concentration of the compounds in function of the time of exposure are determined. Once the steady-state effect is reached, the second concentration is added, etc.

Also, in case of the R-type Ca^{2+} channel current, the effect of the compound are tested on the R-type Ca^{2+} channel amplitude, voltage dependency and probability of opening by using the cell-attached patch clamp technique (Bkaily 1994a, 1996a) and intra and extra patch pipette application of the drug. In all experiment using single channel recording, nifedipine (10^{-6}M) was present in the control and experimental solutions.

Recent results from the inventors laboratories demonstrate that some cardiogenic and

vasoconstrictor hormones such as PAF, ET-1 and bradykinin induced a sustain increase of cytosolic as well as nuclear calcium. This sustained increase of Ca^{2+} induced by depolarization of the cell membrane or some hormones such as PAF, ET-1 and bradykinin is due to the increase of Ca^{2+} influx through the R-type Ca^{2+} channels at the sarcolemmal membrane and/or the nuclear membrane (Bkaily G., 1994a; Bkaily *et al.*, 1996a-e). Using Ca^{2+} fluorescence probes Fura-2 or Fluo-3 and 2 dimension and three-dimension Ca^{2+} imaging technique (Bkaily G., 1994a; Bkaily *et al.*, 1996a-e), the effect of hormones and drugs could be easily tested. These two methods are used with single cells of different types as described earlier.

The inventors tested the effect of the compounds of invention on cytosolic and nuclear Ca^{2+} in different conditions (K^+ depolarization, PAF, ET-1, etc.) that increased the probability of opening of the R-type Ca^{2+} channels and induced cytosolic and/or nuclear Ca^{2+} overload (in presence of L-type Ca^{2+} blocker, nifedipine).

Using Fura-2 or Fluo-3 cytosolic and nuclear Ca^{2+} measurement techniques, the inventors also tested the effect of the compounds of invention on the spontaneous increase of cytosolic and nuclear Ca^{2+} during spontaneous contraction of ventricular single cells. Single cells from human fetal ventricular cells and chick embryonic cells are bathed in normal Tyrode's solution and spontaneous intracellular Ca^{2+} transient are recorded in absence and presence of the compounds of invention.

Title: ***Mandevilla velutina*** and ***Mandevilla illustris*** compounds, derivatives and analogues as blocker of calcium and sodium channels; their chemistry, pharmacological and therapeutical properties.

1. Compounds from *Mandevilla velutina*

The compounds isolated from ***Mandevilla velutina*** that exhibit bradykinin blocking action are:

a) **MV8608** - The structure of this compound denominated velutinol was studied (Yunes et al., 1993 and Bento,Yunes et al. 1996) and it was suggested to be a (15R, 16R, 20S)-14,16:15,20:16,21- triepoxi-15,16-seco 14β, 17α-pregn-5-ene-3β,15-diol. (I)

Pregnanes derivatives have been reported to be present in several species (Abe et al. 1976, 1978, 1979, 1981, 1988). However others isomers could also exist as are shown by structures II, III and IV (Fig. 1). This isomers show also activity (Yunes, Calixto et al. nonpublished results).

b) **MV8612** - The structure os this compound is indicated in Fig 2.

Procedure for isolation and purification of this compound.

The rhizomes of ***Mandevilla velutina*** were ground into small pieces and extracted repeteadly with ethyl acetate. The extract was filtered and evaporated to yield a brown powder that accounts for 9% of the rhizomes. The extract was fractioned by silica gel column chromatography with methylene chloride system containing increasing amounts of ethyl acetate.

Fractions were collected and monitored by thin layer chromatography (Silica Gel G) and eluted with toluene-EtoAc-MeOH (55:45:5) and visualized with short and long wavelength u.v. light or with arylaldehyde-AcOH-MeOH-H_2SO_4 (0:5:10:85:5) spray.

Fractions rich in velutinol glycoside MV8612 were rechromatographed in the same manner several times, further purified by TLC give the pure compound VI (Fig. 2) crystallized in ethanol.

Compound VI (0.0001% of dry weight) mp 148-150° C, white needles from ethanol responded positively to the Lieberman Burchard (Abisch et al., 1960), Xanthydrol (Barton et al., 1952) and Keller-Kiliane (Nagata et al., 1957) indicating to be a stereoidal glycoside of a 2-deoxysugar.

The molecular formula was obtained through elementar analysis [(ρ (60.26%), H (7.94%), 0 (31.10%)] [Cale:((60.80%) H(8.01%), O(31.10%) and fast atom bombardment (FAB) mass spectrum (MS) that afforded a molecular peak at m/z 1205 ($M + Na^+$); 1221 ($M + K^+$) and 1200 ($M + NH_4^+$ suggesting to be $C_{60}H_{94}O_{23}$. The IR spectrum showed peaks (KBr) at cm^{-1}: 3450 (-OH), 1745 ($-COCH_3$), 2920, 1440 (OCH_3), 1230, 1160, 1100, 1080, 1050 (O-C-O). Its methanolic solution is transparent in the UV visible region. In the mass spectrum the loss of fragment 45 from the aglicone following by the loss of a fragment of 244 were indicative of one terminal sugar with two acetyl and one methoxyl groups suggesting one straight chain of sugars. The positive ionization fast atom bombardment mass spectra (FAB-MS) confirmed the result with peaks at m/z (%) 1137 [M-Co-OH]$^+$ (66) 893 [1137-$C_{11}H_{17}0_6$]$^+$(10) 749[893-$C_7H_{12}O_3$)]$^+$ (21), 605 [749-

$C_7H_{12}O_3]^+$ (25); 462 [605-$(_7H_{11}O_3]^+$ (10), 318[462-$C_7H_{12}O_3$]+ (15) and suggesting that are four dideoxy sugars in the molecule.

2. NMR Experiments (Fig. 3, 4, 5, 6)

a) 1D ^{1}HNMR Spectrum

The analysis of the 600 Mhz ^{1}H NMR spectrum can be divided into three distinct regions. The first region [5.78 ppm-4.28 ppm] with the best resolved signals, correspond to the five anomeric protons and protons at C2 and C4 of the sugar ring 5, besides protons 16, 6, 15 (H), 15(OH), 10 and 21b of the genin part (velutinol).

For the second region [3.93 ppm - 3.15 ppm], a very crowded region, the integration is proportional to 31 protons and were assigned as protons 3 and 21a of the genin part, five methoxy and fourteen methine protons of the sugar rings.

The integration of the last region [2.53 - 1.08 ppm] showed the presence of fifty protons; five secondary methyl, eight methylenic, two methyl from acetyl groups and twenty-one protons from the genin part.

b) 1D selective TOCSY

The 1D selective TOCSY was used to define each one of the five spin systems for the sugar rings attached to the genin part. Selective irradiation of an isolated spin multiplet yields a subspectrum of all hydrogens directly or indirectly scalar coupled to the irradiated resonance, if the mixing time is long enough to allow complet transfer of magnetization. A description of the results is given in table 1.

The four anomeric protons of 2,6-dideoxyhexopyranose appeared as a doublet of doublets at δ 4.96; 4.85; 4.76 and 4.45, with J = 10 and 2 Hz. A fifth anomeric proton appeared as a doublet (J = 10 Hz), δ 4.43 and was assigned to the normal hexapyranose unit. The large value of the coupling constant of these anomeric protons were typical of the axial configuration of the hexopyranoses in the C-1 (D) conformation indicating that these sugars were joined through (1 → 4) β-glycosidic linkages.

The spectrum also contained five methoxy groups which appear as singlets and were observed at δ 3.37(3H), 3.44(3H), 3.39(3H), and 3.34(6H); five secondary methyl groups appear as doublets and were observed at δ 1.21(9H), 1.22(3H) and 1.29(3H), (J = 6.0 Hz); two tertiary methyl groups singlets were observed at δ 1.08 and 1.11 and two methyl from acetyl groups were observed at δ 2.07 and 2.18.

The eight C-2 methylene protons of four 2-deoxy sugar units appeared as two sets of four protons multiplets in the regions δ 2.29-2.08 and 1.64-1.55 for the equatorial and axial protons respectively (Abe et al., 1988). There is also a doublet of doublets at δ 5.12 (J = 10 and 8 Hz) attributed to the C-2 proton of the acetylated sugar, it couples with both the signals at δ 4.43 (anomeric proton) and δ 3.33 credited to a C-3 proton. The C-3 signal, part of a multiplet, is coupled with a doublet of doublets at 5.33 (J=3.0 and 2.0 Hz) attributed to the C-4 proton of a diacetyl sugar, which in turn is coupled with a doublet of doublets at δ 3.70 (J=6.0 and 2.0 Hz) attributed to the C-5 proton. This is in turn coupled to a doublet (J=6.0 Hz) at δ 1.21, attributed to the secondary methyl. The chemical shift for C-2 and C-4 is in accordance for acetyl sugar derivatives.

c) **COSY spectrum**

The J coupling relationship described above was also determined from the COSY spectrum. The complete ^{1}H NMR assignment of all the protons in the five sugar rings is given bellow:

a) H1, δ 4.43 ↔ H2, δ 5.12 ↔ H3, δ 3.33 ↔ H4, δ 5.33 ↔ H5, δ 3.70 ↔ CH3, δ 1.21.

b) H1, δ 4.96 ↔ H2, δ 1.55 and 2.16 ↔ H3, δ 3.77 ↔ H4, δ 3.19, ↔ H5, 3.92 CH3, 1.21.

c) H1, 4.45 H2, 1.57 and 2.29 H3, 3.40 H4, 3.15 H5, 3.28 CH3, δ 1.29

d) H1, δ 4.76 ↔ H2, δ 1.64 and 2.11 ↔ H3, δ 3.78 ↔ H4, δ 3.19 ↔ H5, δ 3.34 ↔ CH3, δ 1.21.

e) H1, δ 4.85 ↔ H2, δ 1.58 and 2.08 ↔ H3, δ 3.81 ↔ H4, δ 3.22 ↔ H5, δ 3.85 ↔ CH3, δ 1.22.

d) **C13 spectrum, DEPTs and CH correlations**

The carbon 13 nuclear magnetic resonance spectra (^{13}C NMR) indicated the presence of six quaternary carbons, fourteen methyl, eleven methylene, twenty nine methine and two carbonyl groups (Breitmaier et al.,

1987). The carbon signal were assigned on the ^{1}H-^{13}C COSY one-bond spectrum except for the quaternaries one. The long-range correlations data was used to assign these and the multiplicity of the protonated one was determined from the DEPT spectral data. The ^{13}C assignments of the sugars are indicated in Table 2.

As agreement with the previous determination (ref. of velutinol) of the genin part (Velutinol A), the proton nuclear magnetic resonance spectra (^{1}H NMR) showed a characteristic signal due to the C-6 olefinic proton (δ 5.38, m), as well as those due to C-19 and C-18 (δ 1.08 and 1.11, s) methyl protons, C-3 methine proton δ 3.53, t,t), C-9, C-8, C-17, C-20, C-15 and C-16 methine protons (δ 1.36, m; 2.01, td; 2.53, d,d; 4.44, d; 5.01, d; and 5.78,d, respectively) and C-21 methylene protons (δ, 3.81 and 4.28, d) (Abe et al., 1987, Chen et al., 1987) (Table 3 and 4).

e) <u>CH long range correlations</u>

The analysis of the ^{1}H - ^{13}C long-range data gave the following correlations which are evidence for the fact that the genin and the sugar residue are attached, as well as for the following sequence of the sugar rings: (Table 5)

a) H3α(δ 3.35, V) ↔ C1 (96.11, R1) and H1 (δ 4.85, R1) ↔ C3(δ 77.64, V) define the linkage point between the genin and the sugar residue;

b) H4(δ 3.22, R1) ↔ C1(δ 99.73, R2) and H1 (δ 4.76, R2) ↔ C4(δ 82.59, R1) define the connection between the first and second sugar rings;

c) H4(δ 3.19, R2) ↔ C1(δ 101.45, R3) and H1 (δ 4.45, R3) ↔ C4(δ 83.91, R2) define the connection between sugar rings 2 and 3;

d) H4(δ 3.15, R3) ↔ C1(δ 98.47, R4) and H1(δ 4.96, R4) ↔ C4(δ 82.15, R3) define the attachment of sugar ring 3 to sugar ring 4;

e) H4(δ 3.19, R4) ↔ C1(δ 102.55, R5) and H1(δ 4.43, R5) ↔ C4(δ 83.81, R4) define the linkage point between the last two sugar rings 4 and 5.

f) NOESY spectra

The analysis of the cross peaks in the NOESY (2D n.O.e) spectra also provides evidence for the above connections between the sugar rings and the genin. The most important interactions are the following: H1(δ 4.43, R5) ↔ H4(δ 3.19, R4); H1(δ 4.96, R4) ↔ H4 (δ 3.15, R3); H1(δ 4.45, R3) ↔ H4(δ 3.19, R2); H1 (δ 4.76, R2) ↔ H4(δ 3.22, R1); H1(δ 4.85, R1) ↔ H3 (δ 3.53, V); H1 (δ 4.85, R1) ↔ H4α(δ 2.34, V).

The analysis of the NOESY spectra also showed that in each the sugar rings, proton at C-3 couple with proton in the C1, and this is in turn spatially coupled to proton at C-5 position. These proximities can occur if these protons are all axial, and so provide evidence that the methoxy and the secondary methyl groups are located at equatorial positions.

The values for the coupling constants (J) for protons 2 (10 and 8 Hz) and 4 (3.0 and 2.0 Hz) of the last sugar ring (δ 5.12 and 5.33, respectively) indicate their position as axial configuration at C-2 and an equatorial configuration at C-4. The acetoxy groups are at equatorial and axial positions, respectively. In addition, the long range CH correlation

spectra showed coupling between the two carbonyl at 170.6 ppm (acetyl at C-2) and 172.4 ppm (acetyl at C4), with the methyl signals at 2.08 ppm and 2.17 ppm, respectively.

The analysis of NMR spectra, specially long range CH correlations and cross peaks in the NOESY spectra, provides information for the connection between the sugar rings and the genin. The data from NMR confirm the sequence of sugars indicated by FAB-MS with the 6-deoxy-2,4-acetoxy-3-O-methyl hexopyranose as the terminal of the sugar chain.

Structure - In the formula **ESG** (Fig. 2) structure of **G** part of the molecule is preferably 5-pregnane-3β-ol oxytricyclo 15-ol as shown in Fig. 1 (I, II, III, IV), but also 5-pregnane-3β-ol-20-one, cholesterol, cholic acid, ergosterol, stigmasterol, androstenon, digitoxygenin, β-sitosterol, uvaol, ursolic acid, sarsasapogenin, 18, β-glycylrhetinic acid, betulin, betulinic acid, oleanoic acid, padocarpic acid.

S is preferably α(1-4) (2-deoxy, 3-methoxy) -L-lyxotetrose, α(1-4) (2-deoxy, 3-methoxy) L-xylotetrose, α(1-4) (2-deoxy, 3-methoxy)-L-arabinotetrose, α(1-4) (2-deoxy, 3-methoxy)-l-xylotetrose, α(1-4) (2-deoxy, 3-methoxy-L-ribopyranotetrose, α(1-4) (2-deoxy, 3 methoxy-L-sorbotetrose, α(1-4)-L-lyxotetrose, α(1-4)-L-xylotetrose, α(1-4)-L-arabinotetrose, α(1-4)-L-xylotetrose, α(1-4)-3,4 methoxy-L-lyxotetrose, α(1-4)-3,4 methoxy-L-xylotetrose, α(1-4)-3,4 methoxy-L-arabinotetrose, α(1-4)-3,4 methoxy-L-xylotetrose, α(1-4)-3,4 methoxy-L-ribopyranotetrose, α (1-4)-3,4 methoxy-L-

sorbopyranotetrose, α(1-4)-L-lyxotetrose, α(1-4)-L-xylotetrose, α(1-4)-L-arabinotetrose, α(1-4)-L-sorbotetrose.

E is preferably diacetylfucose but also 4-acetoxy-3 methoxy-L-α-lyxose, 4-acetoxy-3-methoxyl-L-α-xylose, 4-acetoxy-3-methoxylL-α-arabinose, 4-acetoxy-3-methoxy-L-α-xylose, 4-acetoxy-3-methoxy-L-α-ribopyranose, 4-acetoxy-3-methoxy-L-α-sorbose-acetoxy.

MV-86081 - This compound has only one sugar bonded to the genin part G (Fig. 2).

MV-8609 - This compound has in the part S of Fig. 2 only one sugar.

MV-8210 - This compound has on the part S of Fig. 2 two sugars.

MV-8611 - This compound has in the part S of Fig. 2 three sugars.

All of this compounds were demonstrated to be active (Calixto, Yunes, et al., 1987); Calixto et al., 1988).

2. Compounds from *Mandevilla illustris*

MI-07 (Illustrol) . The structure of illustrol (Fig. 1 V) was determined for same of the authors (Yunes, Calixto (1993) to be a derivative of 14:15-seco-15-norpregnane.

MI-15, MI-18 and MI-21. That was demonstrated to be active (Calixto, Yunes, et al., 1991) are of similar structure to that indicated in Fig. 2 where the Genin (part G) correspond to the illustrol, the **part S** has one, two three or more sugars and the terminal sugar E is as was indicated prefereably 6-deoxy-2,4-acetoxy-3-0-methyl hexopyranose.

EXPERIMENTAL

The freshly collected rhizomes of this plant were cut into small pieces and repeatedly extracted with ethyl acetate at room temperature. The extract was filtered and evaporated under reduced pressure and the crude extract was fractioned by column chromatography on silica gel using methylene chloride with increasing amounts of ethyl acetate as eluent.

After repeated column chromatography of the fractions using hexane-acetone as eluents is possible to isolate several compounds that exhibit indirect bradykinin blocking action.

HPLC chromatogram of MV-8608 and MV-8612 are observed in Figs.7 and 8 and a CG chromatogram of MV-8608 in Fig. 9. The CG chromatogram of Illustrol is shown in fig. 10.

M.ps. were determined using a Kofler-stage microscope and are incorrected. Optical rotation were recorded at 18-28° C using a 1 dm cell. IR spectrum was obtained from KBr discs and in $CHCl_3$ solution. Electron-

impact mass spectra were taken on an MS Finnigam model 1020. The FAB-MS were taken on a Fison.

The NMR experiments were made in $CDCl_3$ solution with TMS as internal standard, using AM 250 and Amx 600 instruments, and a JEOL alpha 500 instrument.One-dimensional ^1H spectrum were acquired as 64 K data points with a spectral width of 8.5 ppm (δ 0-8.5). One-dimensional ^{13}C spectrum were recorded as 64 K data points with a spectral width of 200 ppm (δ 0-200). The ^{13}C DEPT experiments (90 and 135) were both recorded on the Bruker AM 250 spectrometer at 62.89 MHz. The 1D selective TOCSY were recorded on the JEOL alpha 500 MHz spectrometer. The phase sensitive DQF-COSY and NOESY were acquired using standard Bruker programs. The hereronuclear (^1H - ^{13}C) correlation experiments, both one-bond and long-range correlation, were performed in reverse ^1H detected mode.

TLC was performed on silica gel (Merck Kilselgel 60 F254 0.25 mm layers). Column Chromatography was carried out on silica gel 200-300 mesh).

The plant material of ***M.velutina*** was collected from Minas Gerais State, Brazil, and was identified by Prof. Ademir Reis and Valério F. Ferreira of the Department of Botany of the Federal University of Santa Catarina. A voucher specimen is deposited in the Herbarium "Flor" of the Department of Botany, Federal University of Santa Catarina, under acession number 17.888-17.892.

EXAMPLE 1

In one series of experiments (n=5), the effect of different concentrations of MV8608 (10^{-11}M to 10^{-7}M) on the TTX-sensitive fast Na^+ current were tested using the whole-cell voltage clamp technique and experimental conditions described by the inventors elsewhere (Bkaily *et al.*, 1988, 1993). MV8608 was found to have no effect on the TTX-sensitive fast Na^+ current at all concentrations used and Figure 4 shows an example using a concentration of 10^{-7}M. Thus, MV8608 had no effect on the fast Na^+ current and can not be used as depressor or blocker of this channel where its reduction has a therapeutic action such as the case of several local anesthetics and antiarrythmic drugs such as Lidocaine.

EXAMPLE 2

In another series of experiments (n=7), the effect of different concentrations of MV8608 were tested on the T-type Ca^{2+} current (I_{Ca}) using the whole-cell voltage clamp technique and classical experimental conditions described elsewhere by the inventors (Bkaily G. *et al.*, 1991, 1992, 1993). MV8608 had no effect on the T-type I_{Ca} amplitude at a concentration of 10^{-9}M to 10^{-7}M and Figure 5 shows an example. As it can be seen in the figure, the inset effect of MV8608 in T-type I_{Ca} is immediate. Thus, the MV8608

was found to be a very weak depressor of the T-type I_{Ca}. These results suggest that MV8608 can not be used as a potent blocker of the T-type Ca^{2+} channel and where its blockade has a therapeutic action. However, its depressing effect on the T-type I_{Ca} could be useful and be used in combination with other drugs to suppress ventricular tachycardia and fibrillation.

EXAMPLE 3

In another series of experiments (n=5), the effect of different concentrations of MV8608 (10^{-11} to 10^{-6}M) were tested on the L-type I_{Ca} of heart cells of chick embryos using the whole-cell and experimental conditions and protocols described elsewhere by the inventors (Bkaily G. *et al.*, 1993). As for the T-type I_{Ca}, the L-type I_{Ca} was not affected by 10^{-11} to 10^{-10}M MV8608. However, increasing the concentration of the compound up to 10^{-9}M decreased the I_{Ca} amplitude by 10% and a further slight increase was found at a concentration of 5 x 10^{-7}M of MV8608 and Figure 6 shows a typical experiment of the time course effect of 10^{-9} and 5 x 10^{-7}M of MV8608.

Our results showed that MV8608 is a very weak depressor of the L-type Ca^{2+} channel. Thus it cannot be considered as a high potent antagonist of the L-type Ca^{2+} channel but its depressor effect could be useful when its used in combination with known L-type Ca^{2+} antagonist drugs. The weak depressor effect of MV8608 on the T-type Ca^{2+}

channel along with the L-type Ca^{2+} channel would be highly beneficial for the treatment of ventricular tachycardia, fibrillation and pathology, where the L-type Ca^{2+} blockers are known and clinicaly used.

EXAMPLE 4

In another series of experiments (n=7), using the cell attached patch clamp technique, we tested the effect of 10^{-7}M of MV8608 on the R-type Ca^{2+} channel in human aortic vascular smooth muscle cell line as described elsewhere by the inventors (Bkaily G. 1994a, Bkaily G. *et al.*, 1996a). In one series of experiments (n=4), in the presence of 10^{-6}M of nifedipine (10^{-6}M) in the patch pipette solution containing 110mM Ca^{2+}, we applied to the pipette 10^{-7}M of MV8608. In this series of experiments, MV8608 applied in the patch pipette solution decreased the single channel amplitude and probability of opening of the single R-type Ca^{2+} channel under the patch pipette without affecting its single channel conductance. In a second series of experiments (n=3), the patch pipette solution was free of MV8608 and after recording the single channel activities at different voltages, we applied MV8608 (final concentration of 10^{-7}M) to the extra-patch pipette solution containing 140mM KCl (where the rest of the cell is bathing) in order to verify if the MV8608 does cross the cell membrane and if so, does its effect from the internal side of the channel under the patch is the same as its effect when it is applied at the outer

side of the channel under the patch pipette. The results showed that effectively, MV8608 did cross the cell membrane and instead of decreasing permanently the amplitude and probability of opening of the single R-type channel as did intra-patch pipette application, MV8608 action on the inner side of the membrane increased the probability and duration of opening of the R-type channel accompanied with a spontaneous decrease and release of blockade the single channel current and Figure 7 shows a typical single R-type Ca^{2+} channel current in absence and presence of extra-patch pipette 10^{-7}M of MV8608. Such a pattern of increase of probability of opening and the open duration accompanied with the sporadic decrease of the single channel current amplitude has never been observed when MV8608 was applied at the outer side of the single channel under the patch pipette. These results highly suggest that MV8608 blocking action of the R-type Ca^{2+} channel is located mainly at the outer side of the channel and that its capability of crossing the cell membrane permits the compound to increase fleckering and duration of opening of the channel which in turn makes the external inhibitory site of the channel accessible to the external molecules of MV8608. These results highly suggest that the MV8608 inhibitory action requires the R-type Ca^{2+} channel to be at the open state and also depends on the frequency of opening of the R-type Ca^{2+} channel. This may explain in part the preventive as well as therapeutic action of MV8608 on the R-type Ca^{2+} channel as will be shown later using Fura-2 and Fluo-3 Ca^{2+} measurement techniques. These results demonstrate that MV8608 does block efficiently the R-type Ca^{2+} at the open state of the channel. The blockade of the R-type Ca^{2+} by MV8608 would reduce the sustained Ca^{2+}

overload that occurred during many abnormal cell function such as sustained vasoconstriction and hormone secretion, self perputing hormone secretion of spontaneously active proliferated cells atherosclerosis, cancer cells proliferation, acute immuno-reaction, arthritis inflammation, pains, ischemia-reperfusion, asthma, acute bronchoconstruction, arrythmia, fibrillation and epiptosis.

EXAMPLE 5

In another series of experiments we tested the effect of MV8608 (10^{-9}M) on R-type Ca^{2+} channels stimulation-induced sustained increase of total intracellular Ca^{2+} by sustained depolarization (Figures 8 to 12), by PAF (10^{-9}M) (Figures 9 to 12 and 14 to 15), by ET-1 (10^{-9}M) (Figures 9 and 12) and bradykinin (BK, 10^{-6}M) (Figures 13 and 14), in embryonic chick heart cells (Figures 8,9,12 and 13), 19-week-old human fetal heart cells (Figures 8,10,11 and 13), rabbit aortic vascular smooth muscle (VSM) cells (Figures 13 and 14), human aortic VSM cell-line (Figure 16) and freshly isolated (Figure 15) as well as in freshly isolated aortic endothelial cells (Figure 15). As can be seen in these results, sustained activation of the R-type Ca^{2+} channel induced sustained increase of $[Ca]_i$ induced by sustained depolarization or sustained superfusion with relatively low concentration of a hormone such as ET-1 (10^{-9}M) PAF (10^{-9}M) and high concentration BK (10^{-6}M) was completely blocked by 10^{-9}M of MV8608 and this effect occurred within 4 to 5 min in presence of the R-type Ca^{2+} blocker. Also, our results showed that the pure

L-type blocker, nifedipine (10^{-7}M to 10^{-5}M) had no effect on the R-type Ca^{2+} channel neither on the sustained increase of $[Ca]_i$ induced stimulation of R-type Ca^{2+} channel (Figures 9 to 12). Also, the pure L-type Ca^{2+} channel blocker did not prevent MV8608 from blocking the stimulation of R-type Ca^{2+} channel induced sustained increase of $[Ca]_i$ (Figures 11 and 12). In some experiments we increased the stimulation of the R-type Ca^{2+} channel by increasing the concentration of PAF from 10^{-9}M up to 10^{-7} and 10^{-9}M of MV8608 failed to significantly decrease the sustained increase of $[Ca]_i$ induced by 10^{-7}M PAF. Only a concentration of 10^{-6}M of MV8608 was able to block the high PAF effect on the sustained increase of $[Ca]_i$ (Figure 16).

All these results demonstrate that MV8608 blocked the R-type Ca^{2+} channel in all cell types used including human osteoblast cancer cell lines (MG63 and FAOS-2) human VSM cells isolated from atherosclerotic patients, arterial and venous endothelial cells, endocardiac endothelial cells, T-lymphocytes and platelets (not shown) and spontaneously proliferative human aortic vascular smooth muscle cells, AOSMC-9 (Figure 21).

In another series of experiments we used the confocal microscopy Fluo-3 3-dimension Ca^{2+} measurement technique in order to verify if the blockade of the R-type Ca^{2+} channel by MV8608 would block both the sustained increase of cytosolic ($[\ ]_c$) and (nuclear ($[\ ]_n$) free Ca^{2+} induced by stimulation of the R-type Ca^{2+} channels induced with

sustained increase of $[Ca]_i$. As can be seen in Figures 22 and 23, and as it was reported by the inventors (Bkaily *et al.*, 1996a) that in presence of nifedipine, sustained depolarization with 30mM KCl and PAF induced sustained increase of both $[Ca]_c$ and $[Ca]_n$ being largely nuclear. The MV8608 blocked both cytosolic and nuclear Ca^{2+} sustained overload with a concentration of $10^{-7}M$ and as was shown using Fura-2 total $[Ca]_i$ measurement technique, the compound did only at $10^{-6}M$ significantly decreased back to the control level the sustained increase of $[Ca]_c$ and $[Ca]_n$ induced with high concentration of PAF ($10^{-7}M$) (Figure 22B). As MV8608, blocked the depolarization induced sustained increase of $[Ca]_i$, the compound at a concentration of $10^{-8}M$ and $10^{-7}M$ also dose dependently prevented the stimulation of the R-type Ca^{2+} channel by the sustained depolarization, thus decreasing back the $[Ca]_c$ and $[Ca]_n$ to the control level (Figure 22A). Extracellular applications of the Ca^{2+} chelator EGTA further decreased the $[Ca]_i$ mainly at the nucleus level. These results demonstrate that blockade of the R-type Ca^{2+} by MV8608 blocked both $[Ca]_c$ and $[Ca]_n$ sustained overload. On the contrary of what was shown for high PAF ($10^{-7}M$) induced sustained increase of $[Ca]_i$, $[Ca]_c$ and $[Ca]_n$, MV8608 succeeded in preventing the high PAF action at a concentration of $10^{-9}M$. Thus, this compound seems to be equally effective in acute sustained Ca^{2+} overload, however, its more effective as a preventive blocker of the R-type Ca^{2+} channel in chronic stimulation of the channel.

All these results showed that MV8608 is an effective R-type Ca^{2+} channel blocker

in acute than in chronic situation. However, this compound seems to be more effective preventive than therapeutic in chronic stimulation of Ca^{2+} influx through the R-type Ca^{2+} channel.

In another series of experiments using the double-perfused bed of the rat (Claing A. *et al.*, 1994), MV8608 was found to induce a concentration-dependent inhibition of the PAF-induced responses (Figure 17). The inhibitory properties of MV8608 are specific for PAF as the response to ACh (arterial) and AngII (venous) are unaffected by the pregnane-containing moiety.

In summary, the potency of blockade of the R-type Ca^{2+} channel by MV8608 depends on the degree of the sustained Ca^{2+} overload at the cytosolic and nuclear Ca^{2+}, thus it depends on the degree of stimulation of the R-type Ca^{2+} channel. A blockade of the R-type Ca^{2+} channel by MV8608 will be beneficial in pathological situation where sustained cytosolic and nuclear Ca^{2+} take place such as those described in Example 4.

EXAMPLE 6

In a series of experiments (n=5), we tested the effect of another MV compound

MV8612 on the TTX-sensitive fast Na^+ current (I_{Na}) of embryonic chick heart cells using the whole-cell voltage clamp technique. Superfusion with 10^{-9}M of MV8612 had no effect on the fast Na^+ current, however, increasing the concentration up to 10^{-8}M decreased the I_{Na} amplitude by 15% and no further decrease was found at 10^{-7}M. Figure 19 shows a typical example of the time course effect of 10^{-8}M of MV8612 on the peak amplitude of the fast I_{Na}.

These results shows that unlike MV8608, MV8612 depresses the fast Na^+ current in heart cells. This compound could be used in situation where depressing of the fast Na^+ channels is beneficial such as in arrythmia, local anaesthetic, and pain. The compound can be used also in combination with drugs acting on fast sodium channel such as lidocaine.

EXAMPLE 7

In another series of experiments (n=4), we tested the effect of MV8612 on the L-type Ca^{2+} current (I_{Ca}) in chick embryonic heart cells using the whole-cell voltage clamp technique. Superfusion with 10^{-9}M of MV8612 decreased I_{Ca} amplitude by 10% and increasing the concentration of the compound up to 10^{-8}M further decreased the current amplitude by 25%. Higher concentration of MV8612 (10^{-7}M) decreased the I_{Ca} amplitude by 62%. These results showed that MV8612 possess a more potent L-type Ca^{2+} channel

antagonist properties than that of MV8608.

The relatively high depressing effect of the L-type Ca^{2+} channel by MV8612 would be beneficial where L-type Ca^{2+} blockade are usually used such as ventricular tachycardia and hypertension.

EXAMPLE 8

In another series of experiments (n=7), we tested the effect of 10^{-7}M of MV8612 on the R-type Ca^{2+} in human aortic VSM cells using the single channel cell attached recording technique and intra and extra patch pipette application of drugs. As for MV8608, the R-type Ca^{2+} channel was recorded in the presence of 10^{-6}M of the L-type Ca^{2+} channel blocker nifedipine (in the patch pipette) and using extra-patch pipette solution (containing 140mM KCl) that mimics the intracellular ionic concentration (to zero the extra-pipette cell membrane potential). In one series of experiments (n=3), we only applied MV8612 (total concentration, 10^{-7}M) to the patch pipette and Figures 20A-C shows examples. As can be seen in this figure, application of 10^{-7}M MV8612 via the patch pipette significantly decreased the R-type single Ca^{2+} channel current amplitude (by about 75% of the control value panel A) and the probability and the opening time of the R-type Ca^{2+} channel (Panel B and C). As for MV8608, in one series of experiments (n=4) we only applied MV8612 (10^{-7}M) to the extra-patch pipette in order to verify if

the compound penetrates into the cytosol and if so, how would it affect the R-type Ca^{2+} channel activity and Figure 20D and E show typical examples. As shown in this figure, extra-patch pipette application rapidly increased the R-type Ca^{2+} opening frequence that was accompanied by a small decrease in the single channel current at all sustained membrane potential (HP) levels used (Figure shows example at HP of -30 where control channel opening is high and a +10mV where control channel opening is low).

These results demonstrate that as MV8608, intra-patch pipette application equivalent to extracellular application in normal working single cell or muscle of MV8612 decreased both R-type Ca^{2+} channel amplitude and probability and duration of opening. However, the extend of blocking of the R-type Ca^{2+} channel amplitude and probability of opening by MV8612 were higher than that of MV8608. Also, these results demonstrate that as MV8608, MV8612 did penetrate the cytosol and did increase the frequency of opening (but not the opening-time) of the channel, however, unlike MV8608, intracellular MV8612 permanently depressed the amplitude of the R-type Ca^{2+} channel. The increase of frequency of opening of the R-type channel by intracellular MV8612 would allow extracellular MV8612 to block the channel activity at the opening state. The large decrease of the R-type Ca^{2+} channel amplitude and activities by intra-patch pipette application of MV8612 when compared to the MV8608 effect could be due to the permanent decrease of the R-type Ca^{2+} channel by intracellular MV8612 but not by MV8608. In summary, the MV8612 seems to be a more effective blocker of the R-

type Ca^{2+} channel than that of MV8608 and this difference is mainly due to the permanent depressing effect of the R-type Ca^{2+} channel by intracellular MV8612. Experiments using $[Ca]_i$, $[Ca]_c$ and $[Ca]_n$ as well as *in vivo* work (will be describe later) confirm these results and show a more potent effect of MV8612 on the R-type Ca^{2+} channel when compared to that of MV8608 described earlier.

Thus, the high potency blockade of the R-type Ca^{2+} channel by MV8612 will be more effective than MV8608 in reducing Ca^{2+} overload that occurred during many abnormal cell function that are described for MV8608 in example 4. Also, since MV8612 (but not MV8608) depressed the fast Na^+ channel and the L-type Ca^{2+} channel, this compound will be highly effective not only in acute but also in chronic diseases such as those described in examples 4 to 7.

EXAMPLE 9

In another series of experiments, as for MV8608, we tested the effect of MV8612 on $[Ca]_i$, $[Ca]_c$, $[Ca]_n$ (in presence of extracellular L-type Ca^{2+} blocker, nifedipine, 10^{-6}M) of embryonic chick heart (Figures 22 to 24 and 27) and human aortic VSM cells (22 to 26) as well as *in vivo* anaesthetized guinea pig (Figure 29).

Using Fura-2 $[Ca]_i$ measurement technique, in one series of experiments we tested the effect of MV8612 (10^{-9}M) on the stimulation of R-type Ca^{2+}-induced sustained increase of $[Ca]_i$ by sustained depolarization (Figures 26 and 27), PAF (10^{-9}M, Figure 27) and ET-1 (Figures 26 and 27). These experiments showed that 10^{-9}M of MV8612 significantly decreased sustained increase of $[Ca]_i$ induced by sustained depolarization and hormones. Also, MV8612 (10^{-8}M) was found to prevent stimulation of the R-type Ca^{2+} channel induced sustained increase of $[Ca]_i$ by sustained depolarization and chronic concentration of PAF (10^{-7}M) (Figure 25). Using 3-dimension Fluo-3 Ca^{2+} measurement of $[Ca]_c$ and $[Ca]_n$, MV8612 was found to be a more potent blocker than MV8608 in the stimulation of R-type Ca^{2+} channel induced sustained increase of $[Ca]_c$ and $[Ca]_n$ by sustained depolarization and high concentration of PAF (10^{-7}M) (Figures 22 and 23). MV8612 was also found to be equipotent in preventing the stimulation of the R-type Ca^{2+} channel by sustained depolarization and high concentration of PAF (10^{-7}M) (Figure 24).

On the other hand, *in vivo* administered PAF, induced a marked hypotension in the anaesthetized rat and guinea pig. In addition, the pro-inflammatory mediator also induced an important bronchoconstriction in the guinea pig, where PAF induced its hypotensive effects through the release of EDRF, its bronchoconstrictive properties are solely mediated by the release of thromboxane A_2.

Characteristically, standard Ca^{2+} blockers such as nifedipine and the dual L and R-type blocker isradipine have marked intrinsic hypotensive properties in the rat (results not shown) and in the guinea pig (Figure 28).

Interestingly, the R-type blocker, MV8612, is devoid of marked intrinsic effect in the guinea pig. As shown in Figure 29, pretreatment of the guinea pig with MV8612 abolished the bronchoconstrictive responses and very significantly reduced the hypotensive effects of PAF. Following withdrawal of the treatment with MV8612, the hypotensive effect of PAF is fully restored in the same animal (for methodology, please refer to Gratton *et al.*, 1995a). Identical inhibition of MV8612 has been observed on the hypotensive effect of PAF in the anaesthetized rat (for methodology, please refer to D'Orléans-Juste et al., 1996; Gratton *et al.*, 1995a,b).

These results again confirm the more potent effect of MV8612 (when compared to MV8608) on blocking the R-type Ca^{2+} channel and related cytosolic and nuclear Ca^{2+} overload. The high potency effect of MV8612 of the R-type Ca^{2+} combined to its depressing of the fast Na^{+} and the L-type Ca^{2+} channels give this compound a high spectrum of action than that of MV8608 and isradipine. The MV8612 as well as MV8608 are unique compounds that did not block the cytosolic Ca^{2+} overload but also blocked nuclear Ca^{2+} overload. This later effect of MV8608 and especially MV8612 gives these compounds a new target other than that of the cytosolic membrane channels

but also a nuclear and a perinuclear ionic channel target blockers. The MV8612 will be beneficial in cell disorders that implicate Ca^{2+} and Na^{+} abnormal transport and preventing cytosolic Ca^{2+} overload such as in diseases cited in example 1 to 8.

In conclusion, our pharmacological results support the unique R-type Ca^{2+} channel blocking properties of the MV8608 and MV8612.

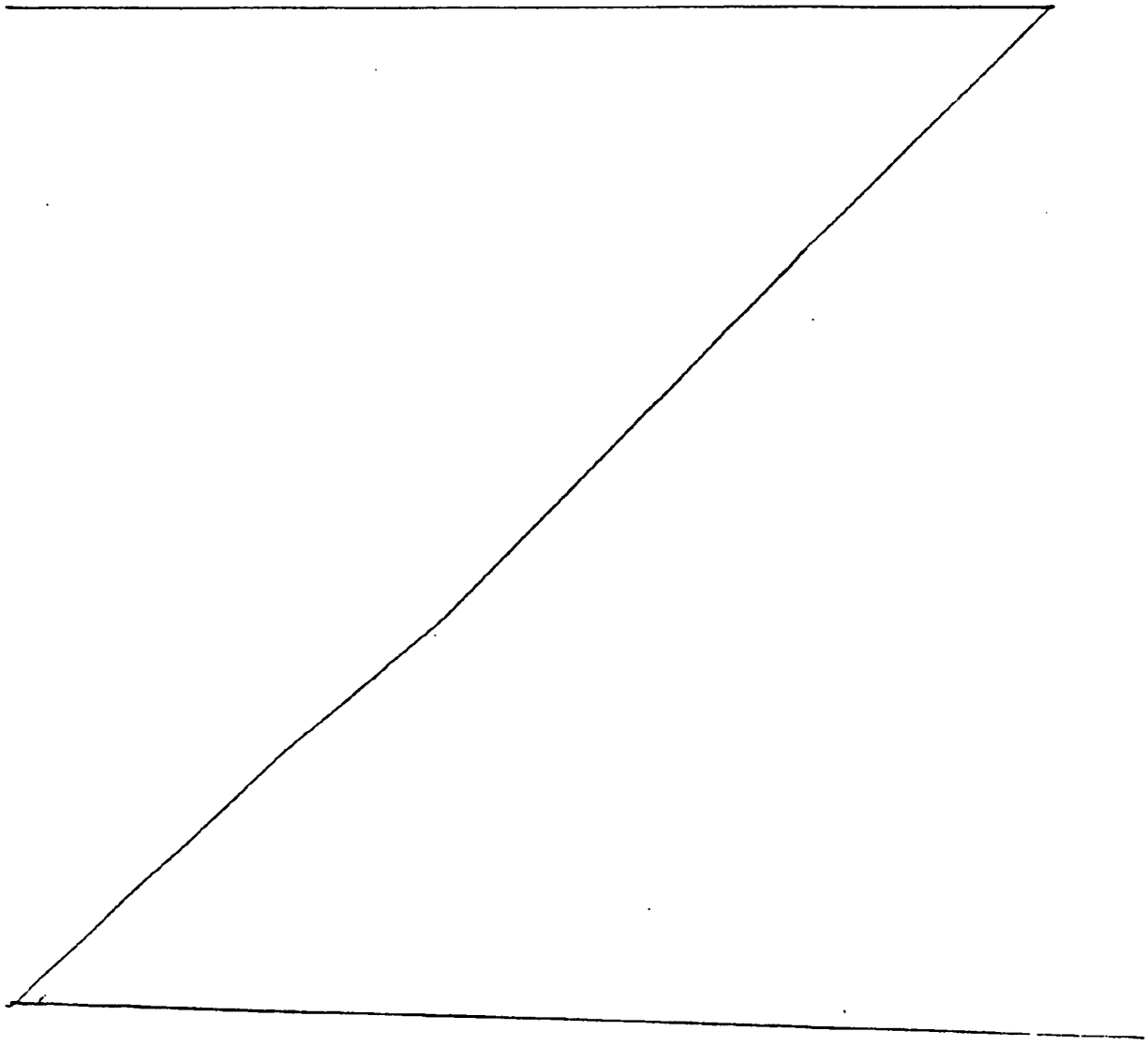

CONFIDENTIAL

NEW "IN VIVO" RESULTS WITH COMPOUNDS MV 8608 AND MV 8612

EXAMPLE 10

In this experiments (N =5 to 6 animals per group) it was evaluated the anti-oedematgenic action of compounds MV 8608 and MV 8612 against bradykinin and several mediators which are reported to be involved in the inflammatory processes. The procedures used to perform these experiments has been reported elsewhere (Neves et al., 1993; Campos and Calixto, 1995; Campos et al., 1996; De Campos et al., 1996). As can be seen in figure 1A, MV 8608 (10 and 100 nmol/paw) when co-injected with des-Arg^9-bradykinin caused a dose-related inhibition of paw oedema induced by this peptide. In contrast, at similar dose MV 8608 had no significant effect against bradykinin-induced hindpaw oedema in animals treated with LPS (Campos et al., 1996) (figure 1B). As reported previously, in rats treated 30 days prior with systemic injection of LPS (Campos et al., 1996), both B_1 and B_2 kinin selective agonists caused marked oedema formation (figure 1C and D). In this experimental condition, compound MV 8608 (100 nmol/paw) significantly inhibited both des-Arg^9-BK and bradykinin-induced rat paw oedema (figure 1C and D). However, this compound was more effective against B_1 agonist-mediated oedema formation. In addition, compound MV 8608 (100 nmol/paw) also consistently

inhibited the paw oedema induced by PAF (figure 2B) and partially the oedema induced by prostaglandin E_2 (PGE_2) (figure 2A), leading oedema induced by substance P unaffected (figure 2C). Interestingly, compound MV 8608 (10 and 100 nmol/paw) also significantly inhibited oedema formation induced by subplantar injection of ovalbumin in animals that had been actively sensitised to this antigen (figure 2D).

Results of figure 3A (A and B) demonstrate that compound MV 8608 (10 and 100 nmol/paw) dose-dependently prevented the potentiation of paw oedema caused by association of low dose of des-Arg^9-BK plus PAF (figure 3A) or with PGE_2 (figure 3B). Compound MV 8608 (10 and 100 nmol/paw) when co-injected in association with carrageenan (figure 4A), dextran (figure 4B), histamine (figure 4C) or with serotonin (figure 4D), significantly prevented the oedemagenic response caused by these substances. However, MV 8608 was much more effective in inhibiting paw oedema induced by carrageenan, an effect which has been reported to be dependent on the release of several mediators, including kinins, histamine, serotonin and PAF (Hargreaves et al., 1988; Burch and DeHaas, 1990; Damas and Remacle-Vólon, 1992; Damas et al., 1996; DeCampos et al., 1996).

In marked contrast, and confirming previous "in vitro" and "in vivo" results (Calixto and Yunes, 1986; Calixto et al., 1985; 1987; 1988; 1991a,b), compound MV 8612 (10 and 100 nmol/paw) significantly inhibited bradykinin and the selective B_2 agonist tyr^8-bradykinin-induced paw oedema (figure 5A and D) while having no significant effect against oedema induced by des-Arg^9-BK in

animals treated with LPS (figure 5B)) (Campos and Calixto, 1996). The anti-oedematogenic effect caused by MV 8612 seems to be systemic, because the controlateral paw treated with saline also revealed an significant anti-oedemagenic action (figure 5C)) On the other hand, MV 8612 (10 and 100 nmol/paw) dose-dependently inhibited PGE_2 and carrageenan-induced oedema formation (figure 6A, C)) but caused only a minimal inhibition of PAF and substance P-mediated paw oedemas (Figure 6B and D)) Compound MV 8612 (10 nmol/paw) significantly inhibited the oedema formation caused by association of low dose of bradykinin plus the calcitonin gene related peptide (figure 7A), PGE_2 (figure 7B) and prostacyclin (figure 7D)) but did not interfere with oedema induced by association of bradykinin plus PAF (figure 7C). The anti-oedematogenic action of MV 8612 against bradykinin-induced oedema was independent on the release of histamine, since a dose-related inhibition was still observed in animals treated with cyprohetadine or with compound 48/80 (figure 8A and B). The inhibition of MV 8612 against oedema caused by bradykinin installs rapidly (30 min) and lasted for at least 2 h (figure 9).

When tested in mice, compound MV 8612 (40 to 160 nmol/paw) inhibited in dose-dependent manner bradykinin and carrageenan-induced paw oedema in mice (Figure 10A and B). At the same dose-, MV 8612 failed to affect significantly PAF-acether or serotonin-induced oedema formation (Figure 10C and D)) Confirming the effect observed with crude extract of *Mandevilla velutina*, when MV 8612 was injected systemically 8612 (7.5 and 15 µmol/kg, i.p.) given 30 min prior, it produced a dose-dependent inhibition of bradykinin and cellulose

sulphate-induced paw oedema (Figure 11 (A and B)). However, at the same range of dose, MV 8612 had no significant effect against paw oedema induced by serotonin and histamine (Figure 11 (C and D)). In marked contrast, compound MV 8608 (7.5 and 15 μmol/kg, i.p) caused a dose-related inhibition of histamine and serotonin-induced oedema formation, leaving paw oedema to bradykinin unaffected (Figure 12 (A ,B and C)). Taken together, these results indicate that both MV 8612 and MV 8608 compounds show topical and systemic potent anti-inflammatory properties through distinct mechanism of action. While MV 8612 was more active against inflammatory response caused by bradykinin via stimulation of B_2 receptors, MV 8608 was effective in preventing oedemas elicited by histamine, PAF-acether and by the B_1 selective agonist des-Arg^9-BK.

EXAMPLE 11

To assess further the anti-inflammatory action of compound MV 8612 and MV 8608, we tested their effects against the inflammatory responses caused by several mediators of inflammation in a murine model of pleurisy (Saleh et al., 1996). In addition, both compounds were tested against the increase of vascular permeability caused by bradykinin in the rat skin (Neves et al., 1993b). Figure 13 shows that compound MV 8612 (30 and 60 μmol/kg, i.p.) given 1 h prior, significantly inhibited plasma extravasation (A) as well as the total (B) and neutrophils cells (C) in response to intrapleural injection of carrageenan. Compound MV 8608 (30 μmol/kg, i.p) also inhibited significantly the total and neutrophil cells migration caused by intrapleural injection of carrageenan (Figure

14A). Confirming our previous results, compound MV 8608 (30 μmol/kg, i.p.) also antagonised significantly the plasma extravasation and the mononuclear cells influx caused by intrapleural injection of PAF (Figure 15A). In contrast, at the same range of dose, MV 8612 did not affect significantly the inflammatory response caused by PAF acether in a murine model of pleurisy (Figure 15A). However, both MV 8612 (8 and 16 μmol/kg, i.p) and MV 8608 (27 and 54 μmol/kg, i.p.) antagonised in a dose-related manner the increase of vascular permeability caused by bradykinin in the rat skin (Figure 16A, A and B). Compound MV 8612 was more active than MV 8608. Such data extend our previous results (Calixto et al., 1991a; Zanini et al., 1992; Neves et al., 1993b) supportting the view that both MV 8612 and MV 8608 exhibit a powerful anti-inflammatory properties.

EXAMPLE 12

We also tested in a separate series of experiments whether compounds MV 8612 and MV 8608 interfere with human lymphocyte proliferation "in vitro". These experiments were carried out as reported previously (Moraes et al., 1996). The results of figure 17A (A and B) show that compound MV 8612 (0.02 to 0.32 μM) and, to a lesser extent, MV 8608 (14.5 to 116 μM) caused graded inhibition of human lymphocyte proliferation, being MV 8612 about 570 fold more potent. These results may account to explain their reported anti-inflammatory properties.

EXAMPLE 13

The antinociceptive actions of compound MV 8612 and MV 8608 were investigated in different models of nociception in mice as reported previously (Vaz et al., 1996). Compound MV 8612 (0.25 to 2.5 µmol/kg, i.p.), given 30 min prior, caused dose-dependent inhibition of acetic acid (Figure 18A (A)) acetylcholine (Figure 19 A) and kaolin (Figure 20A (A)) induced writhing response in mice. However, MV 8612 was about 2-fold more potent against kaolin-induced pain. In contrast, compound MV 8608 (2.7 to 27 µmol/kg, i.p.) caused only partial or even no antinociceptive action when tested in the same model of pain. When compared with morphine and indomethacin (Table 1), compound MV 8612 was about 2-fold more potent when assessed in the kaolin-induced writhes. Given intracerebroventricularly (i.c.v) compound MV 8612 (4.2 to 42 nmol/site), like morphine (0.26 to 13 nmol/site), caused dose-related antinociception when assessed against acetic acid-induced writhes (Figure 21A (A and B)). Compound MV 8612 was about 12-fold less potent than morphine. These results and those reported previously (Corrêa et al., 1993) indicate that MV 8612, exhibits potent antinociceptive actions, comparable to those of morphine and indomethacin. Its antinociceptive property seems to be associated with its anti-bradykinin action, but appear to be unrelated to activation of opioid, ∝-adrenergic, serotonin or interaction with nitric oxide pathway (results not shown).

LEGENDS TO FIGURES

Figure 1A-Effect of subplantar injection of compound MV 8608 isolated from *Mandevilla velutina* on paw oedema caused by subplantar injection of des-Arg^9-bradykinin (DABK) (A) in rats treated 24 h prior with LPS; bradykinin (BK, B) and for des-Arg^9-bradykinin (C) and for bradykinin (D) in animals treated 30 days prior with BCG. Each group represents the mean of 4-5 animals and the vertical bars the S.E.M. The asterisks indicate the significance levels: * $P < 0.05$.

Figure 2A- Effect of subplantar injection of MV 8608 isolated from *Mandevilla velutina* on paw oedema caused by subplantar injection of prostaglandin E_2 (PGE_2) (A), PAF- acether (PAF) (B), substance P (SP) (C) and ovalbumin (OVO) (D). Each group represents the mean of 4-5 animals and the vertical bars the S.E.M. The asterisks indicate the significance levels: * $P < 0.05$. Each group represents the mean of 4-5 animals and the vertical bars the S.E.M. The asterisks indicate the significance levels: * $P < 0.05$.

Figure 3A-Effect of subplantar injection of MV 8608 isolated from *Mandevilla velutina* on paw oedema caused by subplantar injection of low dose of des-Arg^9-bradykinin plus PAF (A) or prostaglandin E_2 (PGE_2) (B). Each group represents the mean of 4-5 animals and the vertical bars the S.E.M. The asterisks indicate the significance levels: * $P < 0.05$.

Figure 4A- Effect of subplantar injection of MV 8608 isolated from *Mandevilla velutina* on paw oedema caused by subplantar injection of carrageenan (Cg) (A), dextran (DEX) (B), histamine (HIST) (C) and for serotonin (5-HT) (D). Each group represents the mean of 4-5 animals and the vertical bars the S.E.M. The asterisks indicate the significance levels: * $P < 0.05$.

Figure 5A- Effect of subplantar injection of MV 8612 isolated from *Mandevilla velutina* on paw oedema caused by subplantar injection of bradykinin (BK) (A and C), des-Arg^9-bradykinin (DABK) (B) and for tyr^8-bradykinin (D). Experiments for DABK were carried out in animals treated with LPS 24 h prior. Each group represents the mean of 4-5 animals and the vertical bars the S.E.M. The asterisks indicate the significance levels: * $P < 0.05$.

Figure 6A-Effect of subplantar injection of MV 8612 isolated from *Mandevilla velutina* on paw oedema caused by subplantar injection of prostaglandin E_2 (PGE_2 (A), PAF acether (PAF) (B), carrageenan (Cg) (C) and substance P (SP) (D). Each group represents the mean of 4-5 animals and the vertical bars the S.E.M. The asterisks indicate the significance levels: * $P < 0.05$. Each group represents the mean of 4 - 5 animals.

Figure 7A-Effect of subplantar injection of MV 8612 isolated from *Mandevilla velutina* on paw oedema caused by subplantar injection of low dose of

bradykinin plus CGRP (A), BK plus prostaglandin E_2 (PGE_2) (B); BK plus PAF C) or BK plus PGI_2 (D). Each group represents the mean of 4-5 animals and the vertical bars the S.E.M. The asterisks indicate the significance levels: * $P < 0.05$.

Figure 8 Effect of intraperitoneal injection of MV 8612 isolated from *Mandevilla velutina* on rat paw oedema caused by subplantar injection of bradykinin in animals treated with cyproheptadine (A) or compound 48/80 (B). Each group represents the mean of 4 animals and the vertical bars the S.E.M. The asterisks indicate the significance levels: * $P < 0.05$.

Figure 9 Time-dependent antioedematogenic effect caused by subplantar injection of compound MV 8612 on bradykinin-induced rat paw oedema. Each group represents the mean of 4-5 animals and the vertical bars the S.E.M. The asterisks indicate the significance levels: * $P < 0.05$.

Figure 10 Dose-dependent antioedematogenic effect caused by co-injection of compound MV 8612 on bradykinin (BK, A), carrageenan (B), PAF (C and serotonin (D)-induced mouse paw oedema. Each group represents the mean of 7 animals and the vertical bars the S.E.M. The asterisks indicate the significance levels:* $P < 0.05$; ** $P < 0.01$.

Figure 11 Dose-dependent antioedematogenic effect caused by intraperitoneal injection of compound MV 8612 on bradykinin (BK, A), cellulose sulphate (B)-

serotonin (5-HT, C) and histamine (Hist, D)-induced mouse paw oedema. Each group represents the mean of 5-6 animals and the vertical bars the S.E.M. The asterisks indicate the significance levels: ** $P < 0.01$.

Figure 12A-Dose-dependent antioedematogenic effect caused by intraperitoneal injection of compound MV 8608 on histamine (Hist, A) -serotonin (5-HT, B) and bradykinin (BK, C)-induced mouse paw oedema. Each group represents the mean of 5-6 animals and the vertical bars the S.E.M. The asterisks indicate the significance levels: *$P < 0.05$; ** $P < 0.01$.

Figure 13A Effect of compound MV 8612 given intraperitoneally on carrageenan (1mg/site)-induced pleurisy in mice. Each group represents the mean of 8 to 10 animals and the vertical bars the S.E.M. The asterisks indicate the significance levels: *$P < 0.05$; ** $P < 0.01$.

Figure 14A Effect of compound MV 8608 given intraperitoneally on carrageenan (1mg/site)-induced pleurisy in mice. Each group represents the mean of 8 to 10 animals and the vertical bars the S.E.M. The asterisks indicate the significance levels: ** $P < 0.01$.

Figure 15A Effect of compounds MV 8608 and MV 8612 given intraperitoneally on PAF-acether (1 µg/site)-induced pleurisy in mice. Each group represents the

mean of 10 animals and the vertical bars the S.E.M. The asterisks indicate the significance levels: ** $P < 0.01$.

Figure 16 Dose-dependent inhibition of bradykinin-induced skin vascular permeability in rats caused by intraperitoneal injection of MV 8612 and MV 8608. Each group represents the mean of 8 animals and the vertical bars the S.E.M. The asterisks indicate the significance levels: *$P < 0.05$; ** $P < 0.01$.

Figure 17 Concentration-dependent inhibition of human lymphocyte proliferation caused by compounds MV 8612 and MV 8608. Each group represents the mean of 6-7 experiments and the vertical bars the S.E.M.

Figure 18 Dose-related antinociceptive effect caused by intraperitoneal injection of compounds MV 8612 and MV 8608 against acetic-acid-induced writhe responses in mice. Each group represents the mean of 8 animals and the vertical bars indicate the S.E.M.

Figure 19 Dose-related antinociceptive effect caused by intraperitoneal injection of compounds MV 8612 and MV 8608 against acetylcholine-induced writhe responses in mice. Each group represents the mean of 8 animals and the vertical bars indicate the S.E.M.

Figure 20A Dose-related antinociceptive effect caused by intraperitoneal injection of compounds MV 8612 and MV 8608 against kaolin-induced writhe responses in mice. Each group represents the mean of 8 animals and the vertical bars indicate the S.E.M.

Figure 21A Dose-related antinociceptive effect caused by i.c.v. injections of compounds MV 8612 and morphine against acetic acid- induced writhe responses in mice. Each group represents the mean of 8 animals and the vertical bars indicate the S.E.M.

Table 1 - Antinociceptive potencies of compound MV 8612, morphine and indomethacin in mice .

	ID_{50} µmol/kg, i.p			
DRUG	KAOLIN	ACETYLCHOLINE	ACETIC ACID	TAIL-FLICK
MV 8612	0.4 (0.3-0.6)	2.2 (2.0-2.3)	2.4 (1.9-2.6)	no effect
MORPHINE	1.4 (1.2-1.7)	1.4 (1.0-1.8)	1.3 (1.0-1.6)	6.0 (5.7-6.4)
INDOMETHACIN	1.6 (1.4--1.8)	0.8 (0.5-1.0)	1.2 (0.9-1.4)	no effect

each groups represents the mean of 6 to 8 animals

CONFIDENTIAL

Table 1 - 1 D selective TOCSY

Irradiated proton	Observed signals (δ, ppm)					
	H1	H2	H3	H4	H5	H6
I11,R1 δ=4.45ppm	X	Ax: 1.58 Eq: 2.08	3.81	3.22	3.85	1.22
I11,R2 δ=4.76ppm	X	Ax:1.64 Eq: 2.11	3.78	3.19	3.34	1.21
I12,R3(ax) δ=1.57ppm	4.45	Ax: 1.57 Eq: 2.29	3.40	3.15	3.28	1.29
I11,R4 δ=4.96ppm	X	Ax: 1.55 Eq: 2.16	3.77	3.19	3.92	1.21
I12,R5 δ=5.12ppm	4.43	5.12	3.33	5.33	3.70	1.21

Table 2 - ^{13}C assignments (sugars) (δ, ppm)

	C1	C2	C3	C4	C5	-CH3	-OMe
R1	96.11	35.63	68.38	82.59	70.87	18.25*	56.74
R2	99.73	36.15	77.10	83.91	71.19	18.27*	58.33
R3	101.45	36.35	78.75	82.15	71.54	18.41	56.39
R4	98.47	35.37	76.39	83.81	69.29	18.06	58.03
R5	102.55	70.72	80.34	68.45	71.02	16.58	57.81

(*) These assignments can be interchangeable

CH3-CO			
CH3		CO	
20.87**	C2-R5	170.6	C2-R5
20.97**	C4-R5	172.4	C4-R5

(**) These assignments can be interchangeable

Table 3 - ^{13}C assigments for the genin part (velutinol) in compound-12 (δ, ppm)

Position	Velutinol(ref. 12)	Compound-12
1	37.4	37.57
2	31.4	29.67
3	71.3	77.64
4	42.0	38.89
5	139.3	140.49
6	121.4	121.56
7	25.9	26.07
8	33.5	33.69
9	45.8	45.94
10	37.6	37.96
11	18.6	18.68
12	26.6	26.80
13	43.5	43.70
14	87.1	87.40
15	92.5	92.67
16	108.7	108.84
17	52.3	52.47
18	21.6	21.74
19	19.1	19.17
20	73.8	73.96
21	78.0	78.19

Table 4 - ^{1}H NMR assignements of velutinol and of the aglycone of 8612 compound

Position	ppm $\delta.^1$H	
	Velutinol	Compound 12
1	1.12(a); 1.82(b)	1.14(a)qd; 1.82(b)dt.J=13.5;3.5
2	1.85(a); 1.50(b)	1.95(a); 1.56(b)
3	3.53(H.a); 1.80(OH)	3.53(tt.J=11.5;4.5)
4	2.30(a); 2.23(b)	2.34(a); 2.23(b)
5	--	--
6	5.38	5.38(m)
7	2.16(a); 1.89(b)	2.16(a); 1.90(qd.J=18.0;5.0;2.5)β
8	2.01	2.01(td.J=11.5;5.5)
9	1.36	1.36(dd)
10	--	--
11	1.64(a.b)	1.64(a.b)m
12	2.35(a); 1.65(b)	2.35(a); 1.65(b)
13	--	--
14	--	--
15	5.01(H); 4.75(OH)	5.01(H)d.J=12.0; 4.75(OH)d.J=12
16	5.78	5.78(d.J=4.5)
17	2.53	2.53(dd.J=6.0; 4.5)
18	1.11	1.11(s)
19	1.09	1.08(s)
20	4.45	4.44(dd.J=6.0; 3.5)
21	3.81(A) 4.28(B)	3.81(A)dd.J=10.0; 3.5 4.28(B)d.J=10.0

CONFIDENTIAL

Table 5 - ^{13}C - ^{1}H correlation long range

C-1 (δ, ppm)		H (δ, ppm)	
R-1	96.11	3.53	H3 (Vel.)
R-2	99.73	3.22	H4-R1
R-3	101.45	3.19	H4-R2
R-4	98.47	3.15	H4-R3
R-5	102.55	3.19	H4-R4

C (δ, ppm)		H-1 (δ, ppm)	
C-3 (velutinol)	77.64	4.85	R-1
C4-R1	82.59	4.76	R-2
C4-R2	83.91	4.45	R-3
C4-R3	82.15	4.96	R-4
C4-R4	83.81	4.43	R-5

The embodiments of the invention in which an exclusive property or privilege is claimed are defined as follows:

1. The compounds of the general formula (III):

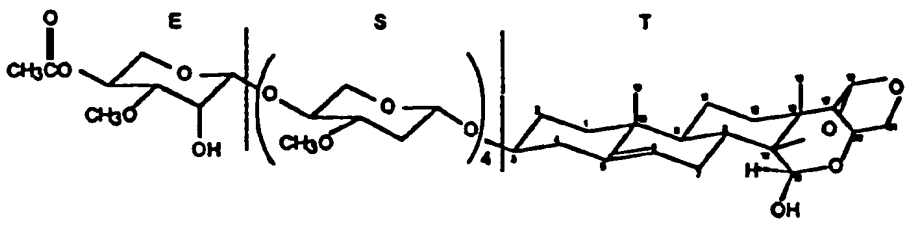

and pharmaceutically aceptable salts thereof.

2. The use of the compounds of claim 1 as a R-type Ca2+ channel blocker.

3. In the above formula ETS, T is preferably α(1-4) (2-deoxy, 3-methoxy) -L-lyxotetrose, α(1-4) (2-deoxy, 3-methoxy) L-xylotetrose, α(1-4) (2-deoxy, 3-methoxy)-L-arabinotetrose, α(1-4) (2-deoxy, 3-methoxy)-L-xylotetrose, α(1-4) (2-deoxy, 3 methoxy-L-ribopyranotetrose, α(1-4) (2-deoxy, 3 methoxy-L-sorbotetrose, α(1-4)-L-lyxotetrose, α(1-4)-L-xylotetrose, α(1-4)-L-arabinotetrose, α(1-4) -L-xylotetrose, α(1-4)-3, 4 methoxy-L-lyxotetrose, α(1-4)-3,4 methoxy-L-xylotetrose, α(1-4)-3,4 methoxy-L-arabinotetrose, α(1-4)-3,4 methoxy-L-xylotetrose, α(1-4) 3,4 methoxy-L-ribopyranotetrose, α(1-4) 3,4 methoxy-L-sorbopyranotetrose, α(1-4)-L-lyxotetrose, α(1-4)-L-xylotetrose,α(1-4)-L-arabinotetrose,α(1-4)-L-ribopyranotetrose,α(1-4)-L-sorbotetrose.

T has preferably tetra sugar derivative but also monomeric to aligomeric of mentioned sugar derivatives. The terminal E part is preferably 4-acetoxy-3 methoxy-L-α-lyxose, 4-acetoxy-3-methoxy-L-α-xylose, 4-acetoxy-3-methoxy-L-α-arabinose, 4-acetoxy-3-methoxy-L-α-xylose, 4-acetoxy-3-methoxy-L-α-ribopyranose, 4-acetoxy-3-methoxy-L-α-sorbose-acetoxy.

4) Compounds of the general formula **I, II, III, IV, V and VI** indicated in Fig. 1 and Fig. 2 that present inhibitory activity on calcium and sodium channel. Compounds of formula **VI ESG** (in Fig. 2) as was mentioned has three parts:

Part G - structure of **G** part of the molecule is preferably 5-pregnane-3β-ol oxytricyclo 15-ol as shown in Fig. 2, but also illustrol, 5-pregnane-3β-ol-20-one, cholesterol, cholic acid, ergosterol, stigmasterol, androstenon, digitoxygenin, β-sitosterol, uvaol, ursolic acid, sarsasapogenin, 18, β-glycyrrhetinic acid, betulin, betulinic acid, oleanoic acid, padocarpic acid.

Part S - is preferably α(1-4) (2-deoxy, 3-methoxy) -L-lyxotetrose, α(1-4) (2-deoxy, 3-methoxy) L-xylotetrose, α(1-4) (2-deoxy, 3-methoxy)-L-arabinotetrose, α(1-4) (2-deoxy, 3-methoxy)-l-xylotetrose, α(1-4) (2-deoxy, 3-methoxy-L-ribopyranotetrose, α(1-4) (2-deoxy, 3 methoxy-L-sorbotetrose, α(1-4)-L-lyxotetrose, α(1-4)-L-xylotetrose, α(1-4)-L-arabinotetrose, α(1-4)-L-xylotetrose, α(1-4)-3,4 methoxy-L-lyxotetrose, α(1-4)-3,4 methoxy-L-xylotetrose, α(1-4)-3,4 methoxy-L-arabinotetrose, α(1-4)-3,4 methoxy-L-xylotetrose, α(1-4)-3,4 methoxy-L-ribopyranotetrose, α (1-4)-3,4 methoxy-L-sorbopyranotetrose, α(1-4)-L-lyxotetrose, α(1-4)-L-xylotetrose, α(1-4)-L-arabinotetrose, α(1-4)-L-sorbotetrose.

Part E - is preferably diacetylfucose but also 4-acetoxy-3 methoxy-L-α-lyxose, 4-acetoxy-3-methoxyl-L-α-xylose, 4-acetoxy-3-methoxylL-α-arabinose, 4-acetoxy-3-methoxy-L-α-xylose, 4-acetoxy-3-methoxy-L-α-ribopyranose, 4-acetoxy-3-methoxy-L-α-sorbose-acetoxy.

7) All the derivatives obtained from the compounds indicated in the general formulas **I, II, III, IV , V and VI** . These derivatives could be made specialy by alkylation, benzoylation, or glycosidation of the hydroxyl groups, chain of sugar extension or contraction and other possible modifications.

8) All the synthetic analogues of compounds **I, II, III, IV, V and VI** .

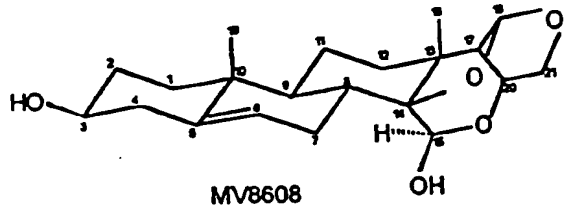

COMPOUND (Ia)

MV8608

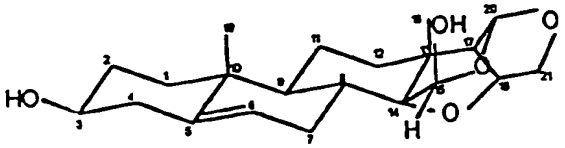

COMPOUND (Ib)

MV8608

Figure 1

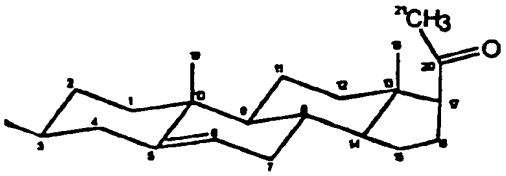

COMPOUND (II)

5-Pregnen-3beta-ol-20-one

Figure 2

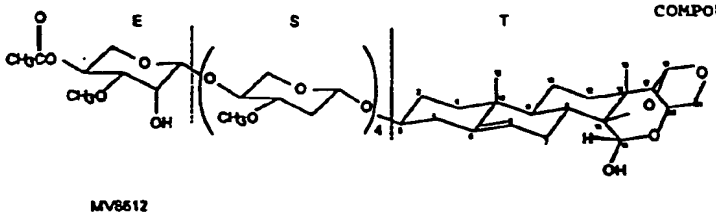

COMPOUND (III)

MV8612

Figure 3

FIGURE 4

EFFECT OF MV8608 ON FAST-Na IN 10 DAY EMBRYONIC CHICK HEART

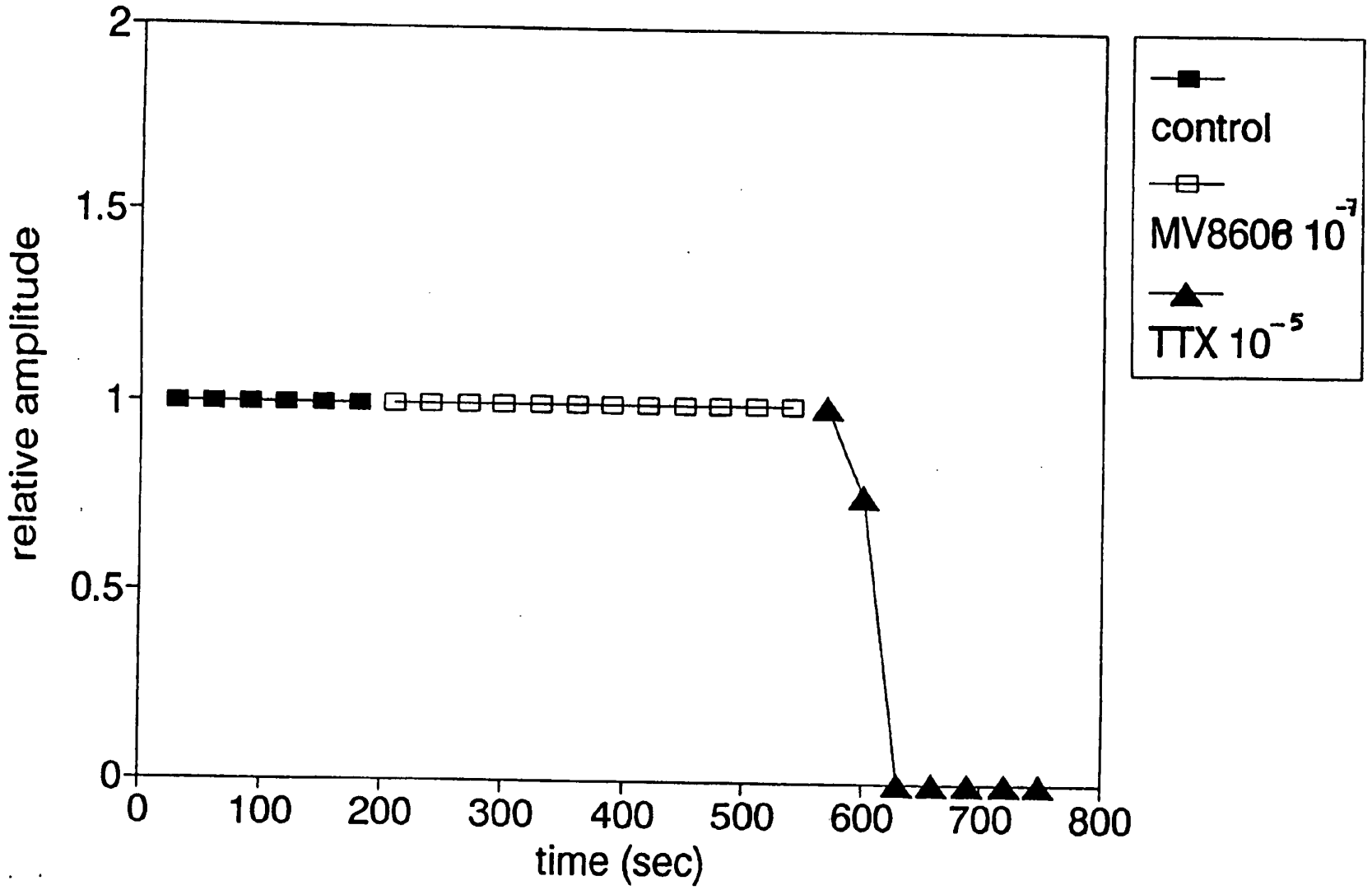

FIGURE 5

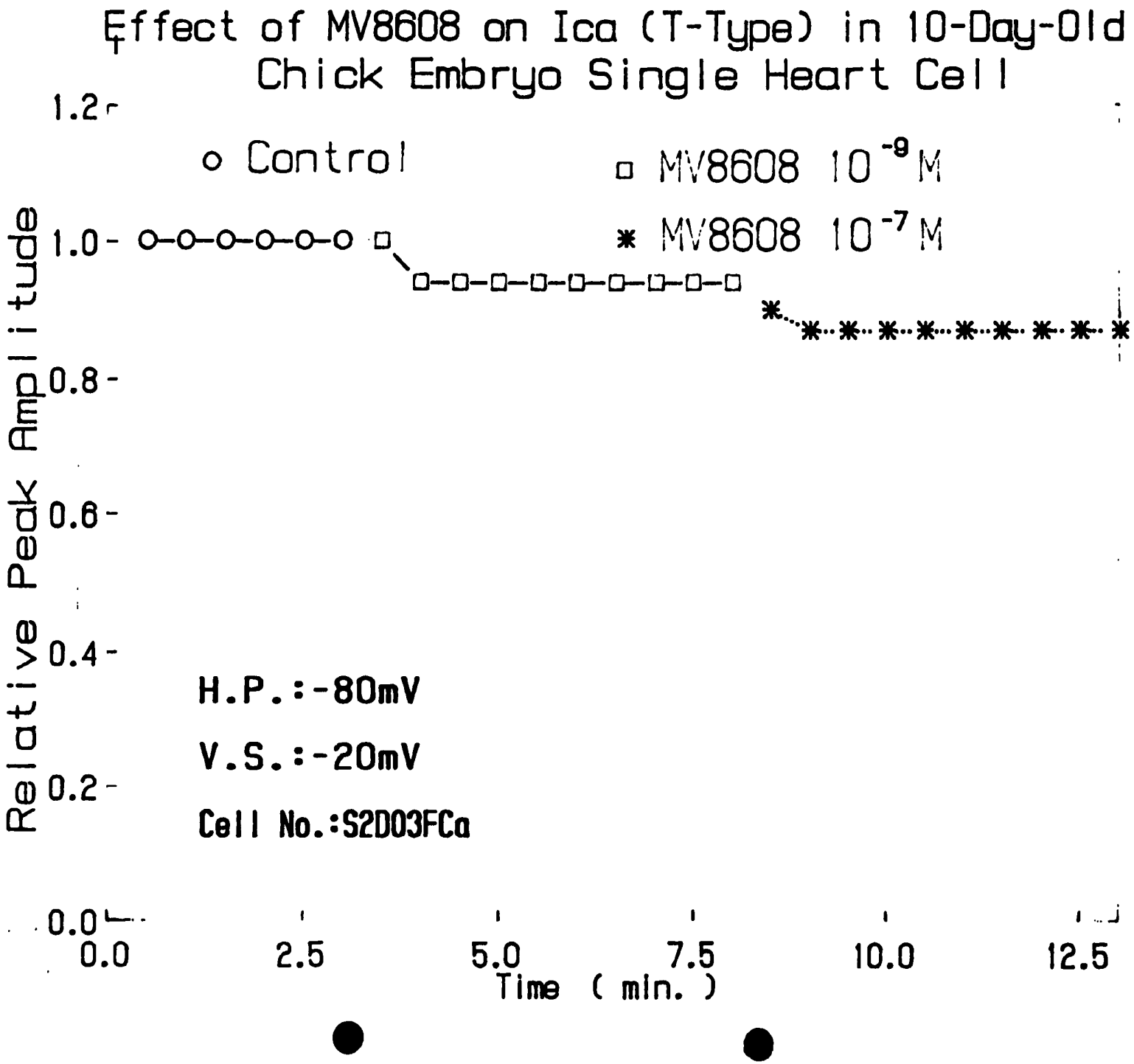

FIGURE 6

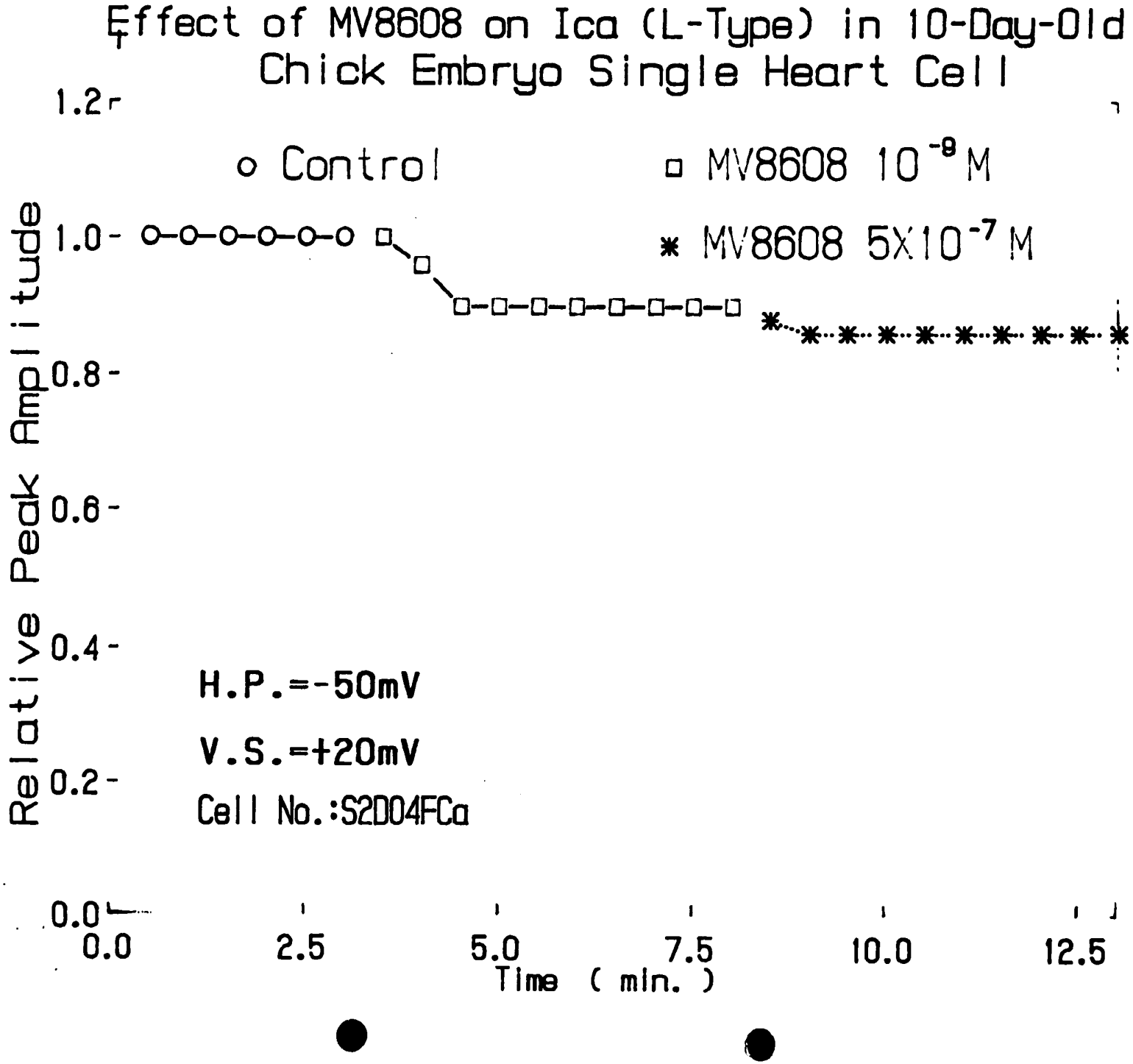

FIGURE 7

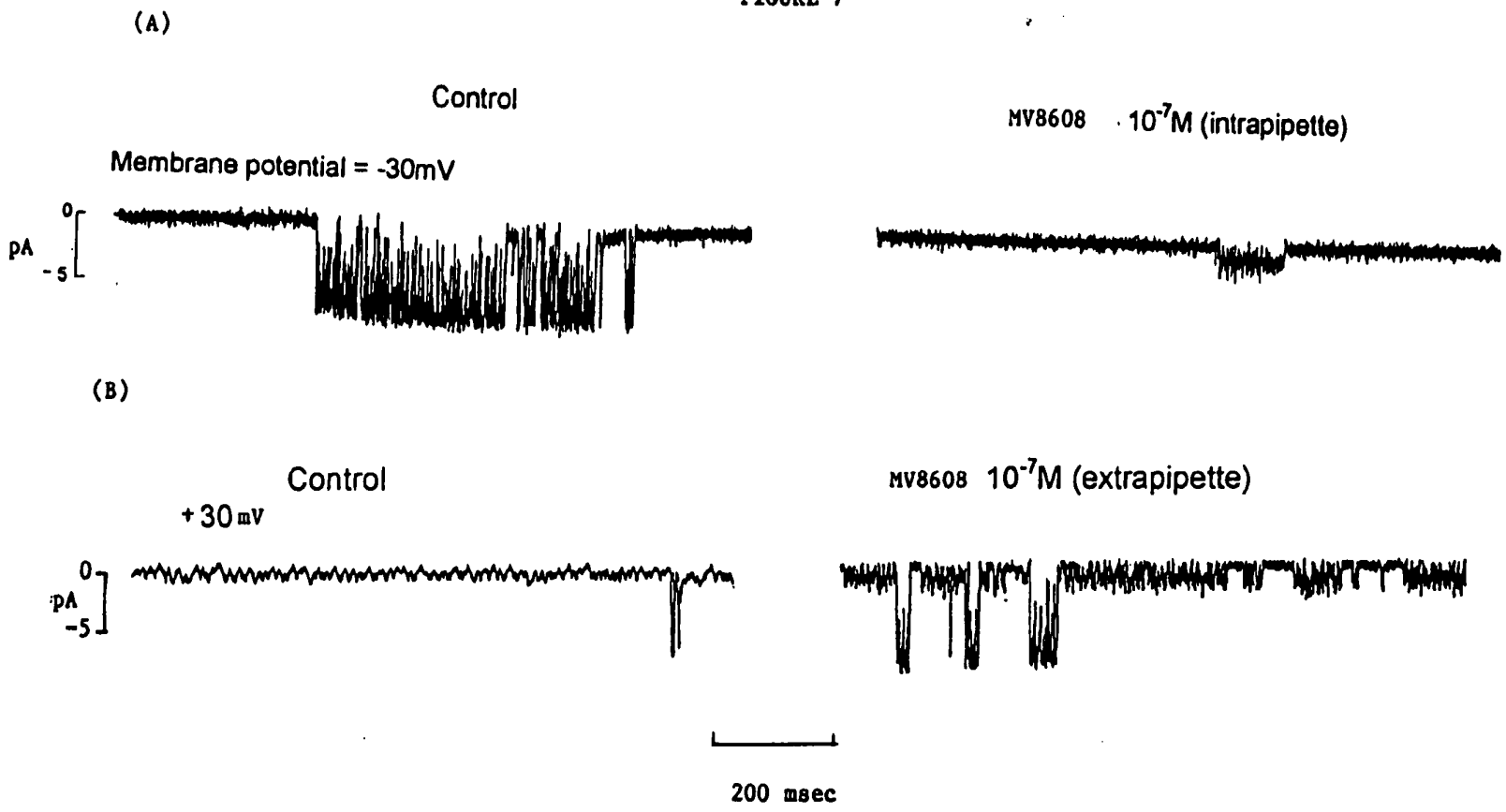

FIGURE 8 CHICK HEART

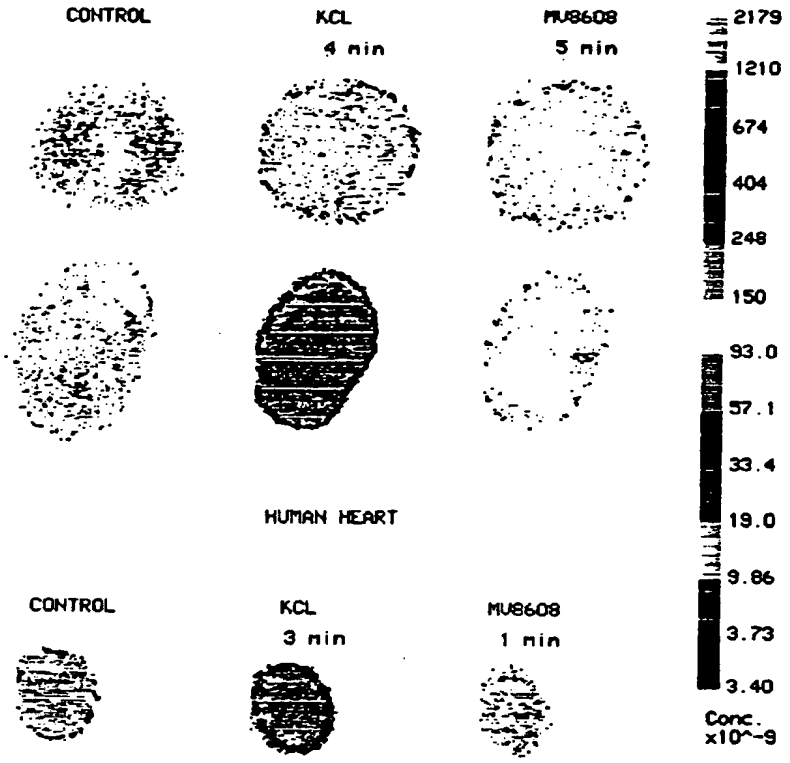

CA 02217088 1997-09-30

FIGURE 9 CHICK HEART

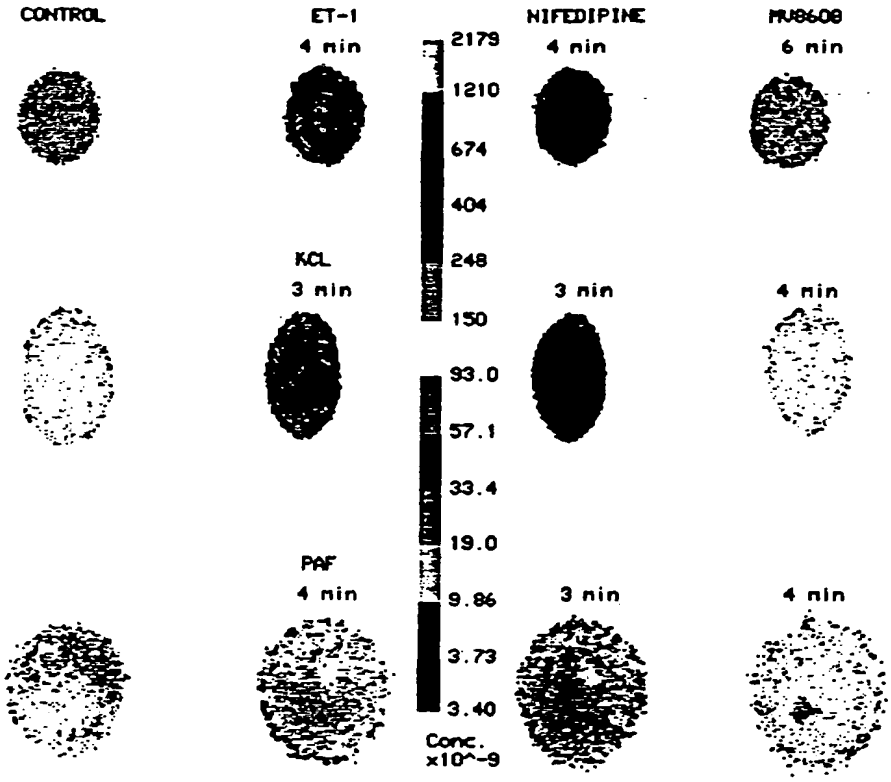

FIGURE 10 HUMAIN HEART

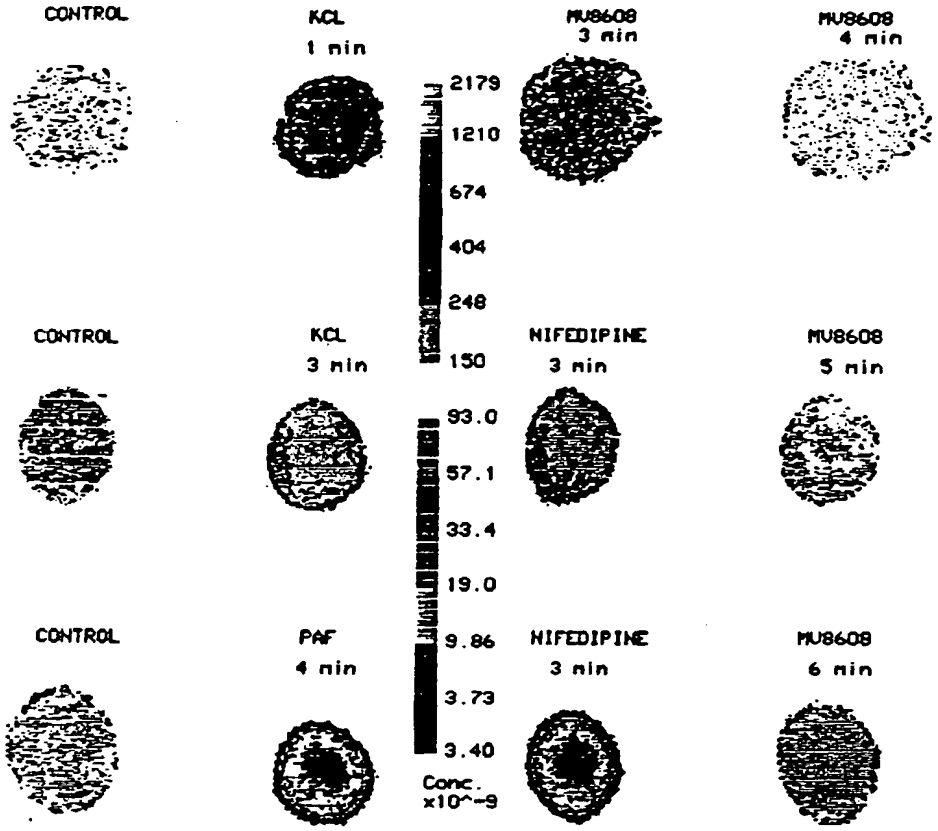

Blockade by MV8608 (MV08) of PAF- and sustained depolarization- induced sustained increase in $[Ca^{2+}]_i$ via activation of the R-type Ca^{2+} channel in human heart cells

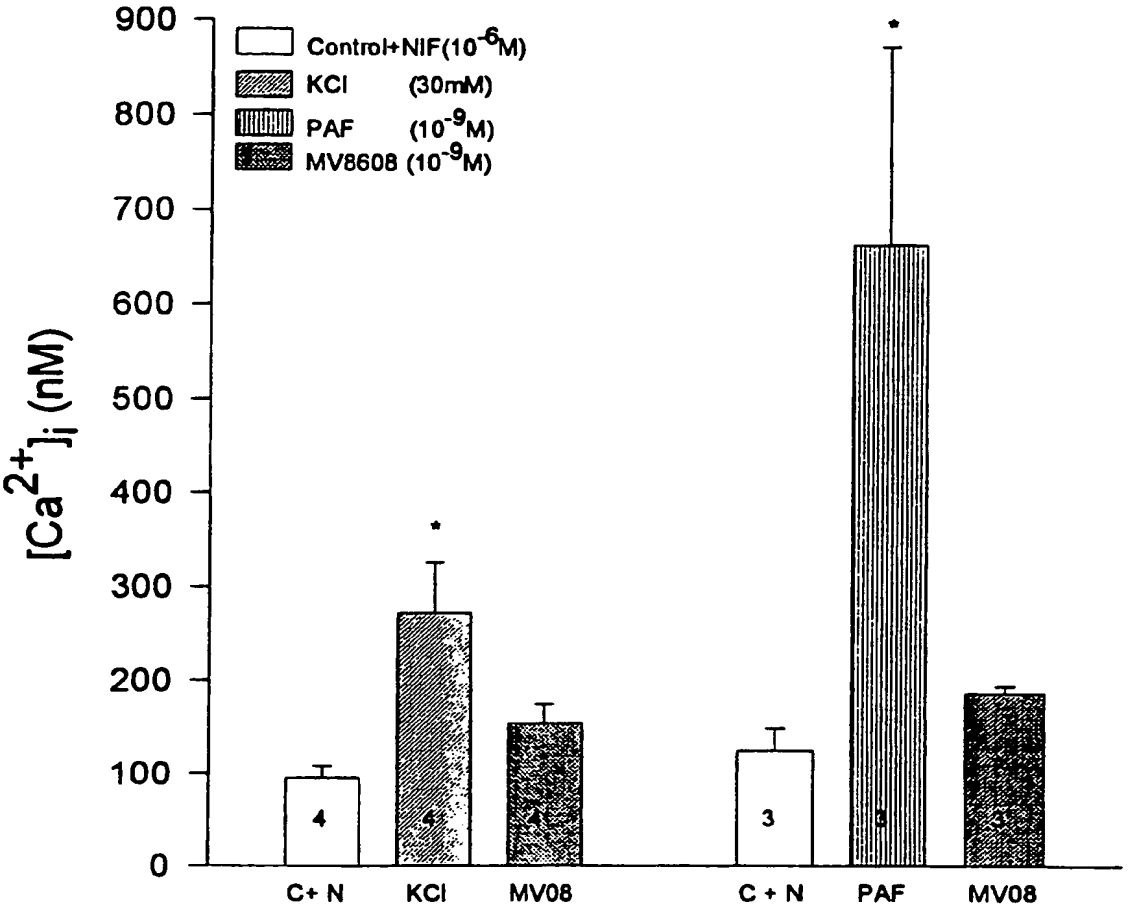

X

Blockade by MV8608 (MV08) of agonist- and sustained depolarization-induced sustained increase in $[Ca^{2+}]_i$ via activation of the R-type Ca^{2+} channel in chick embryonic heart cells

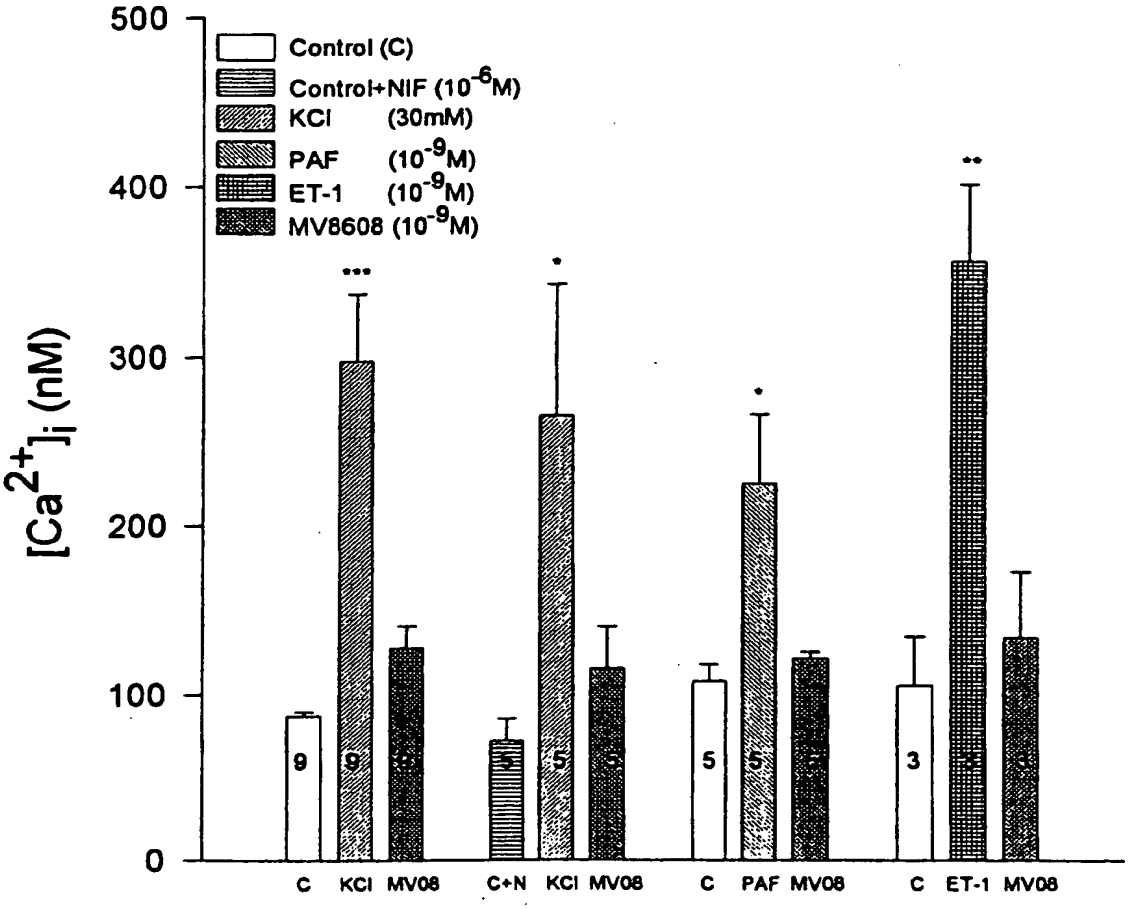

FIGURE 13

CA 02217088 1997-09-30

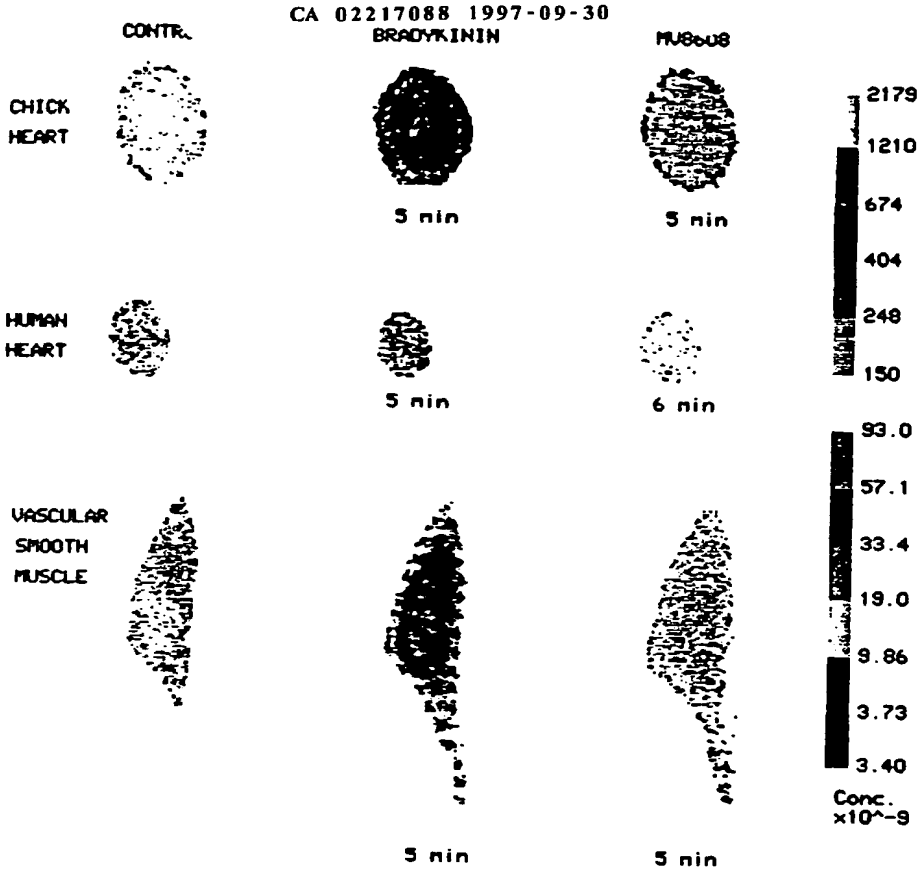

Blockade by MV8608 (MV08) of bradykinin (BK)- and PAF-induced sustained increase in $[Ca^{2+}]_i$ via activation of the R-type Ca^{2+} channel in rabbit aortic vascular smooth muscle cells

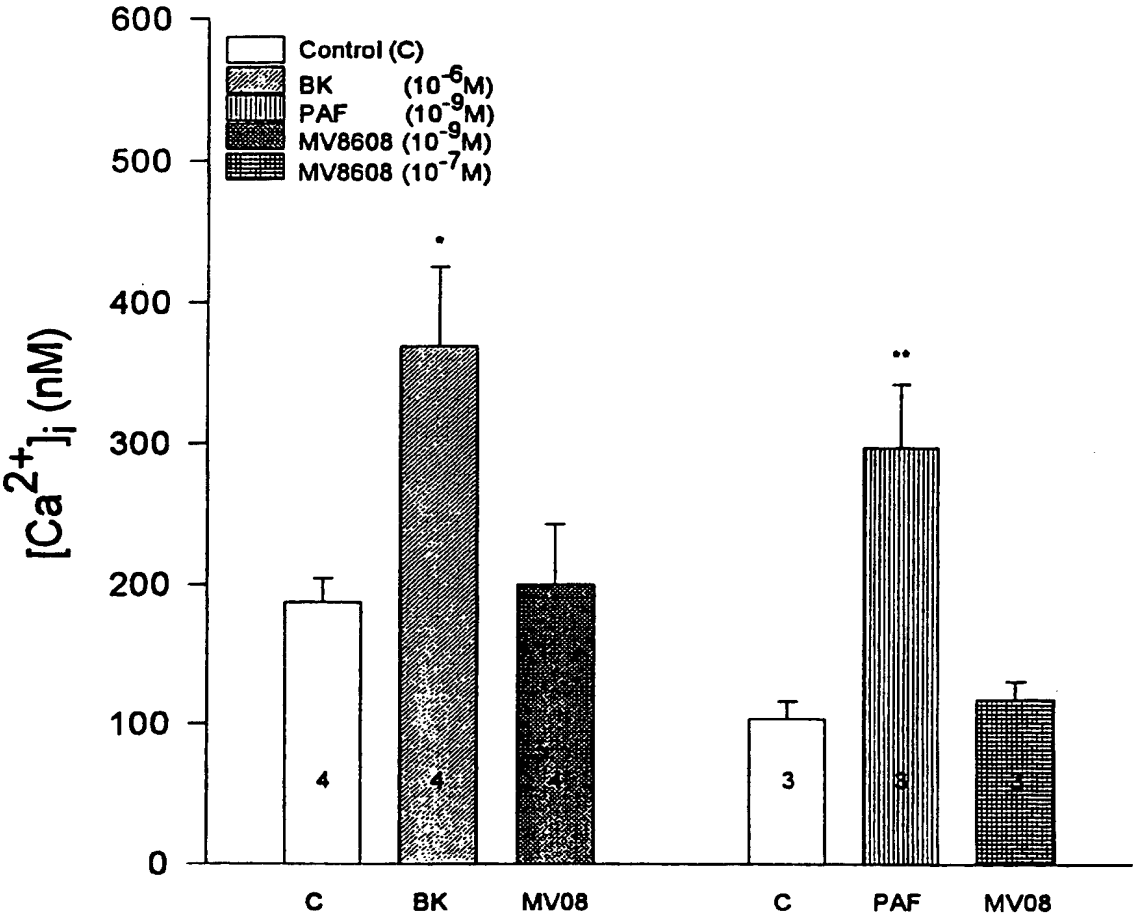

CA 02217088 1997-09-30

FIGU 15 HUMAN ENDOTHELIAL CELLS

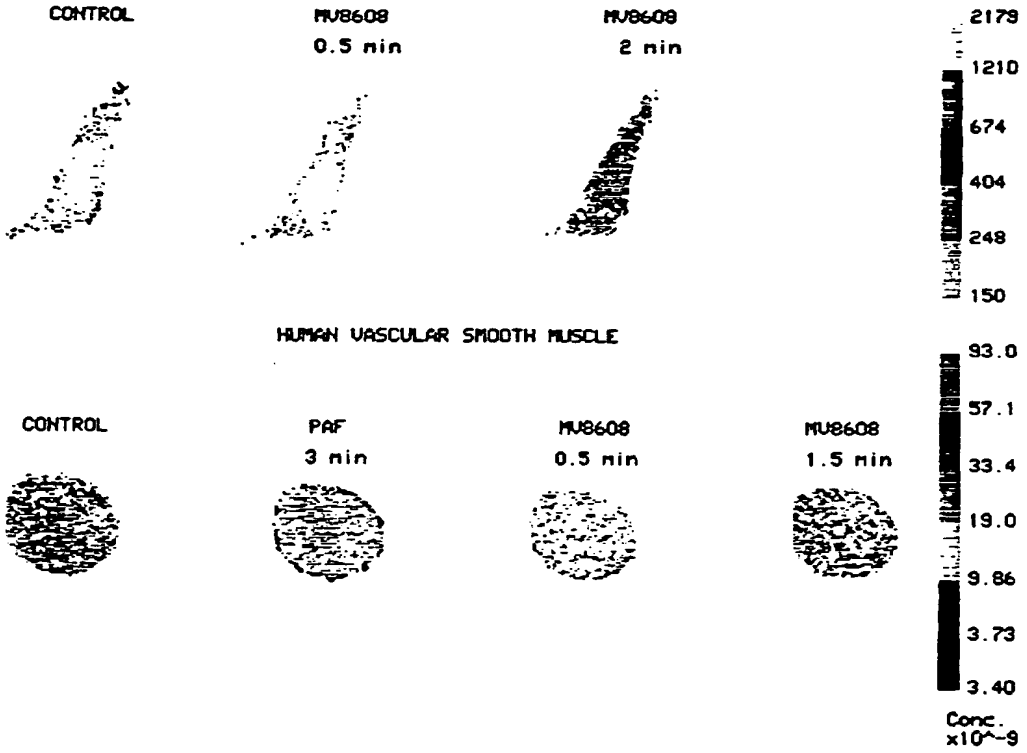

MV8608 (MV08) blocked PAF-induced sustained increase in $[Ca^{2+}]_i$ via activation of the R-type Ca^{2+} channel in human aortic vascular smooth muscle cells

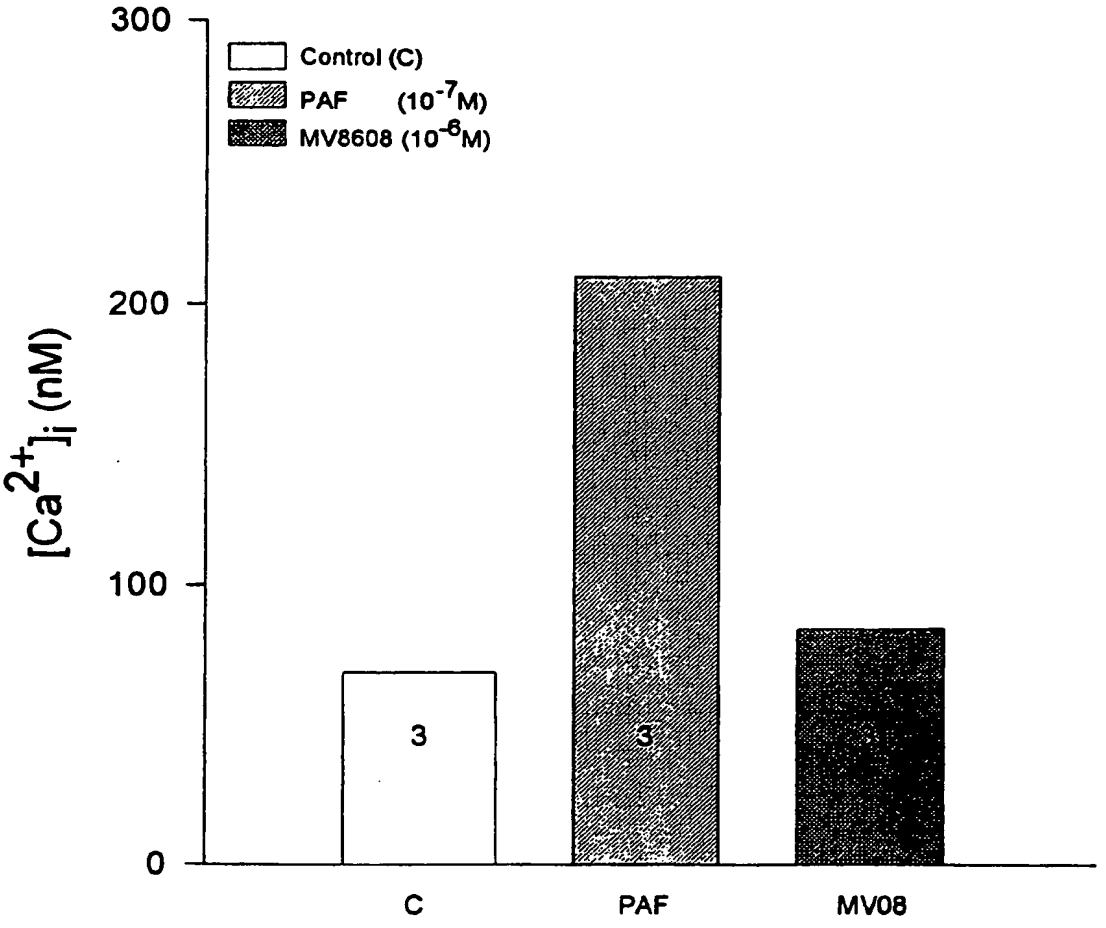

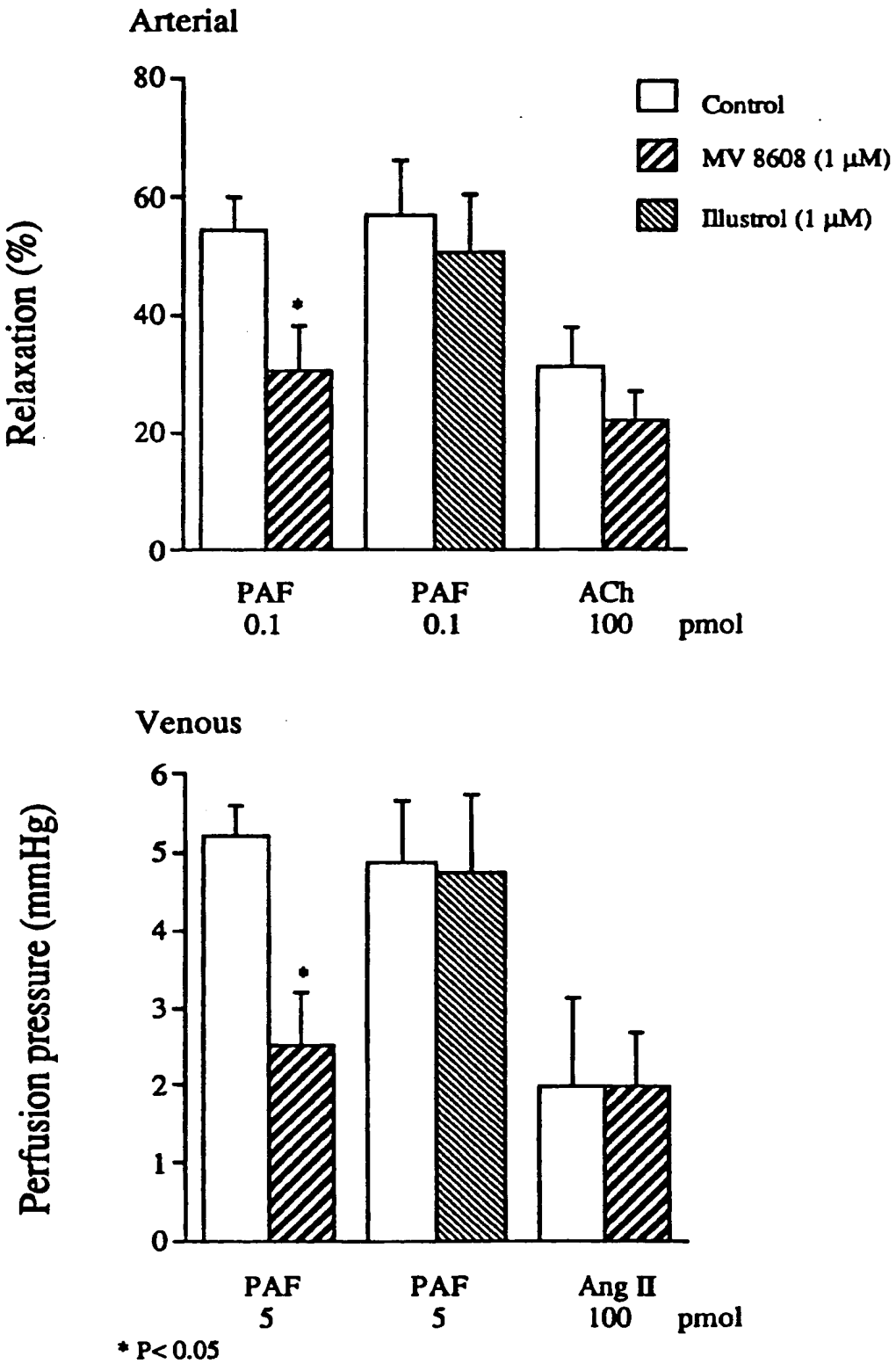
Arterial
Relaxation (%)
80
60
40
20
0
Control
MV 8608 (1 µM)
Illustrol (1 µM)
*
PAF 0.1
PAF 0.1
ACh 100
pmol
Venous
Perfusion pressure (mmHg)
6
5
4
3
2
1
0
*
PAF 5
PAF 5
Ang II 100
pmol
* P< 0.05

FIGURE 18

THE EFFECT OF 10^{-8} M MV8612 ON 15 DAY OLD EMBRYONIC CHICK HEART I_{NA}

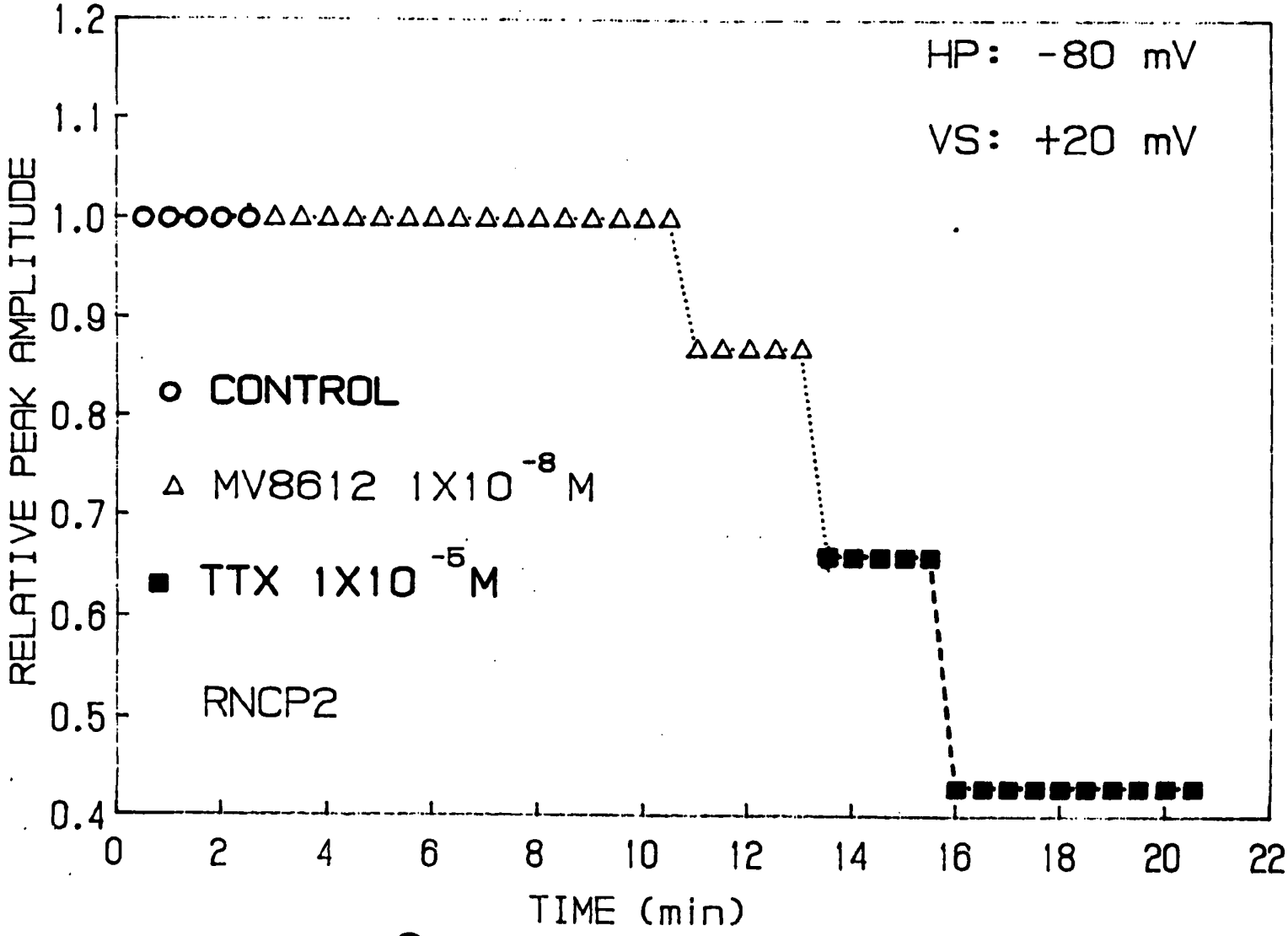

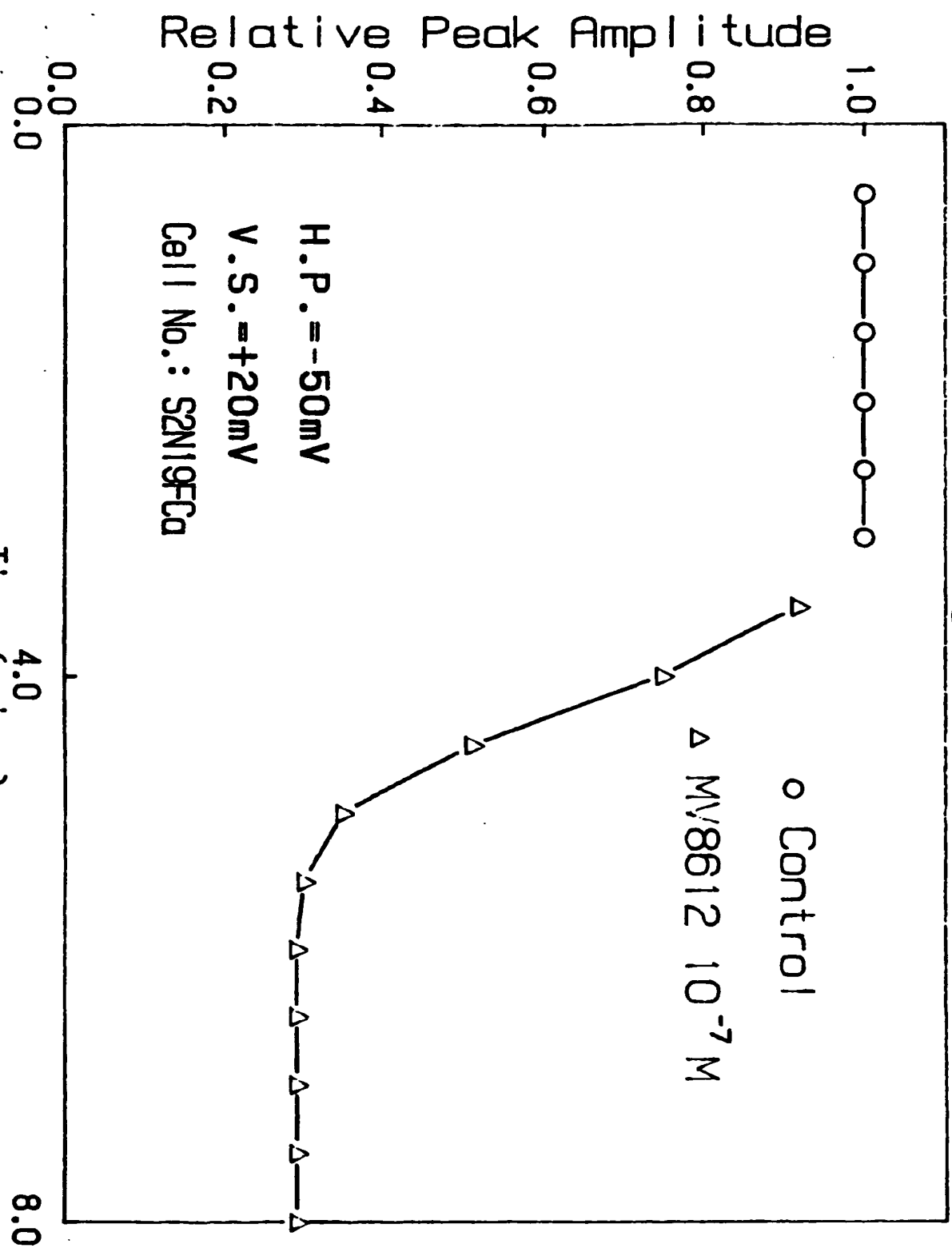
Effect of MV8612 on Ica (L-Type) in
Human Single Heart Cell
Relative Peak Amplitude
0.0
0.2
0.4
0.6
0.8
1.0
0.0
4.0
8.0
Time (min.)
o Control
Δ MV8612 10⁻⁷M
H.P.=-50mV
V.S.=+20mV
Cell No.: S2N19FCa

FIGURE 19

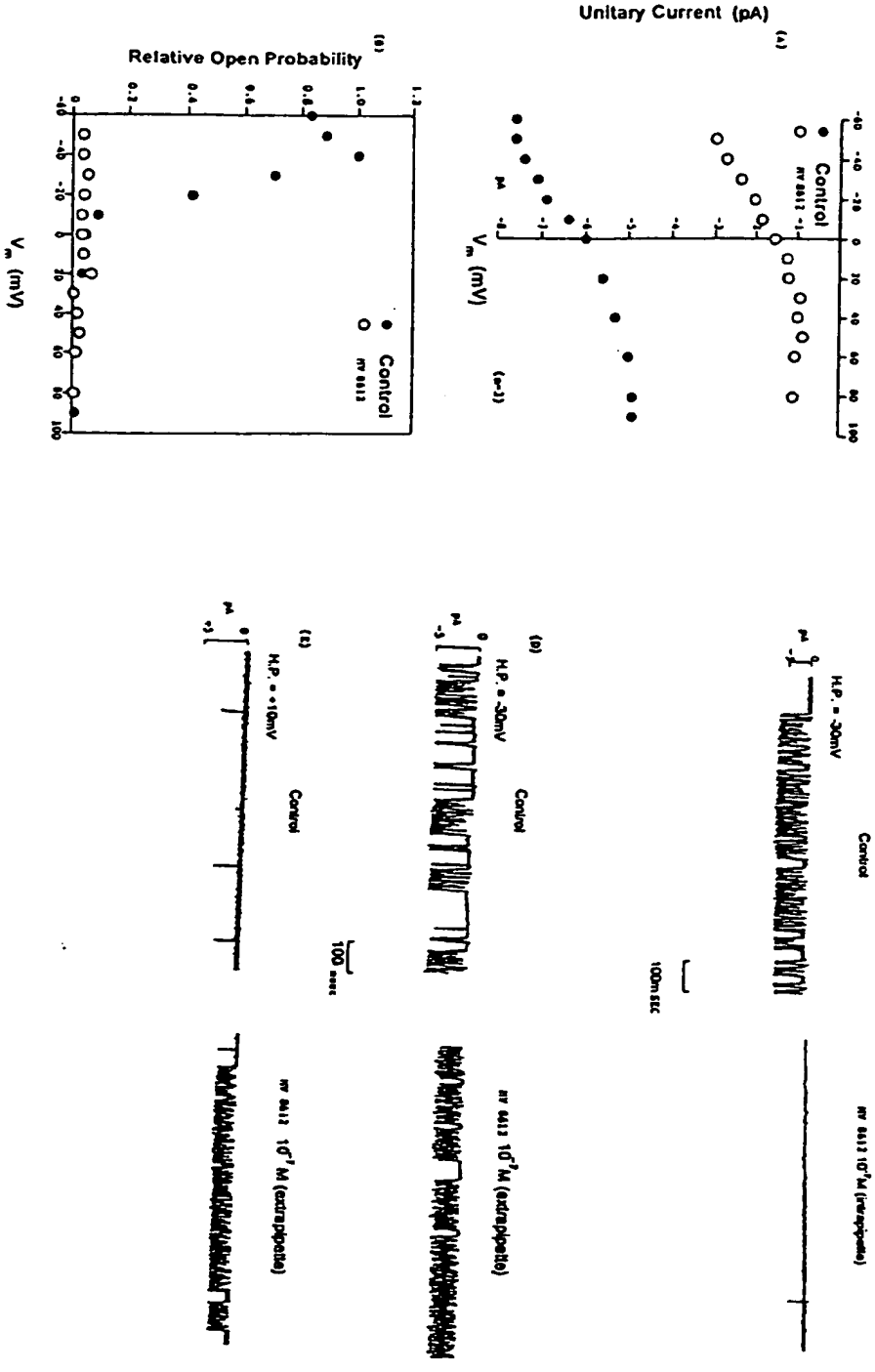
Relative Open Probability
(b)
Control
Unitary Current (pA)
(a)
Control
(c)
H.P. = -30mV
Control
100msec
(d)
H.P. = -30mV
Control
(e)
H.P. = -10mV
Control
100 msec

FIGURE 20

Blockade by MV8608 and MV8612 of human aortic VSMC proliferation

(AOSMC-9, passage #1)

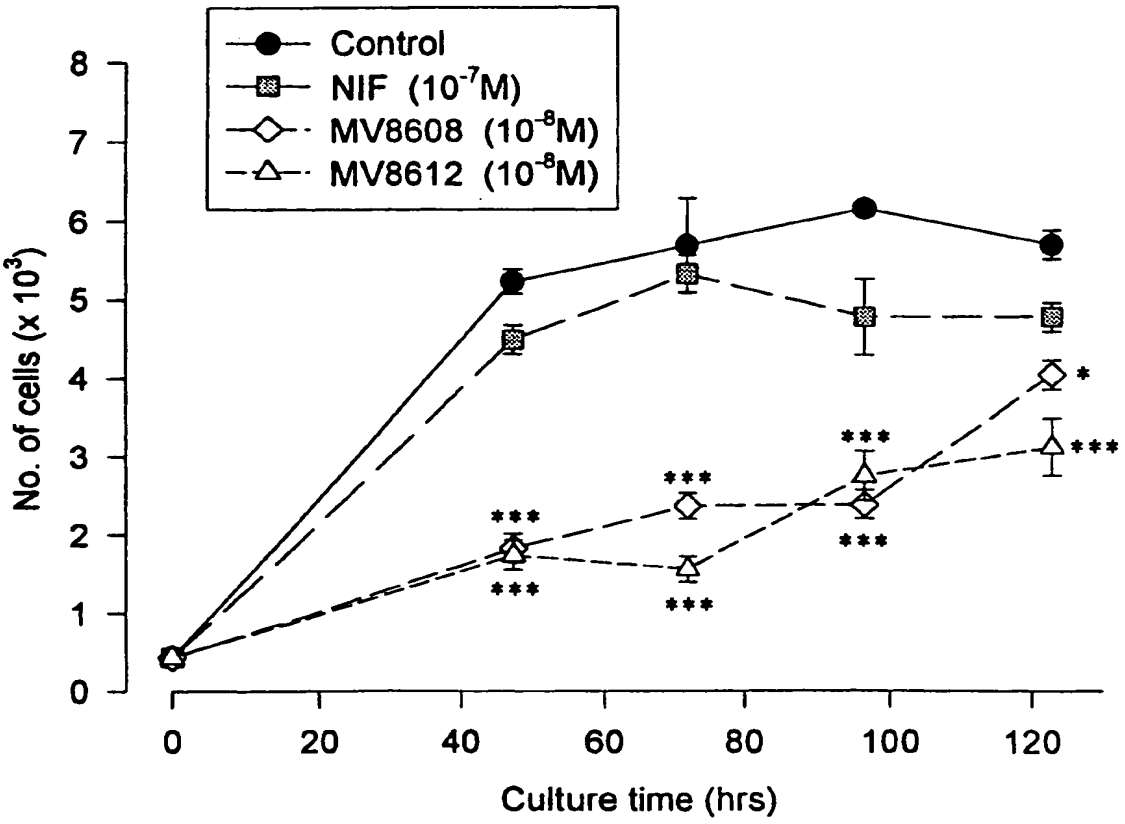

* $p < 0.05$ *** $p < 0.001$

Blockade by MV8608 (08) and MV8612 (12) of agonist- and sustained depolarization-induced sustained increase of $[Ca]_c$ and $[Ca]_n$ via activation of the R-type Ca^{2+} channel in heart and VSM cells

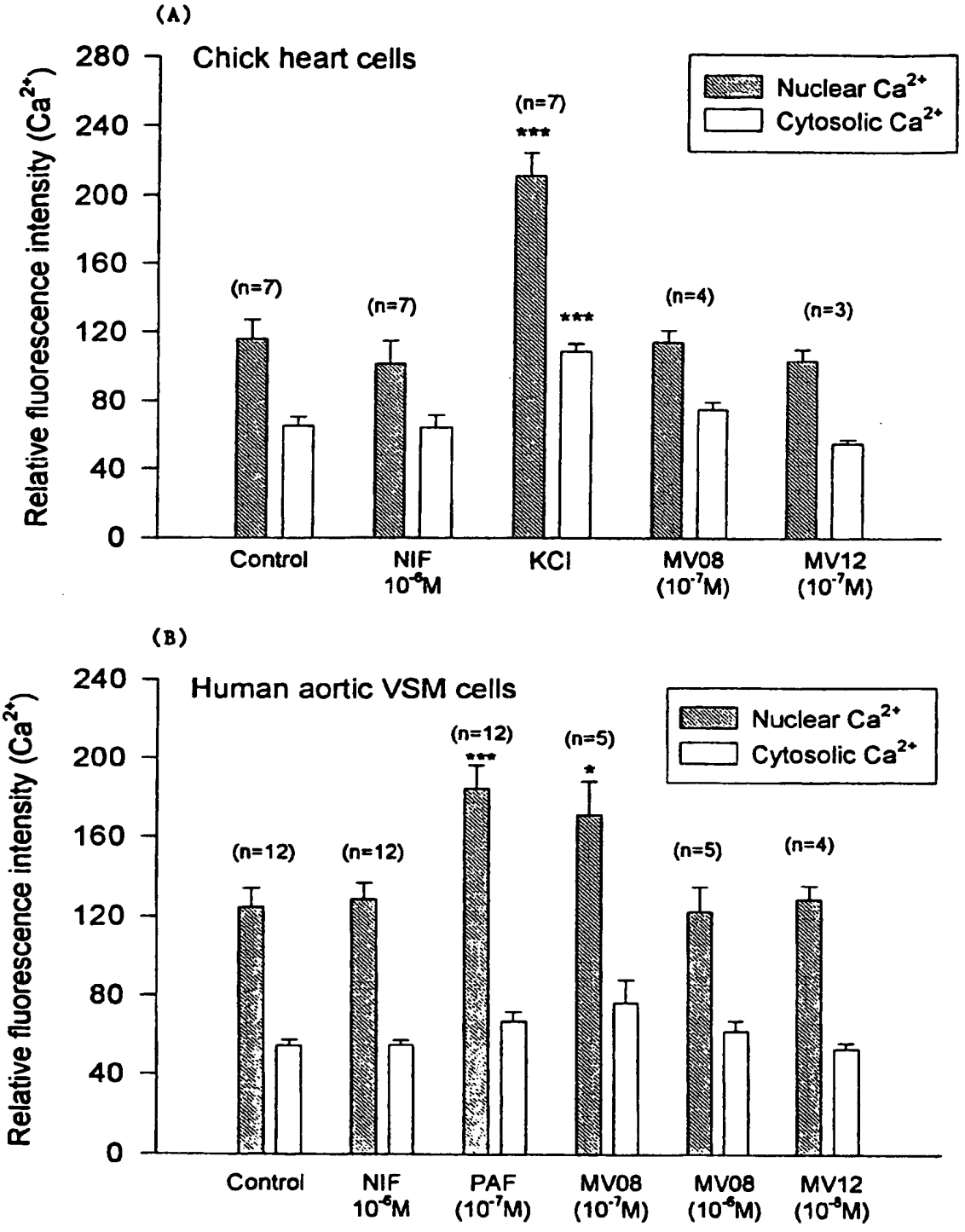

Effect of MV08 and MV12 on agonist- and sustained depolarization-induced sustained increase of $[Ca]_n$ and $[Ca]_c$ via activation of the R-type Ca^{2+} channels in heart and aortic VSM cells

Chick heart cells

Human aortic VSM cells

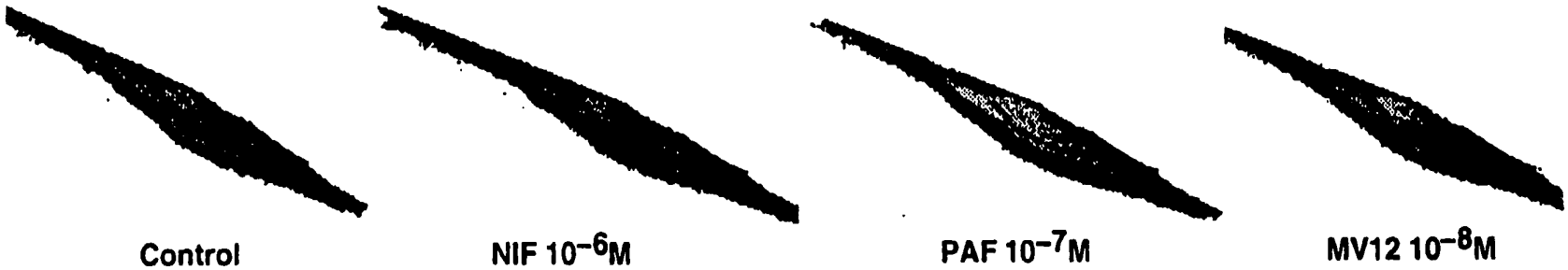

Preventive effect of MV8608 (MV08) and MV8612 (MV12) on agonist- and sustained depolarization-induced sustained increase in nuclear and cytosolic Ca^{2+} fluorescence via activation of the R-type Ca^{2+} channels in chick heart and human VSM cells

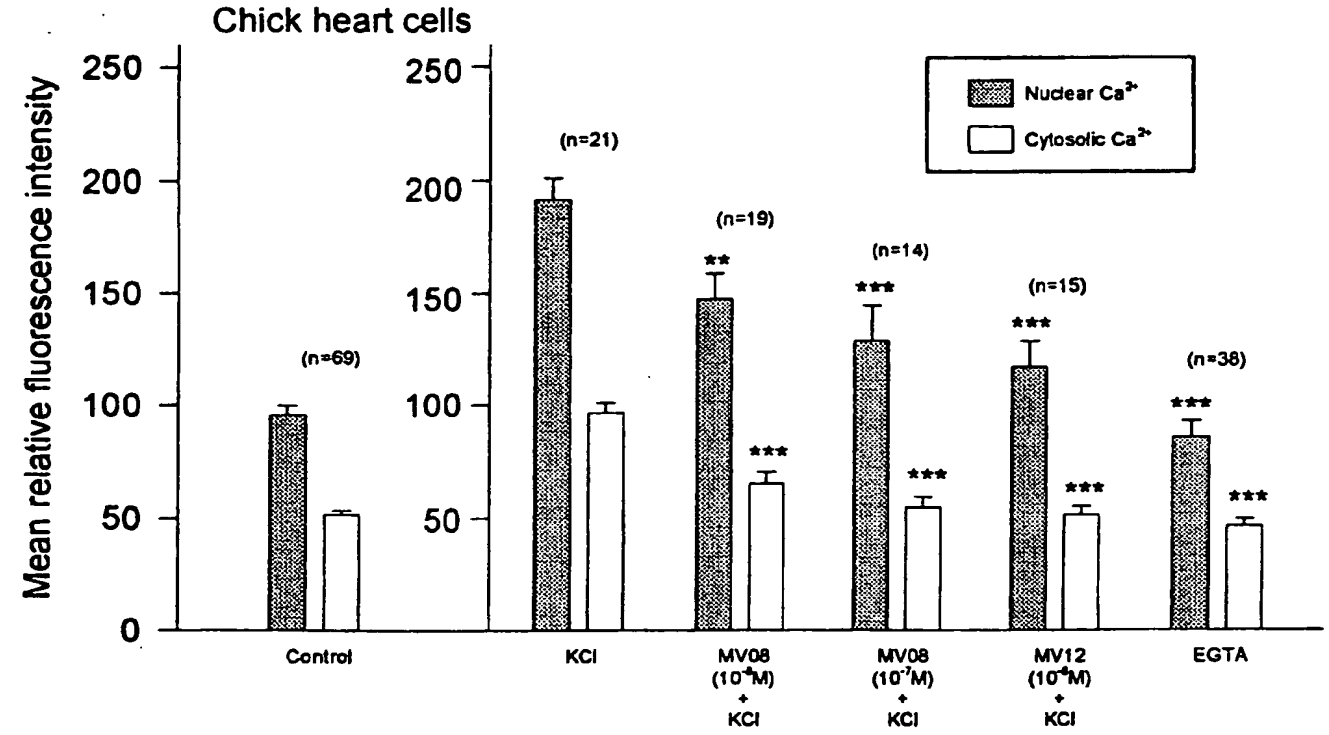

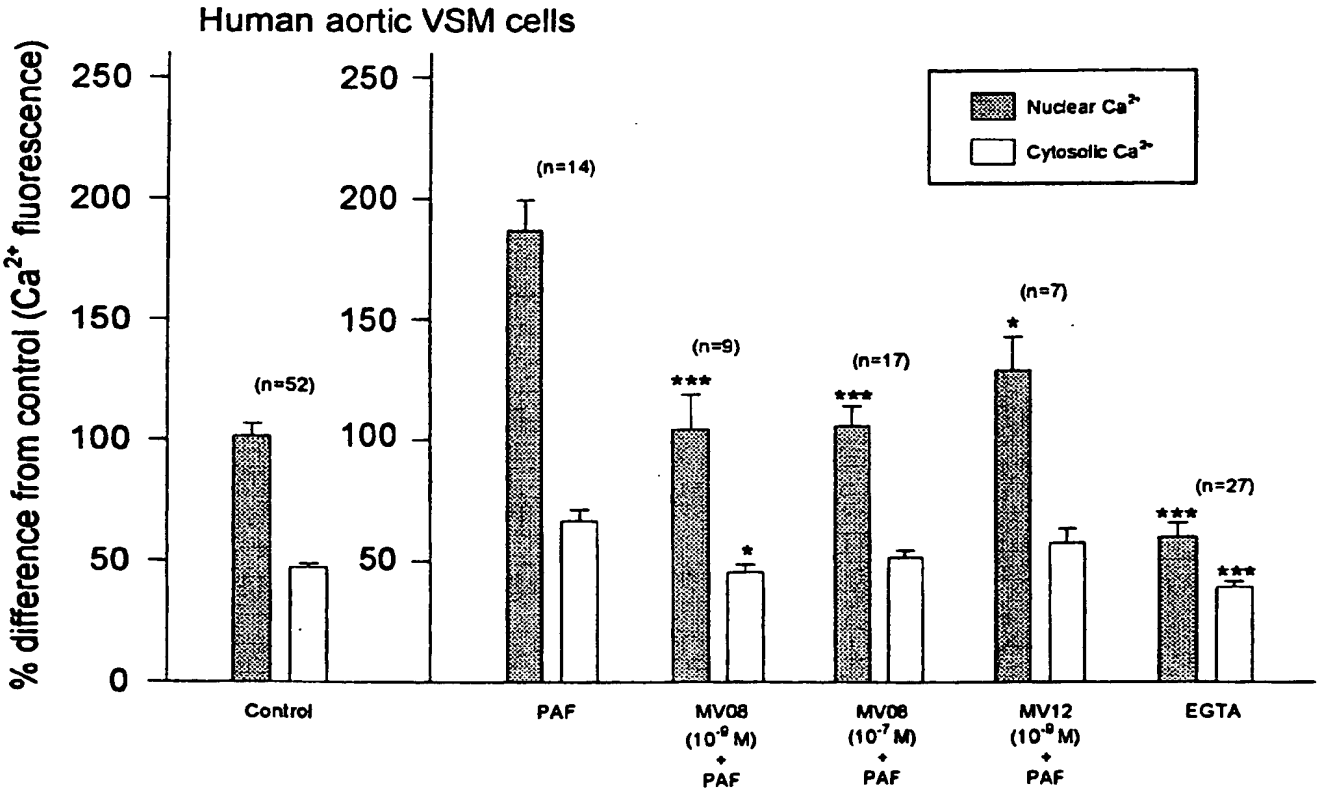

* $p< 0.05$ ** $p<0.01$ *** $p<0.001$

MV8612 (MV12) prevented PAF and sustained depolarization from inducing a sustained increase in $[Ca^{2+}]_i$ via activation of the R-type Ca^{2+} channel in human aortic vascular smooth muscle cells

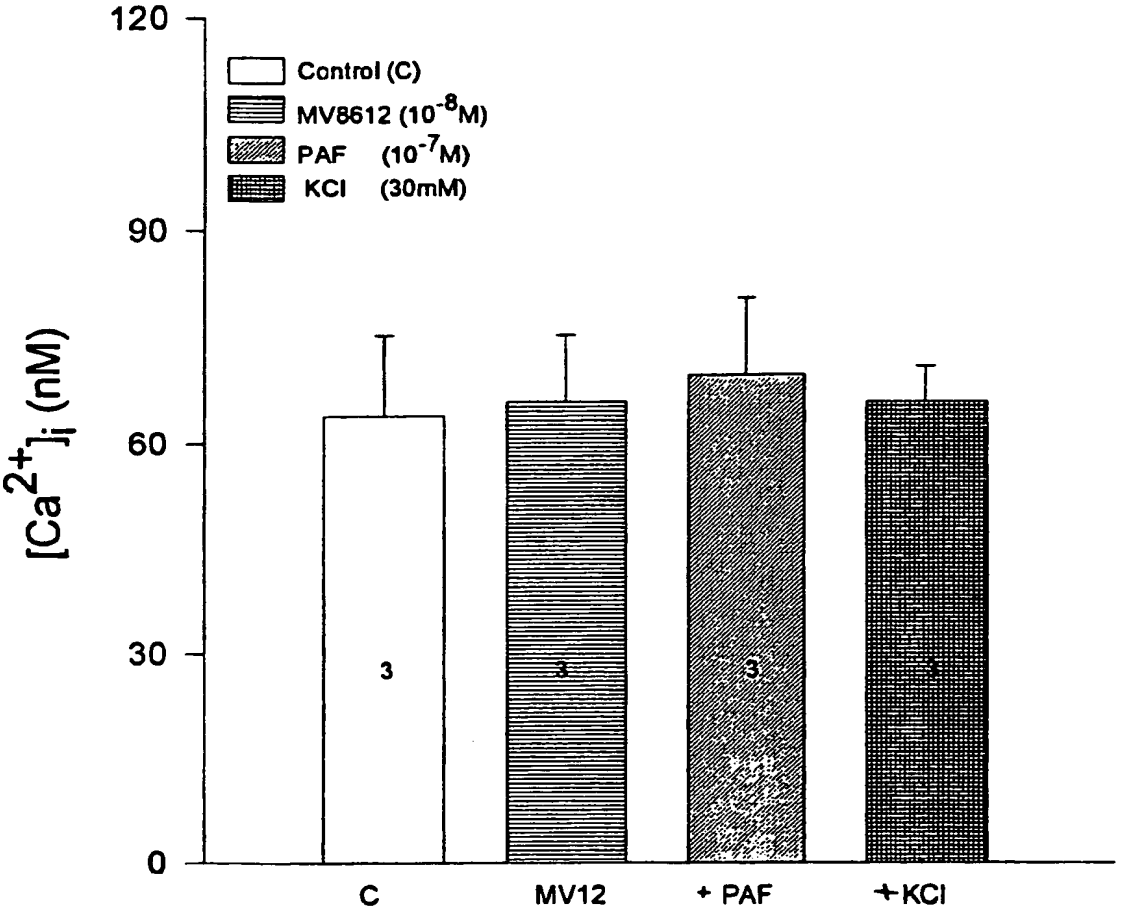

Blockade by MV8612 (MV12) of ET-1 and sustained depolarization-induced sustained increase in $[Ca^{2+}]_i$ via activation of the R-type Ca^{2+} channel in rabbit aortic vascular smooth muscle cells

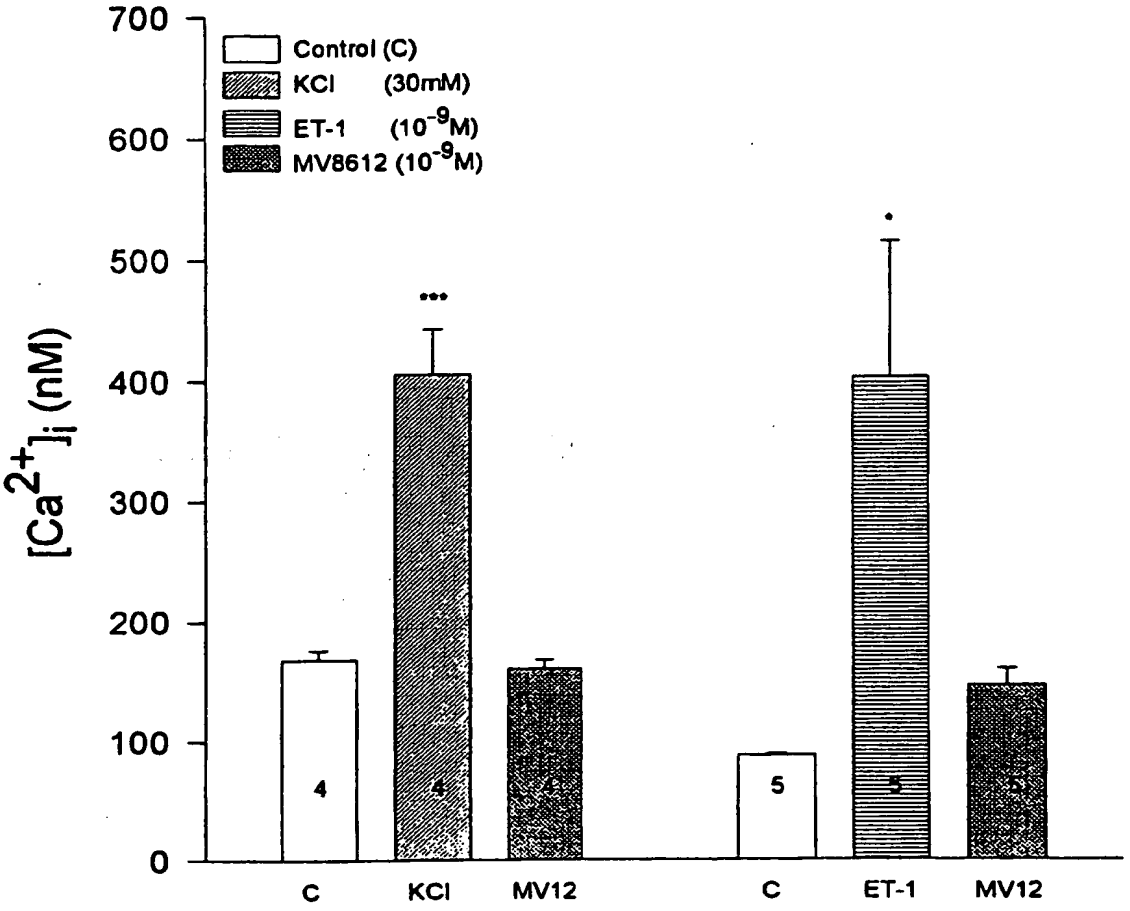

Blockade by MV8612 (MV12) of agonist- and sustained depolarization-induced sustained increase in $[Ca^{2+}]_i$ via activation of the R-type Ca^{2+} channel in chick embryonic heart cells

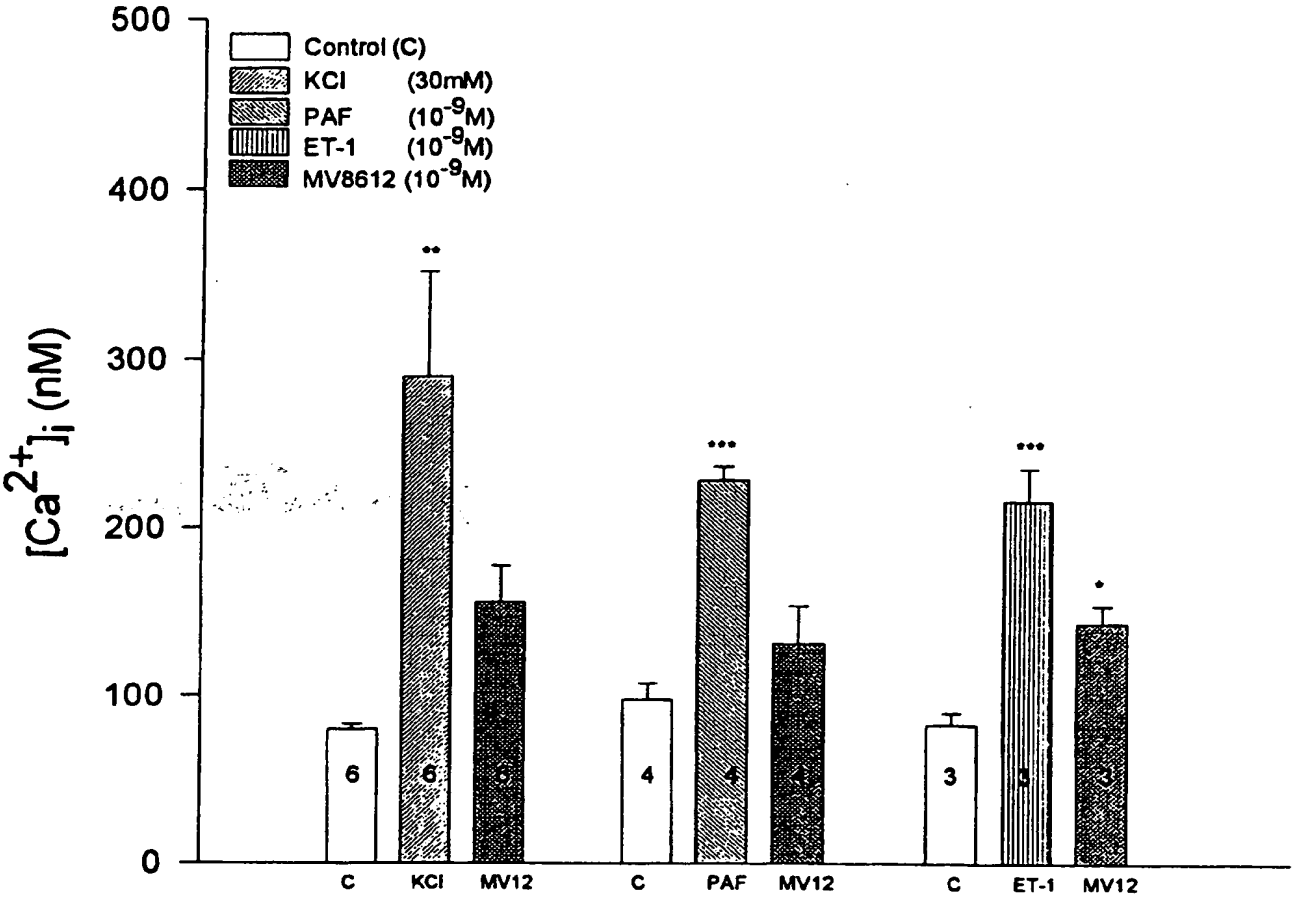

Intrinsic activity of Nifedipine and Isradipine in the anaesthetized guinea pig

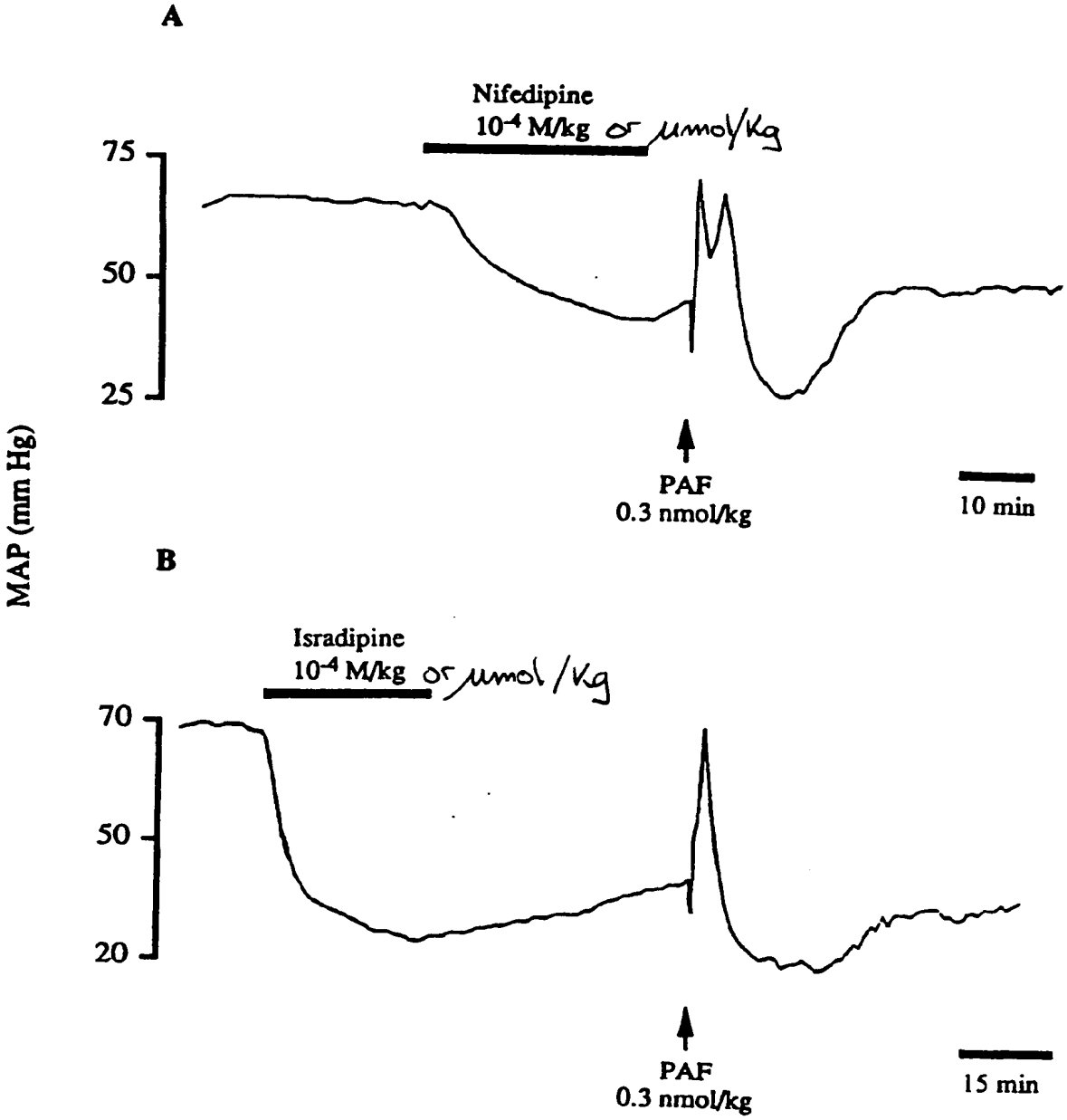

Effect of V8612 on hypotensive and ronchoconstrictive (PIP) effects of PAF in the anaesthetized guinea pig

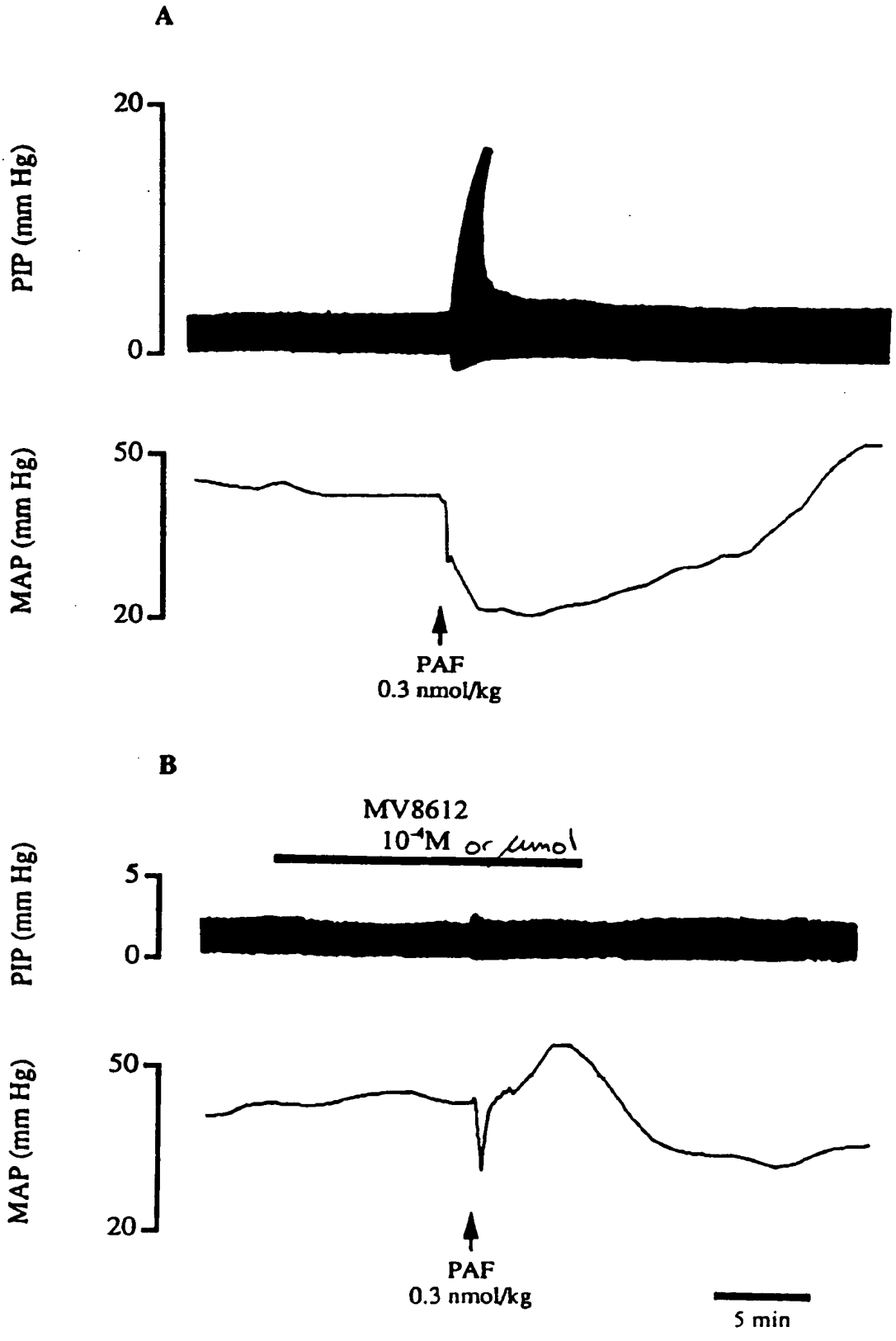

FIGURE 1A

CONFIDENTIAL

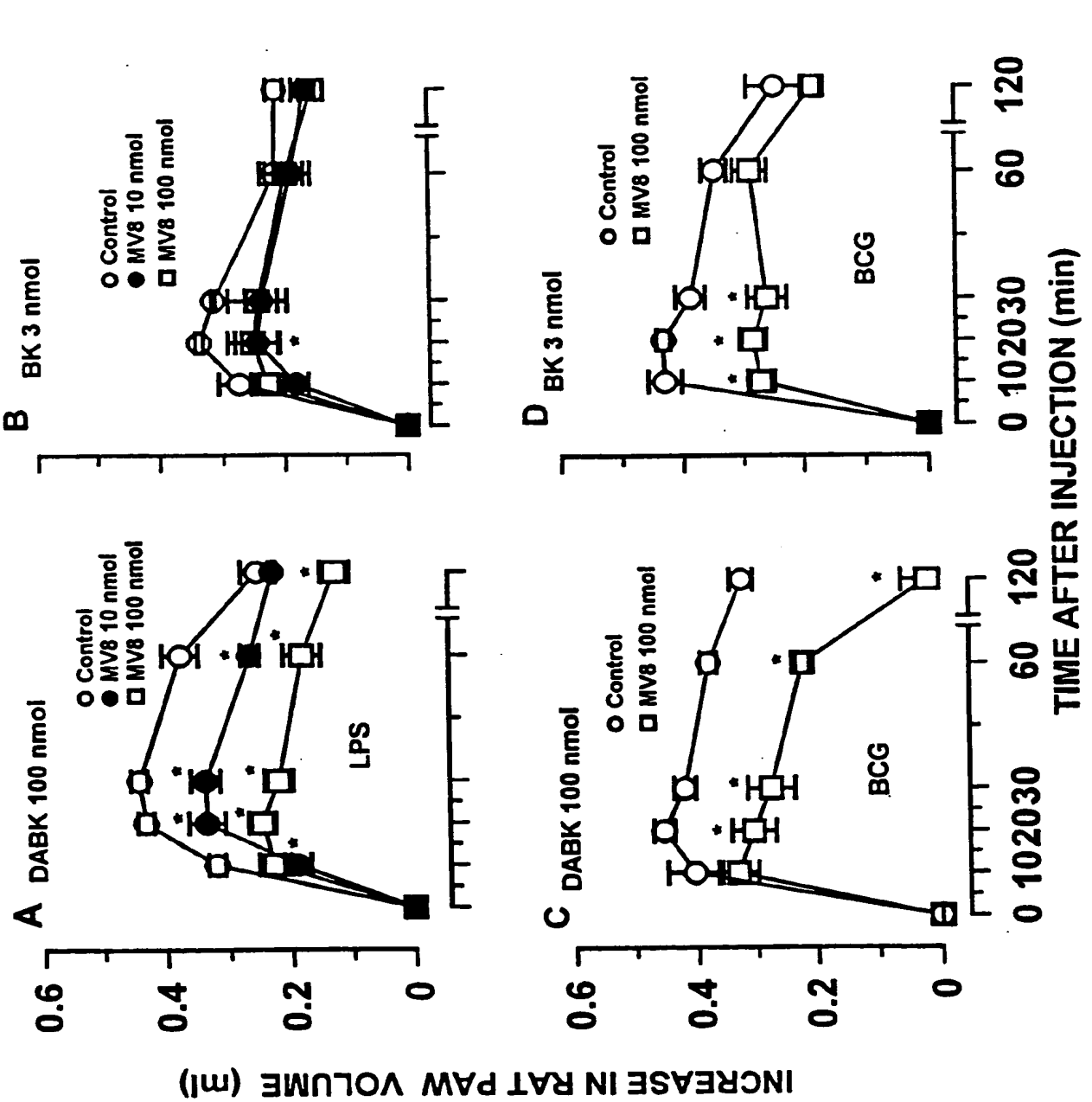

:ECTS OF MV8608 ON RAT PAW OEDEMA INDUCED BY SEVERAL FLOGISTIC AGENTS

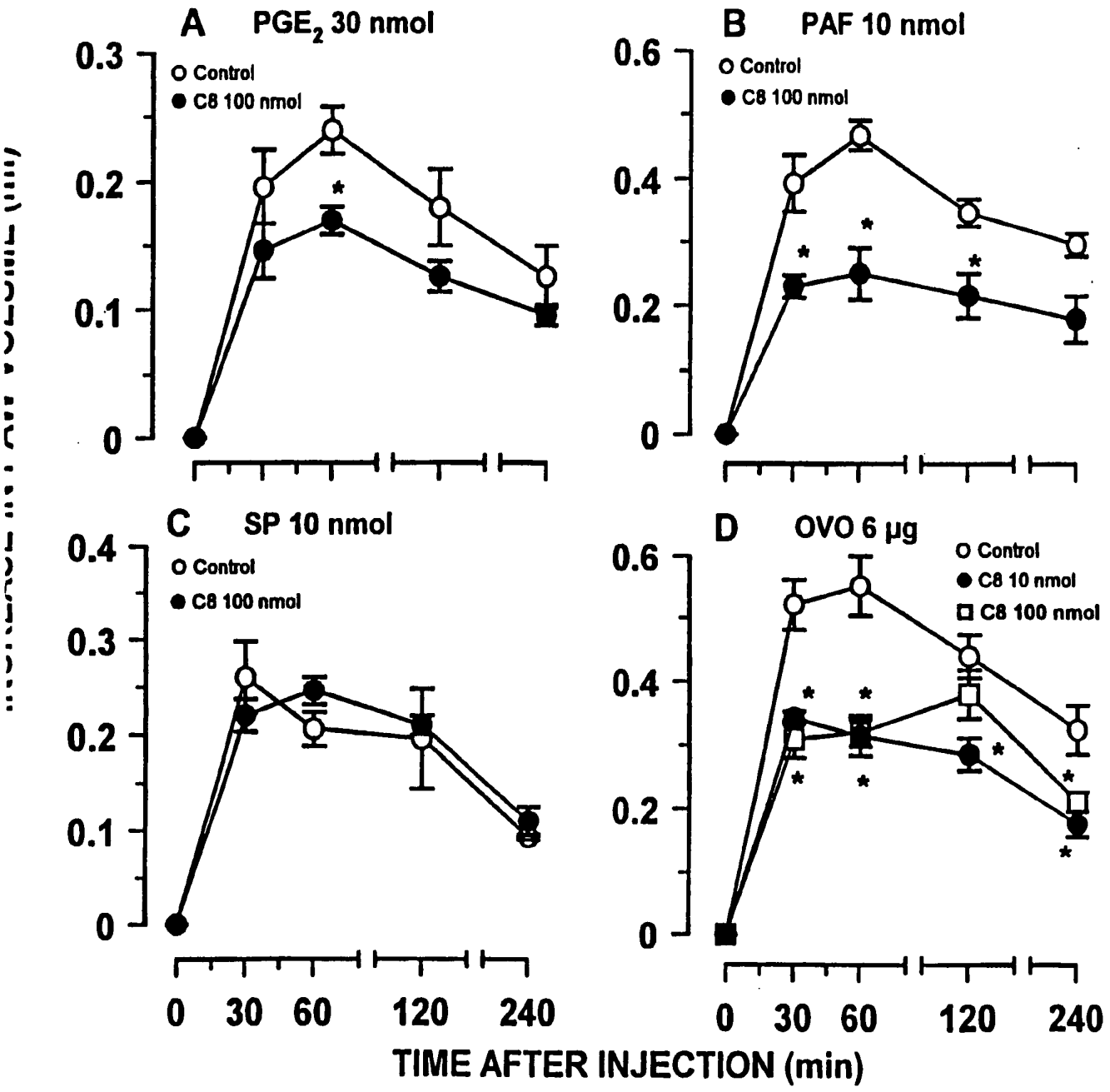

Figure 2

FIGURE 2

FIGURE 3A

CONFIDENTIAL

EFFECTS OF MV8608 ON KININ INDUCED- RAT PAW OEDEMA.

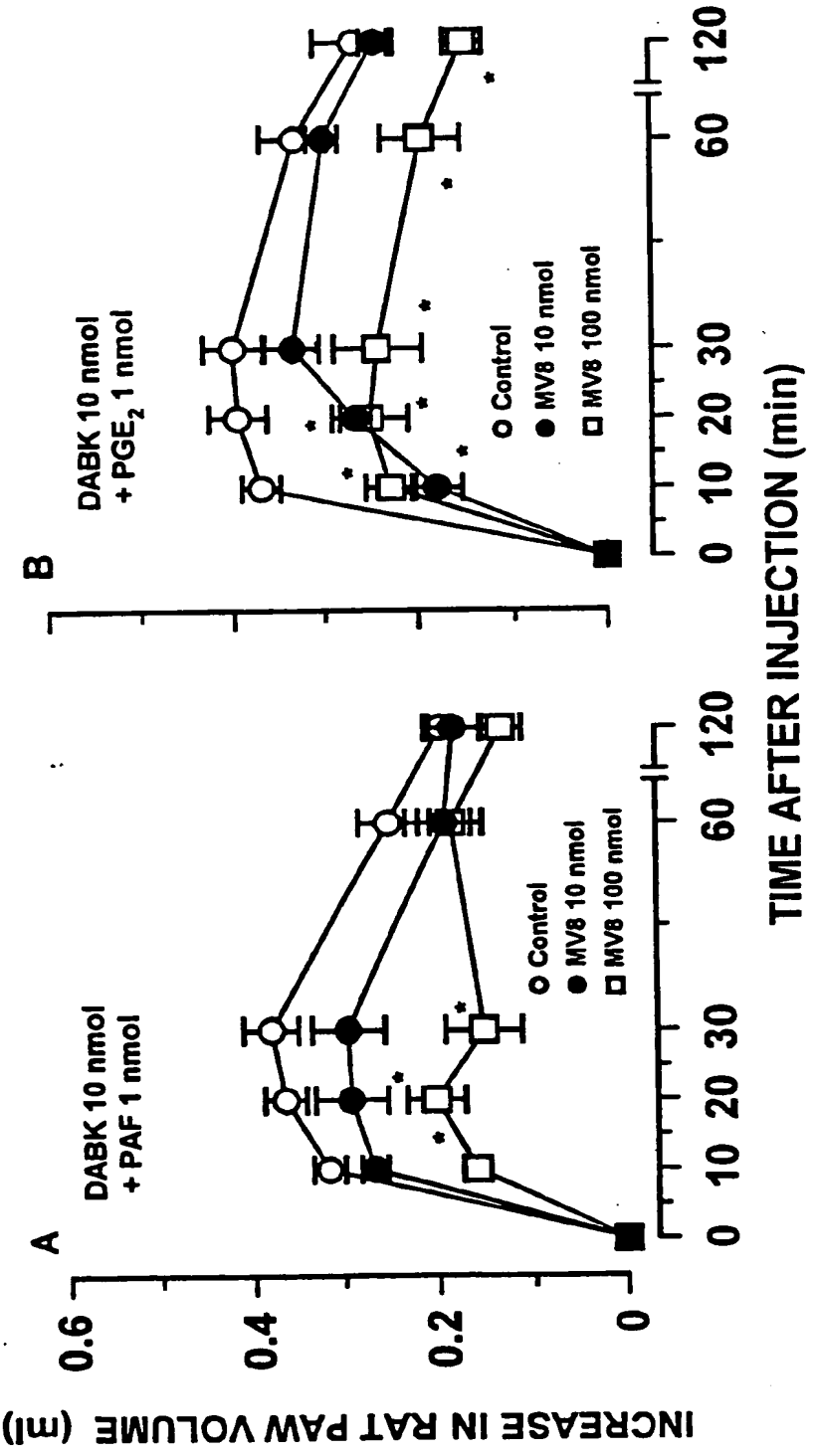

e 3

FECTS OF MV 8608 ON RAT PAW OEDEMA INDUCED BY SEVERAL FLOGISTIC AGENTS

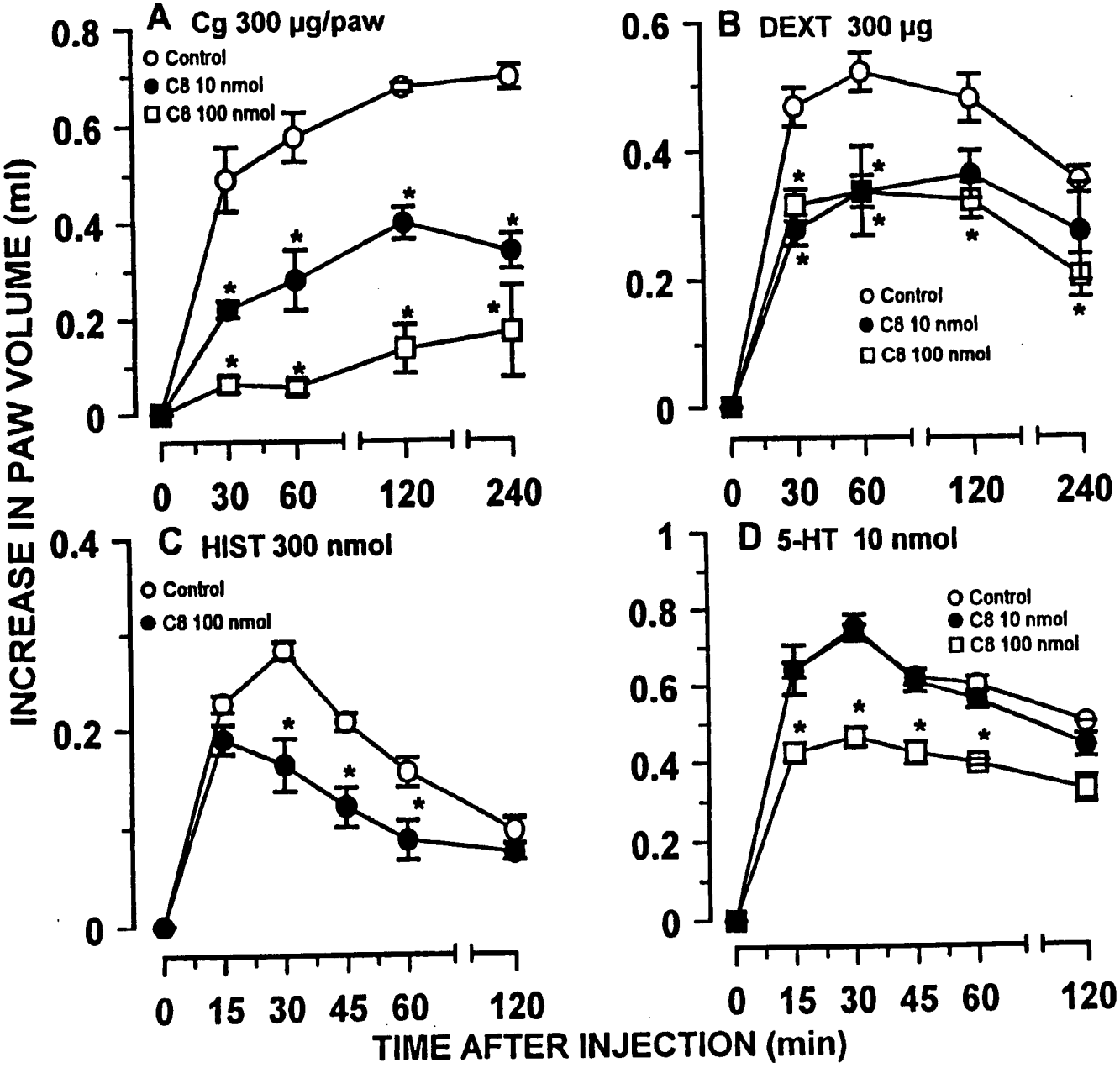

Figure 4

FIGURE 4

FIGURE 5

CONFIDENTIAL

EFFECT OF MV8612 ON KININ-INDUCED RAT PAW OEDEMA

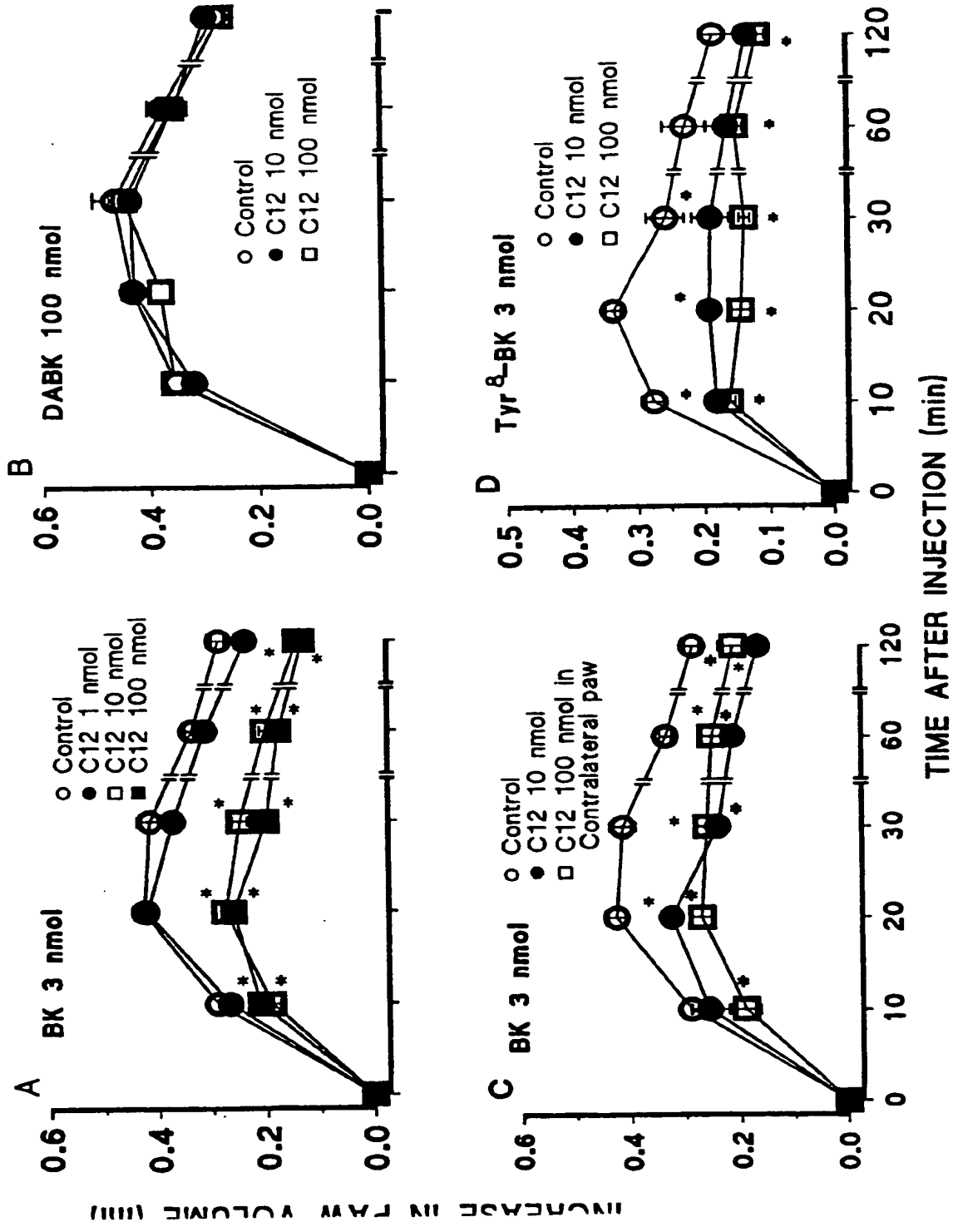

EFFECTS OF MV8612 ON SEVERAL AGONISTS-INDUCED RAT PAW OEDEMA

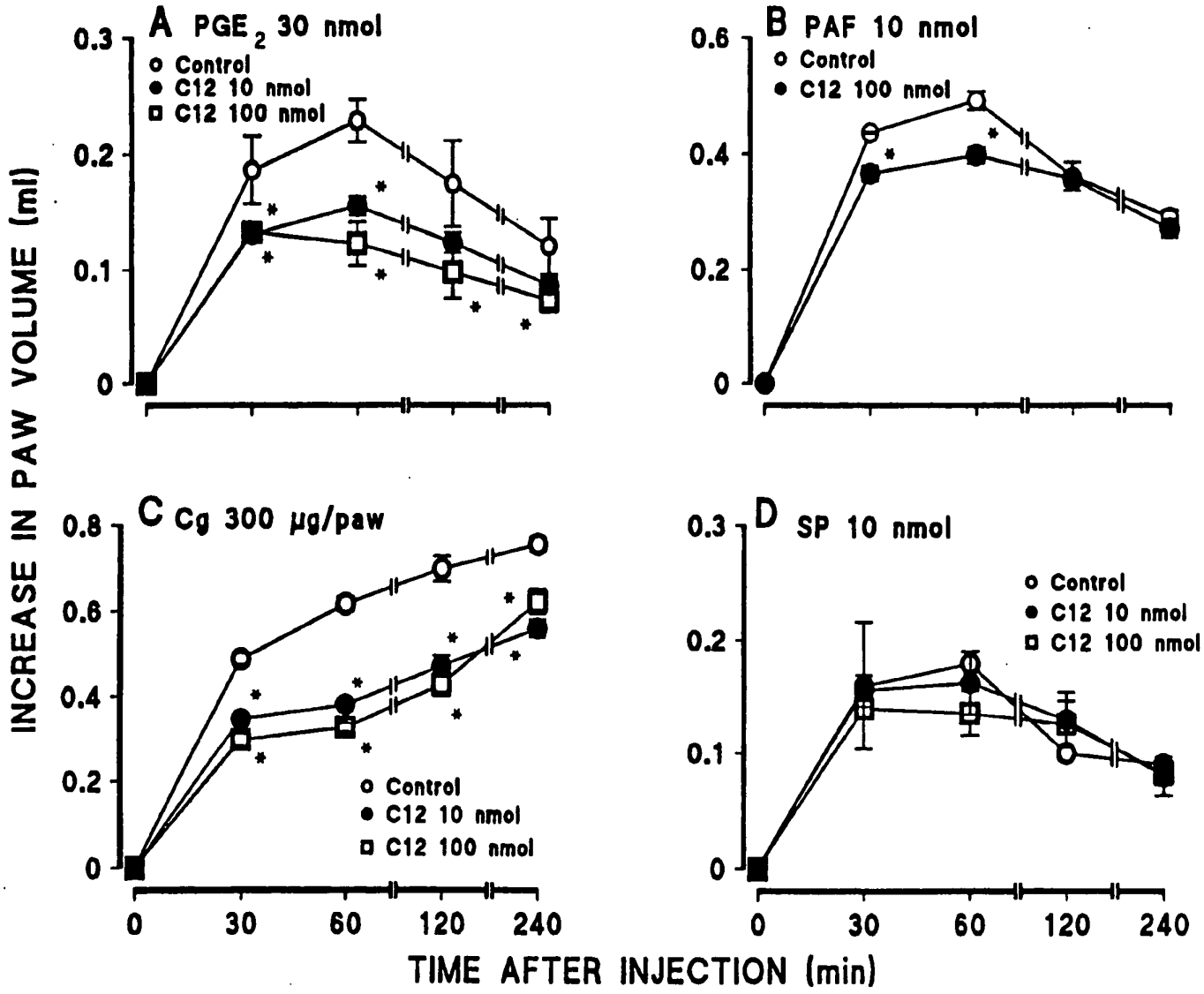

FIGURE 6A

FIGURE 7A .

CONFIDENTIAL

EFFECTS OF COMPOUND MV12 ON PAW OEDEMA CAUSED BY CO-INJECTION OF BK AND INFLAMMATORY MEDIATORS

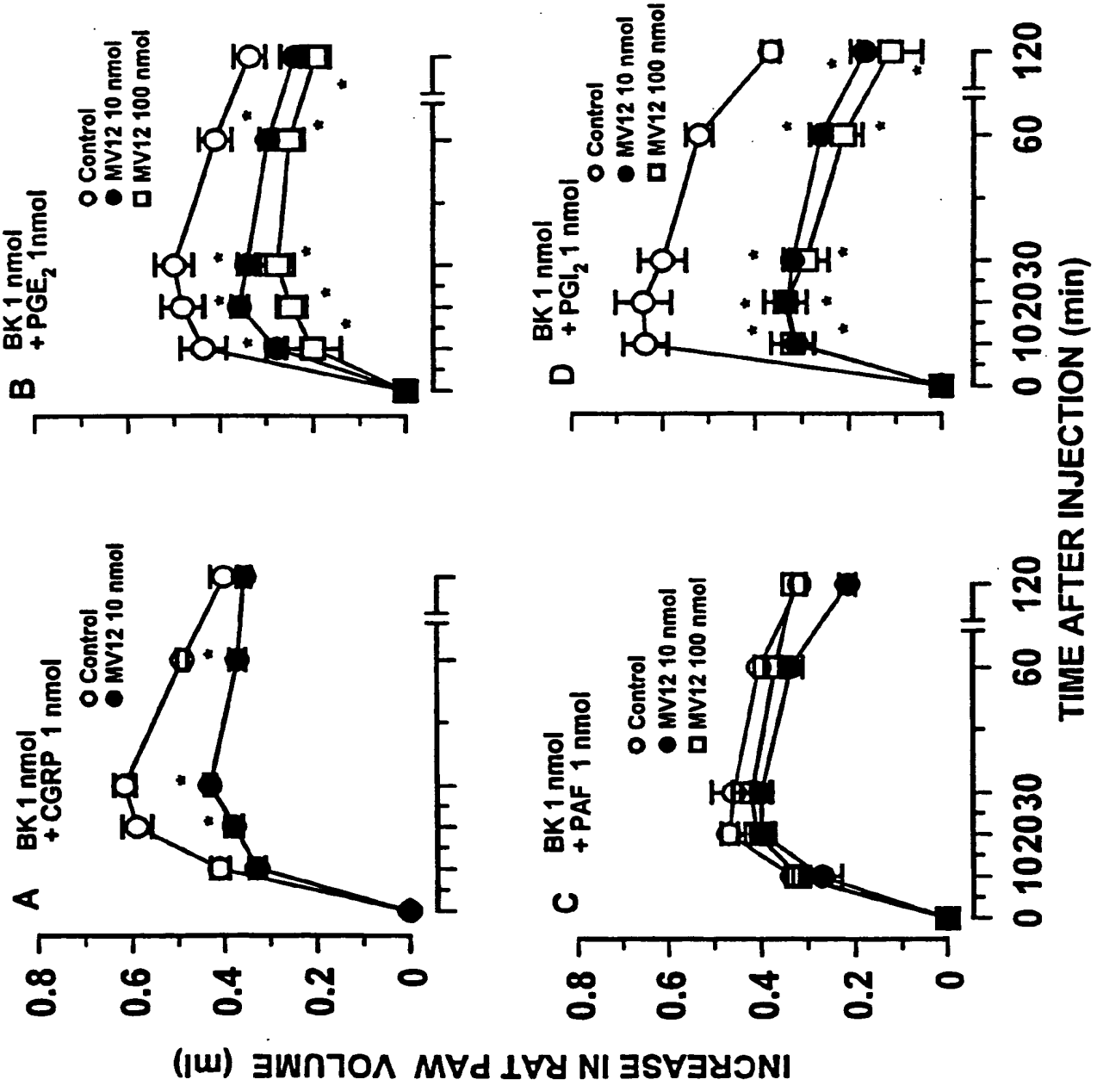

FIGURE 1

EFFECT OF MV8612 ON BK-INDUCED RAT PAW OEDEMA

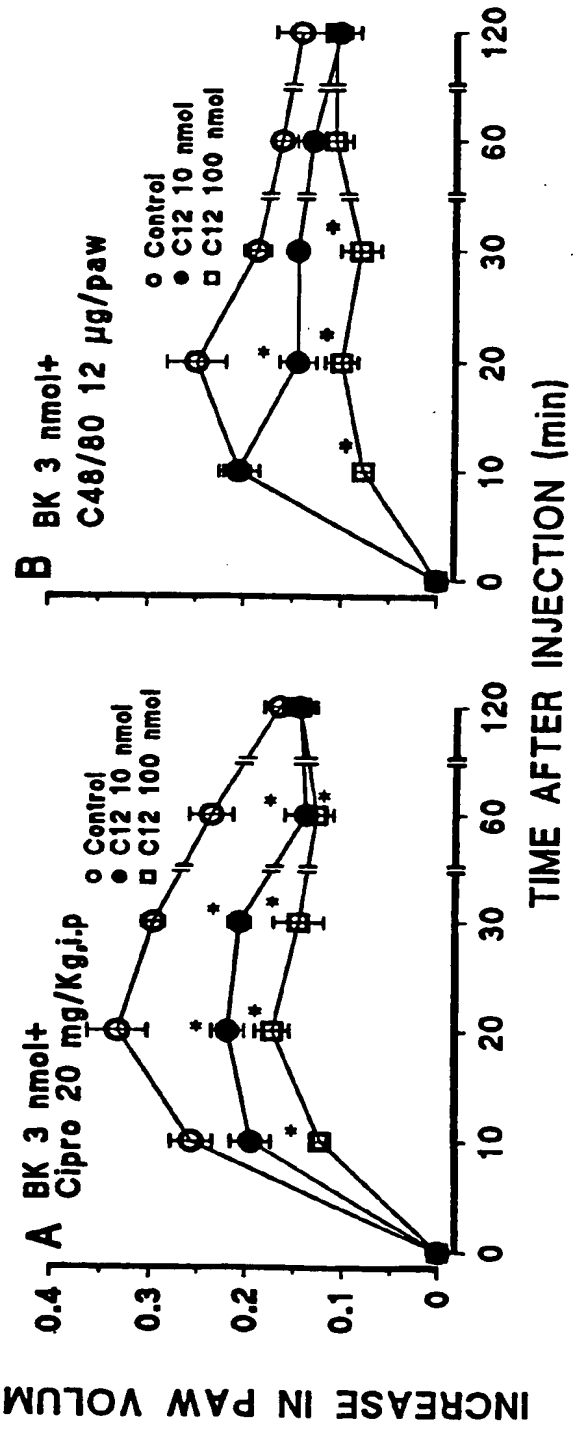

Figure 8

FIGURE 9A

CONFIDENTIAL

EFFECT OF COMPOUND MV8612 (10 nmol) ON
BK-INDUCED RAT PAW OEDEMA

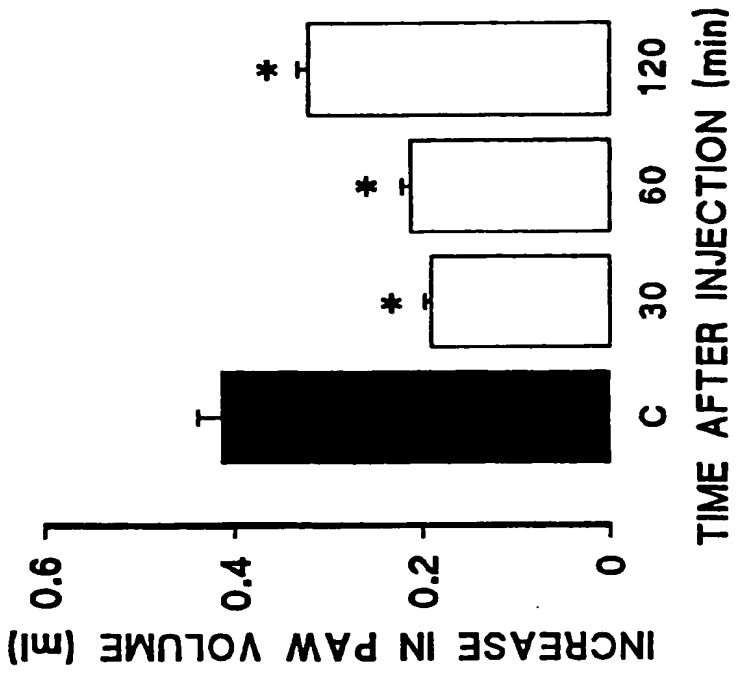

Figure 9

FIGURE 10A

EFFECT OF MV 8612 IN MOUSE PAW OEDEMA

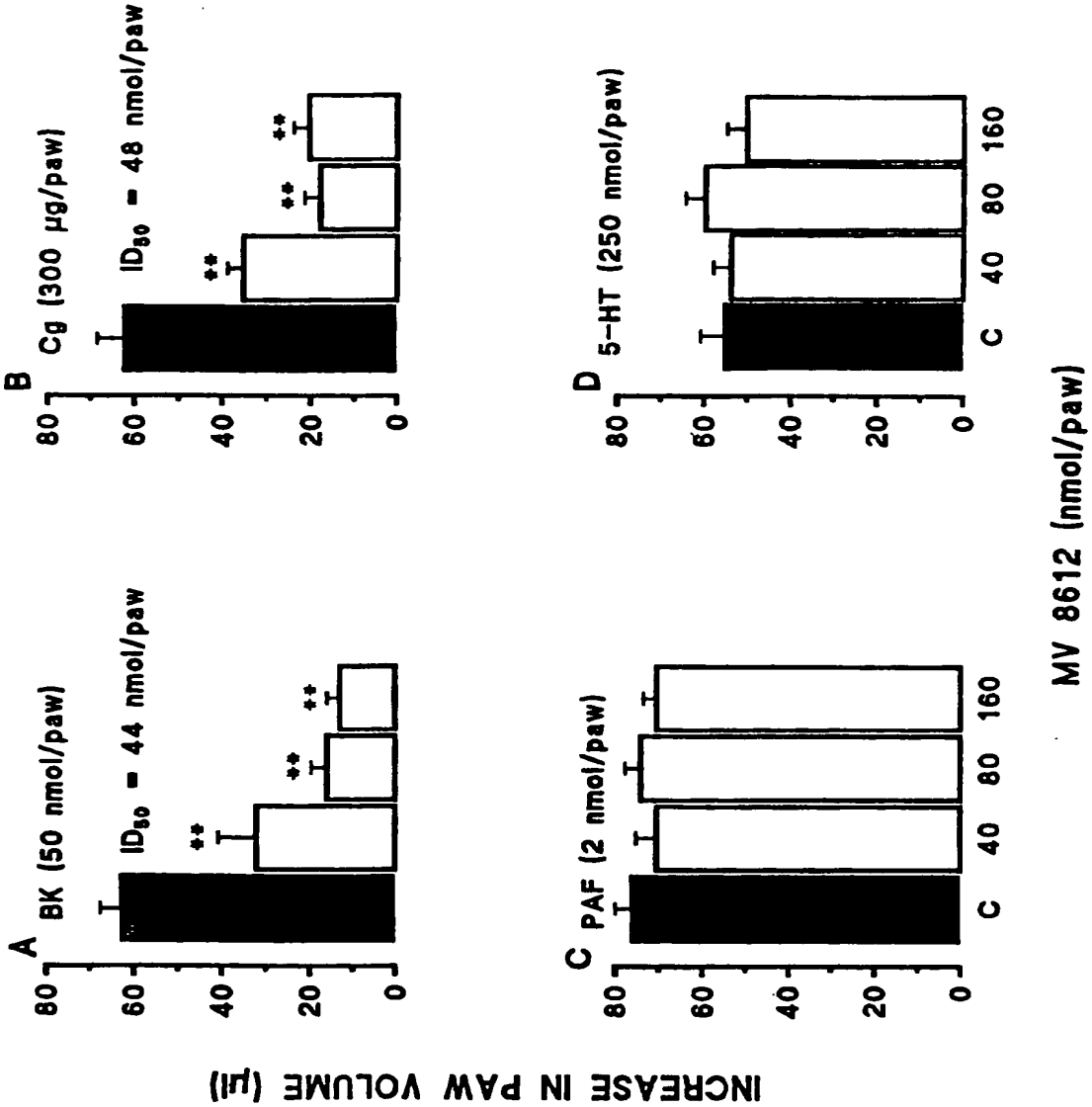

Figure 10

ıre 11

EFFECT OF MV 8612 IN MOUSE PAW OEDEMA

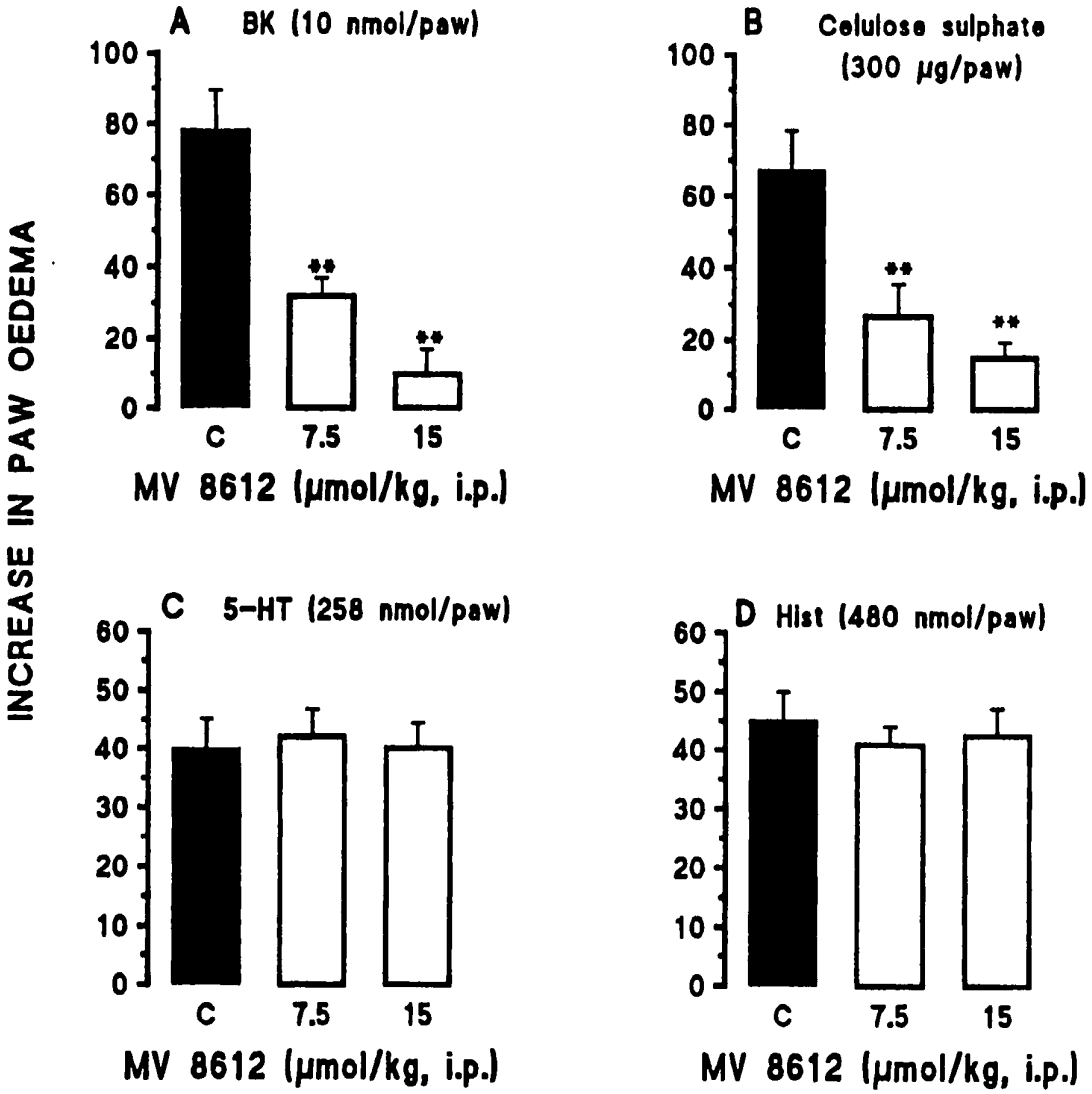

FIGURE 12A

EFFECT OF COMPOUND MV 8608 IN MOUSE PAW OEDEMA

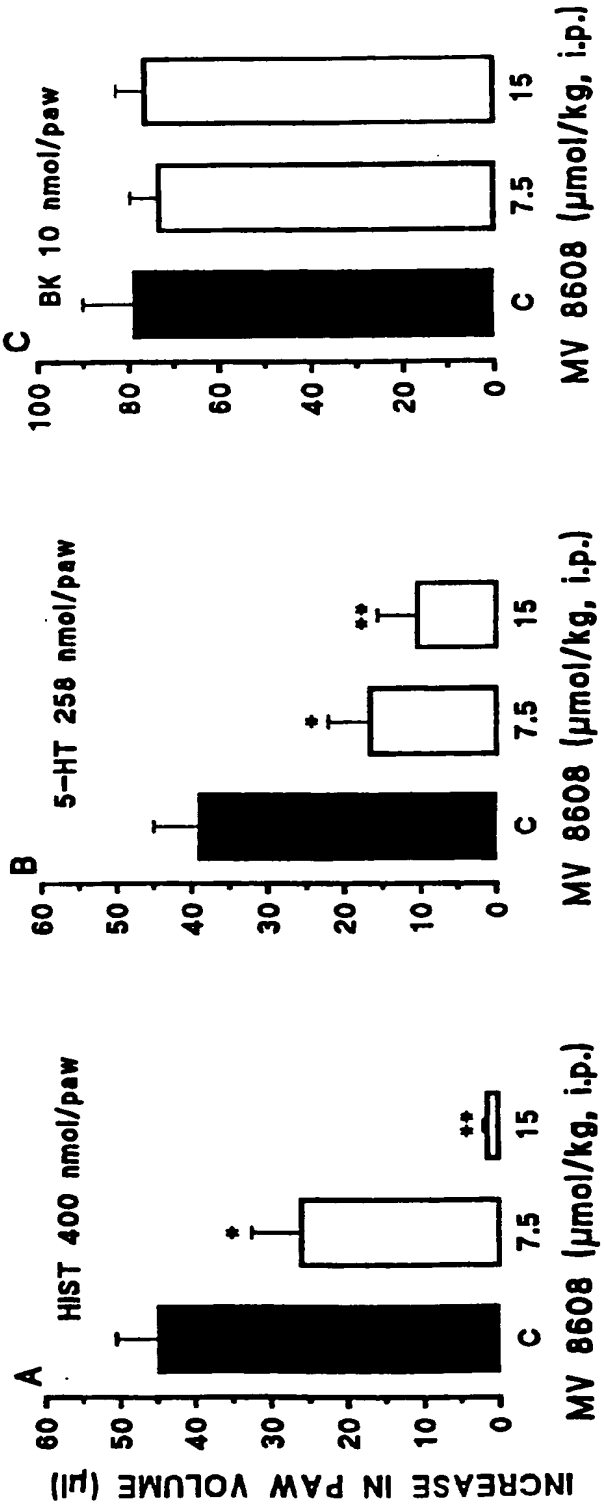

ure 12

FIGURE 13

CONFIDENTIAL

EFFECT OF COMPOUND MV8612 OF *Mandevilla velutina* ON CARRAGEENAN (1 mg PER SITE)-INDUCED PLEURISY IN MICE

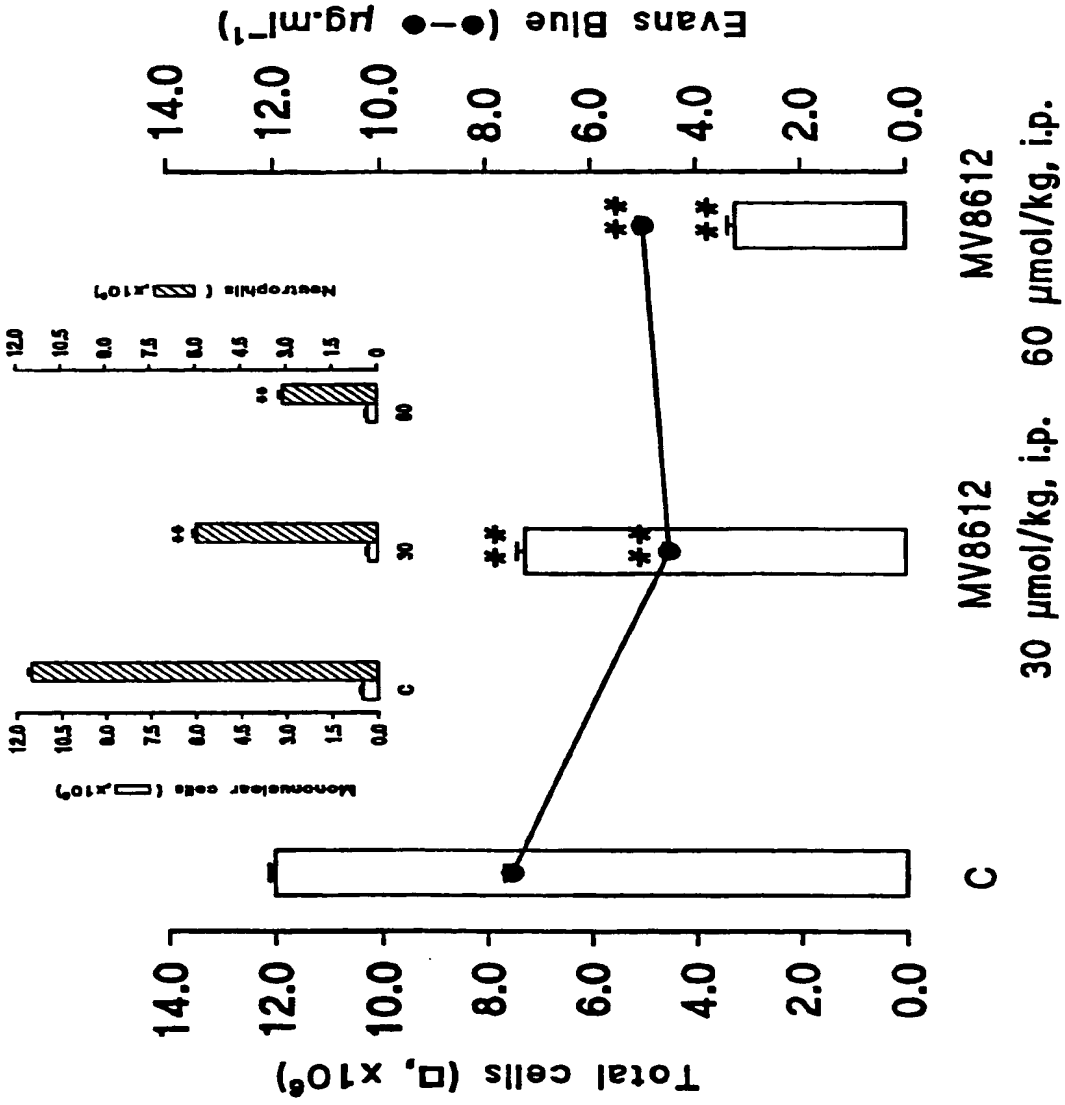

ure 13

FIGURE 14

EFFECT OF COMPOUND MV8608 OF *Mandevilla velutina* ON CARRAGEENAN (1 mg PER SITE)–INDUCED PLEURISY IN MICE

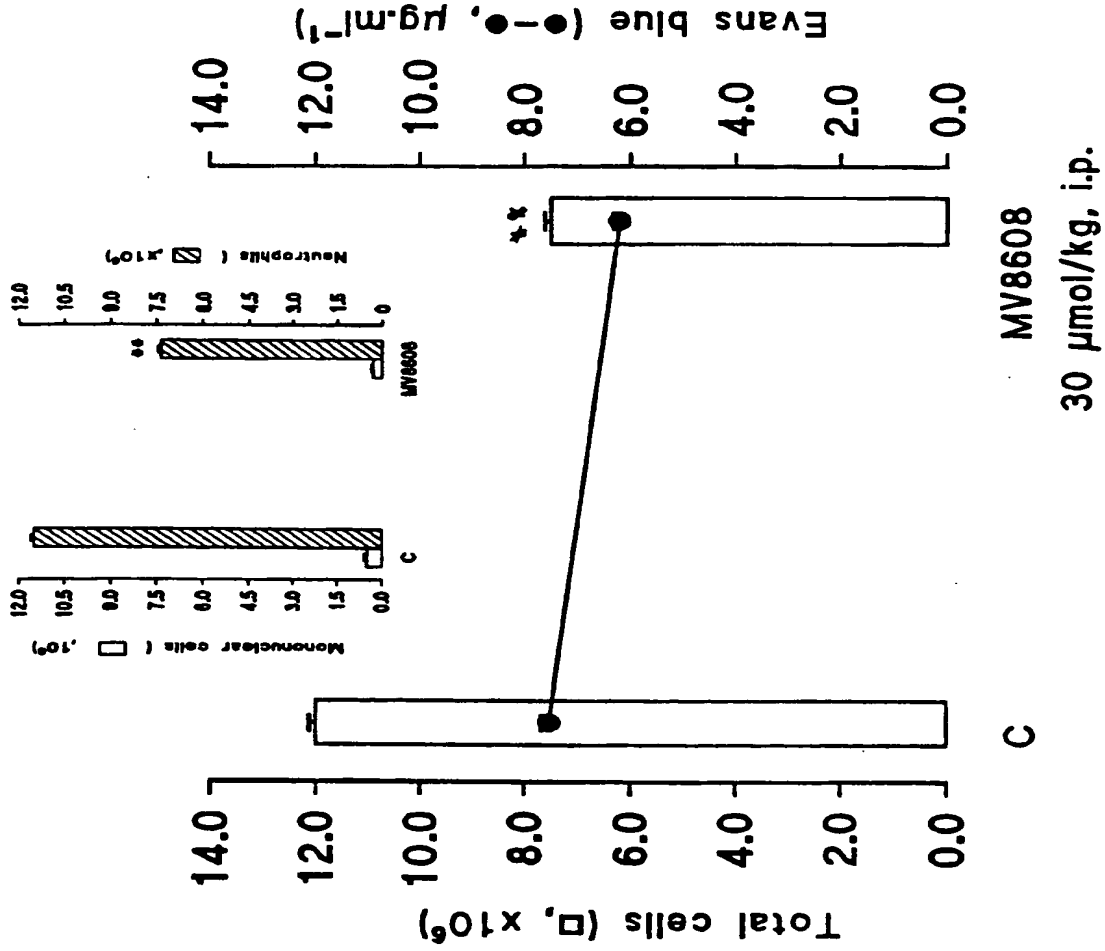

FIGURE 15A.

CONFIDENTIAL

EFFECT OF COMPOUNDS MV8608 AND MV8612 OF *Mandevilla velutina* ON PAF-ACETHER (1 µg PER SITE)-INDUCED PLEURISY IN MICE

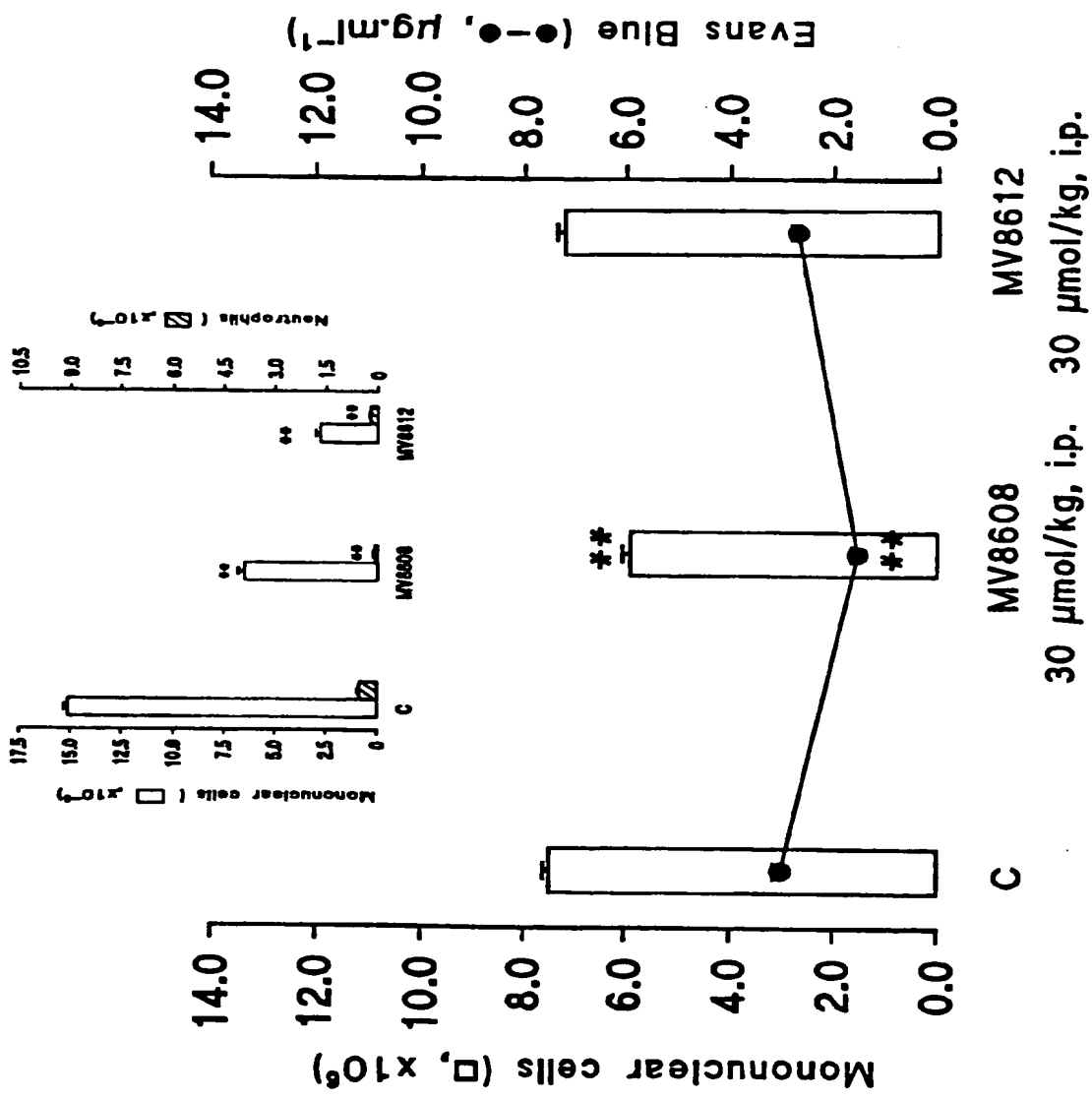

15

EFFECT OF MV 8612 AND MV 8608 ON BK (1 nmol/site)–INDUCED INCREASE OF RAT VASCULAR PERMEABILITY

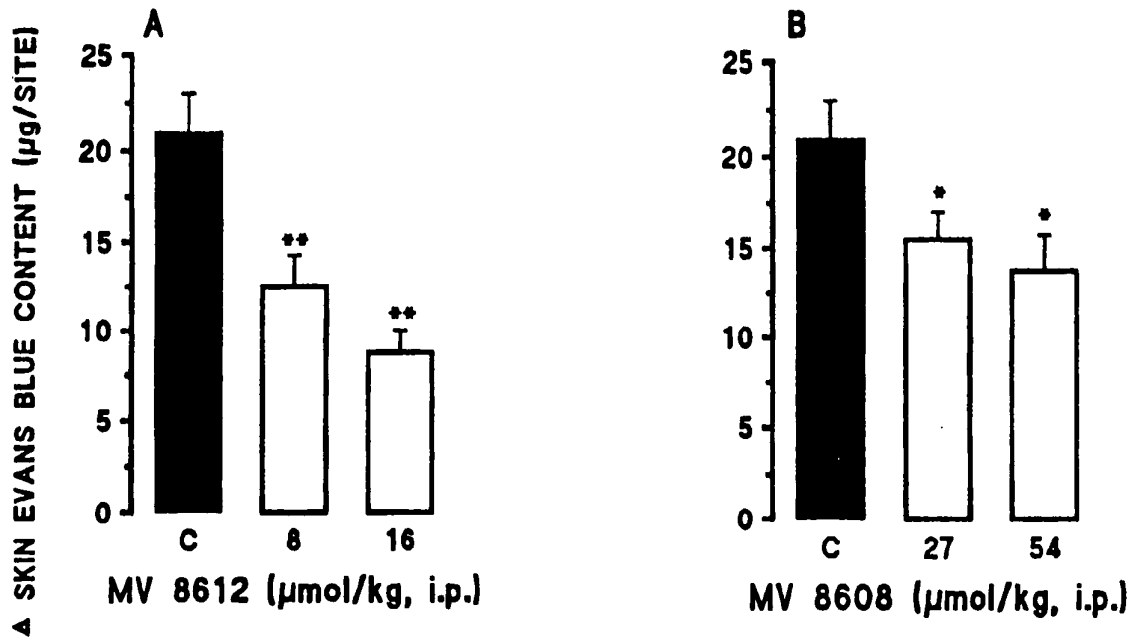

FIGURE 14A

FIGURE 17.

CONFIDENTIAL

EFFECT OF COMPOUNDS MV 8612 AND MV 8608 IN HUMAN LYMPHOCYTE PROLIFERATION

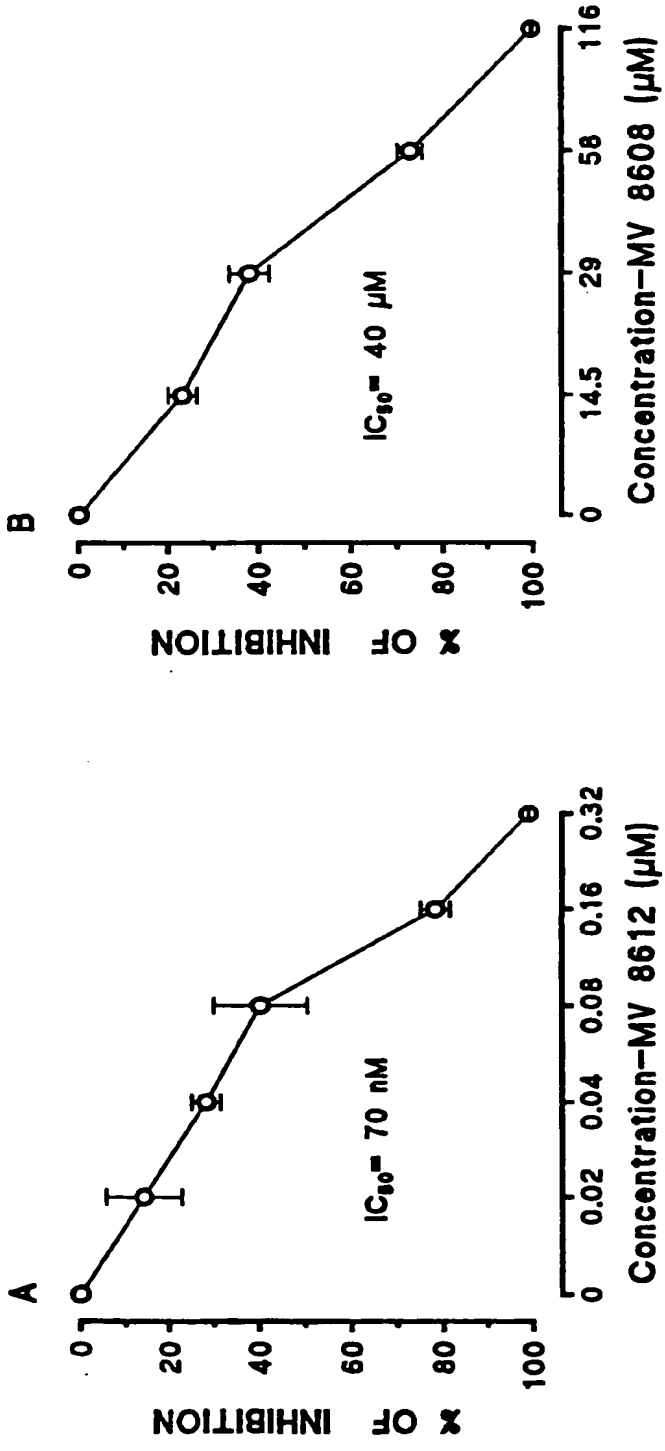

re 17

FIGURE 18A

EFFECT OF MV 8612 AND MV 8608 ON ACETIC ACID-INDUCED WRITHING IN MICE

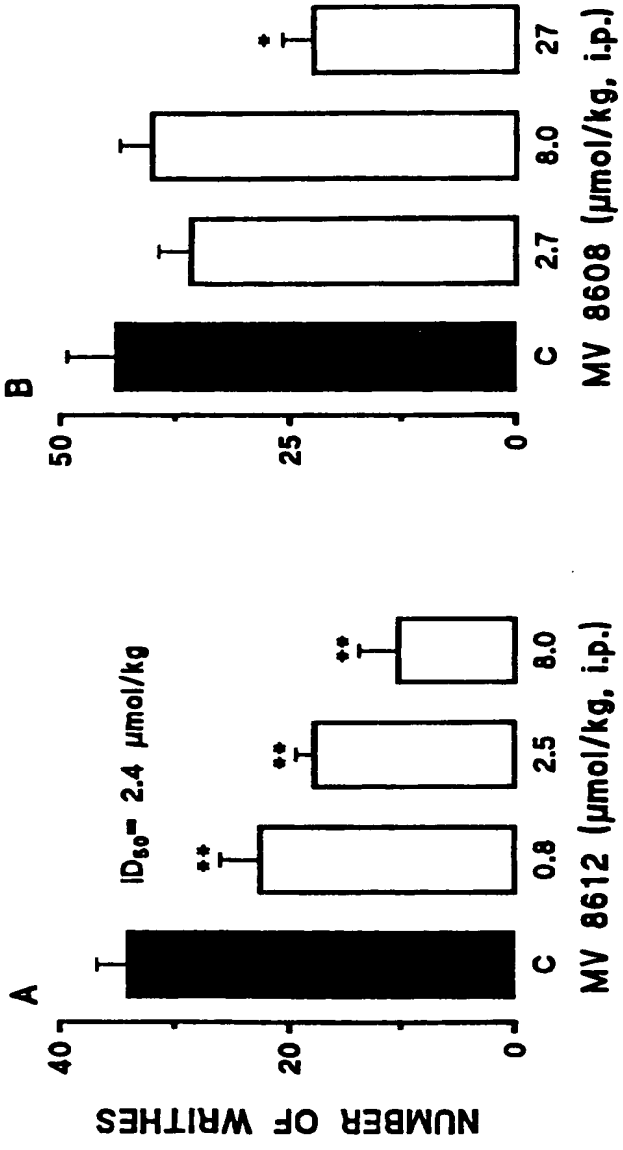

ıre 18

FIGURE 19.

CONFIDENTIAL

ANTINOCICEPTIVE ACTIVITY FROM M. velutina COMPOUNDS
ON ACETYLCOLINE-INDUCED WRITHING IN MICE

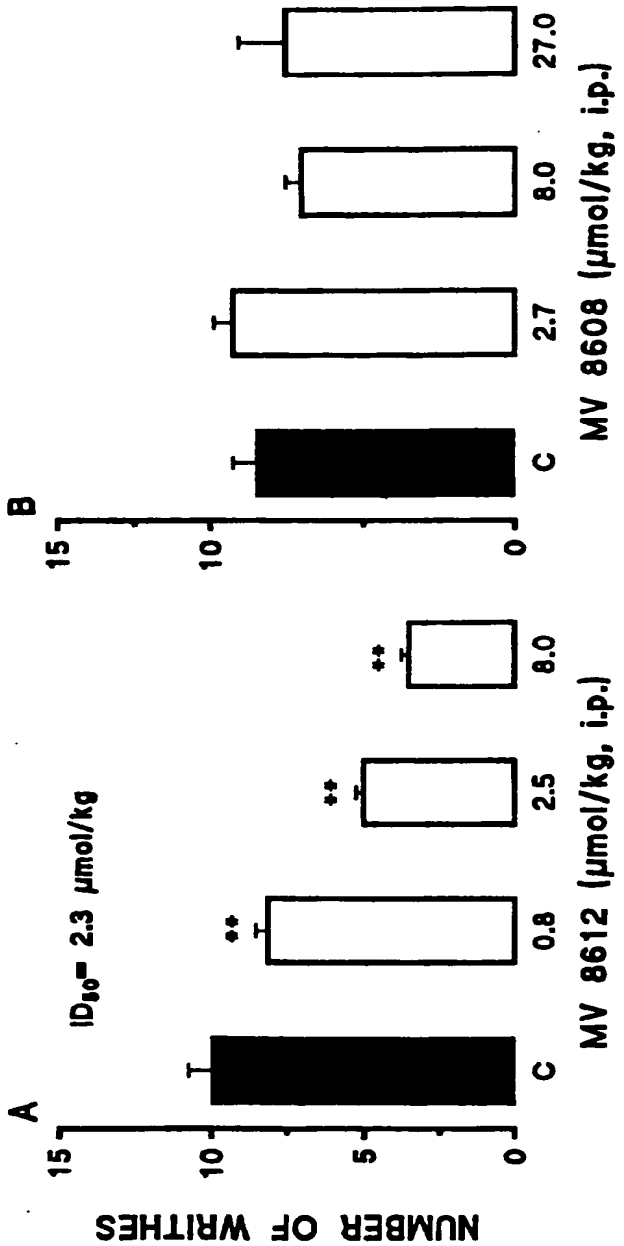

re 19

FIGURE 2

CONFIDENTIAL

EFFECT OF MV 8612 AND MV 8608 ON KAOLIN-INDUCED WRITHING IN MICE

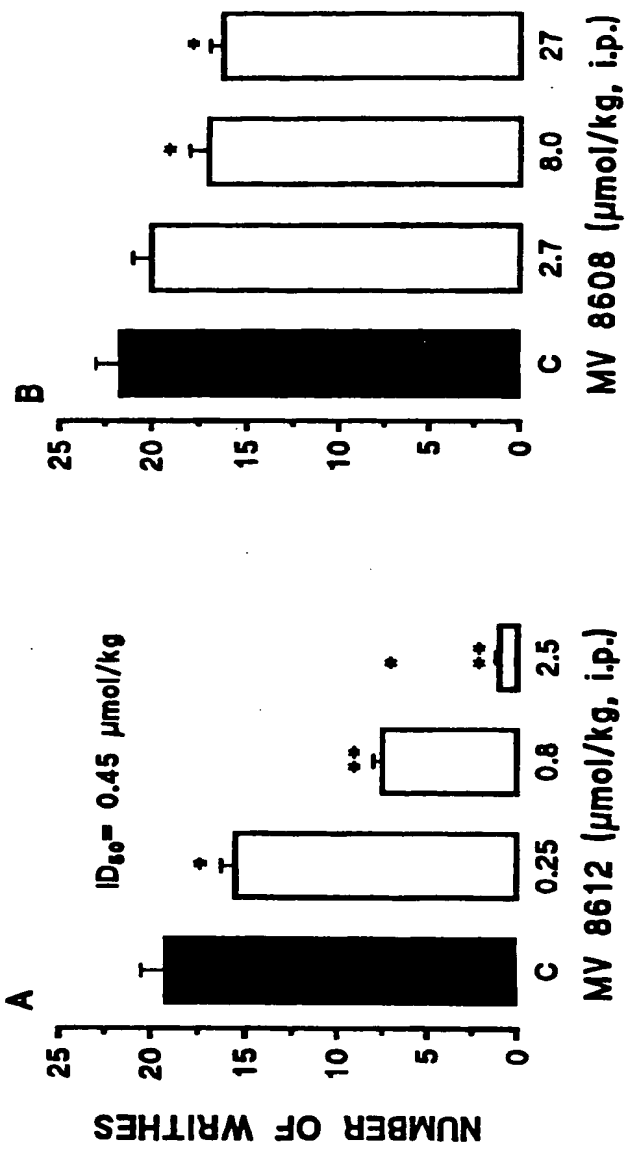

re 20

ANTINOCICEPTIVE EFFECTS OF INTRACEREBROVENTRICULAR INJECTION OF MV 8612 AND MORPHINE IN ACETIC ACID-INDUCED WRITHING IN MICE

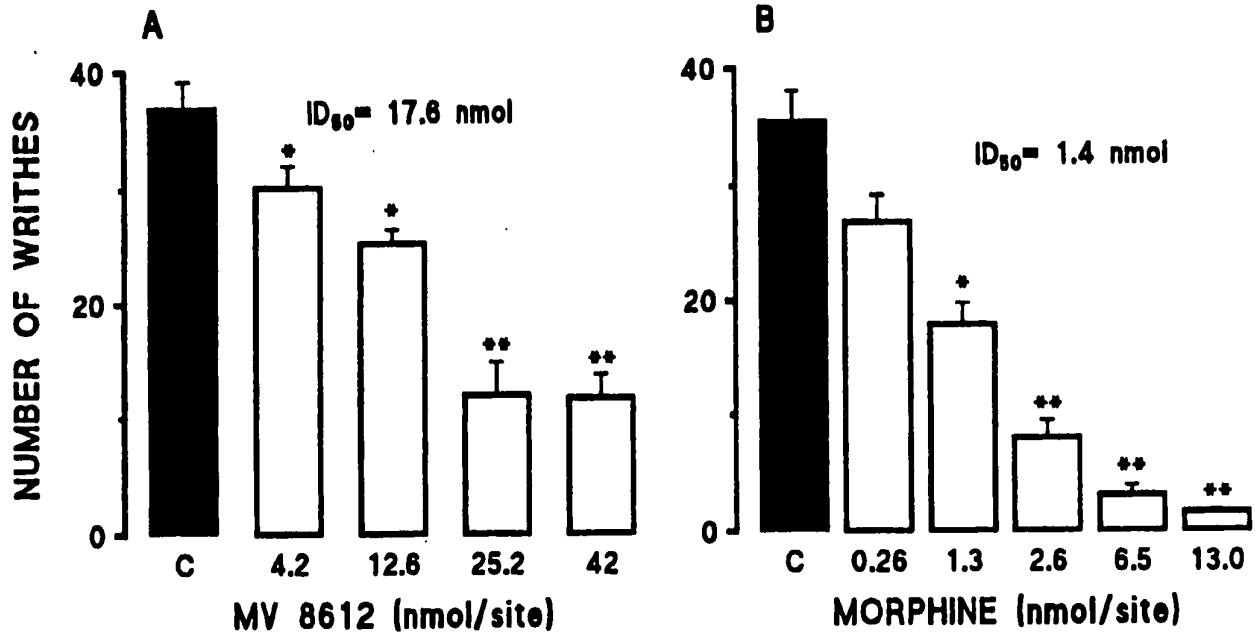

FIGURE 2K.

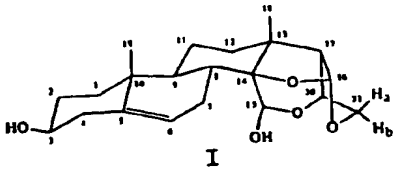

I

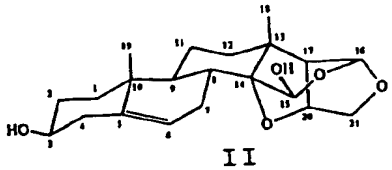

II

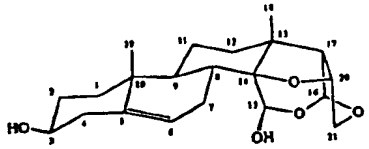

III

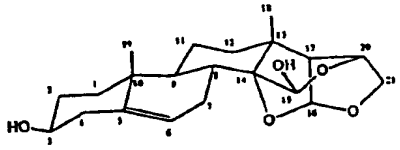

IV

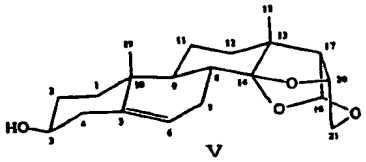

V

Fig 22A- Structures of compound MV-8608 (Velutinol) (I,II,III,IV) and Illustrol (V)

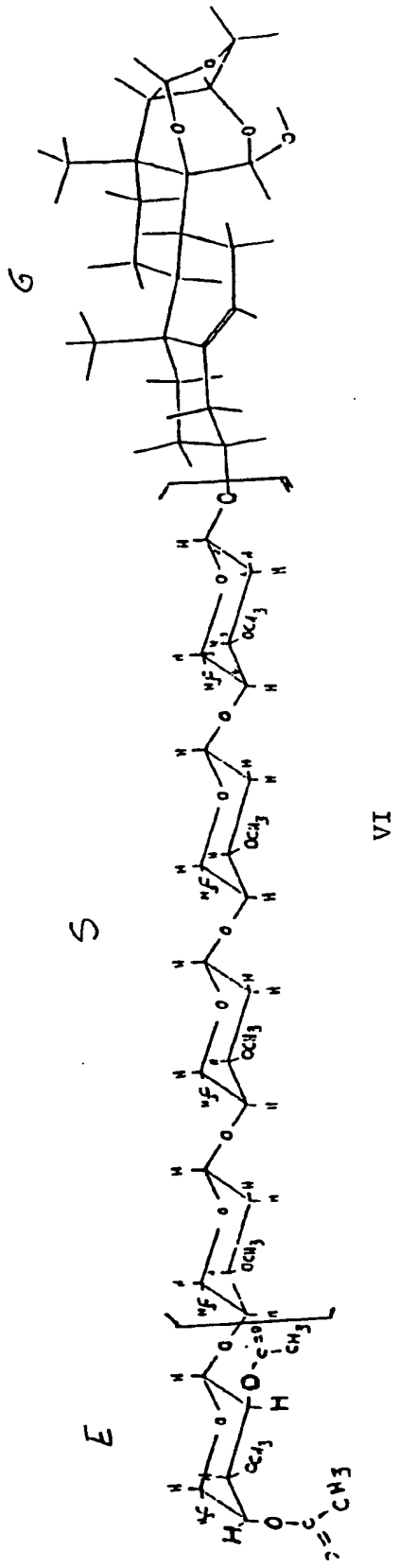

Fig 24 Structure of compound MA-8612

Fig. 4 ^{1}HNMR of compound NV-8612 isolated from Mandevilla velutina

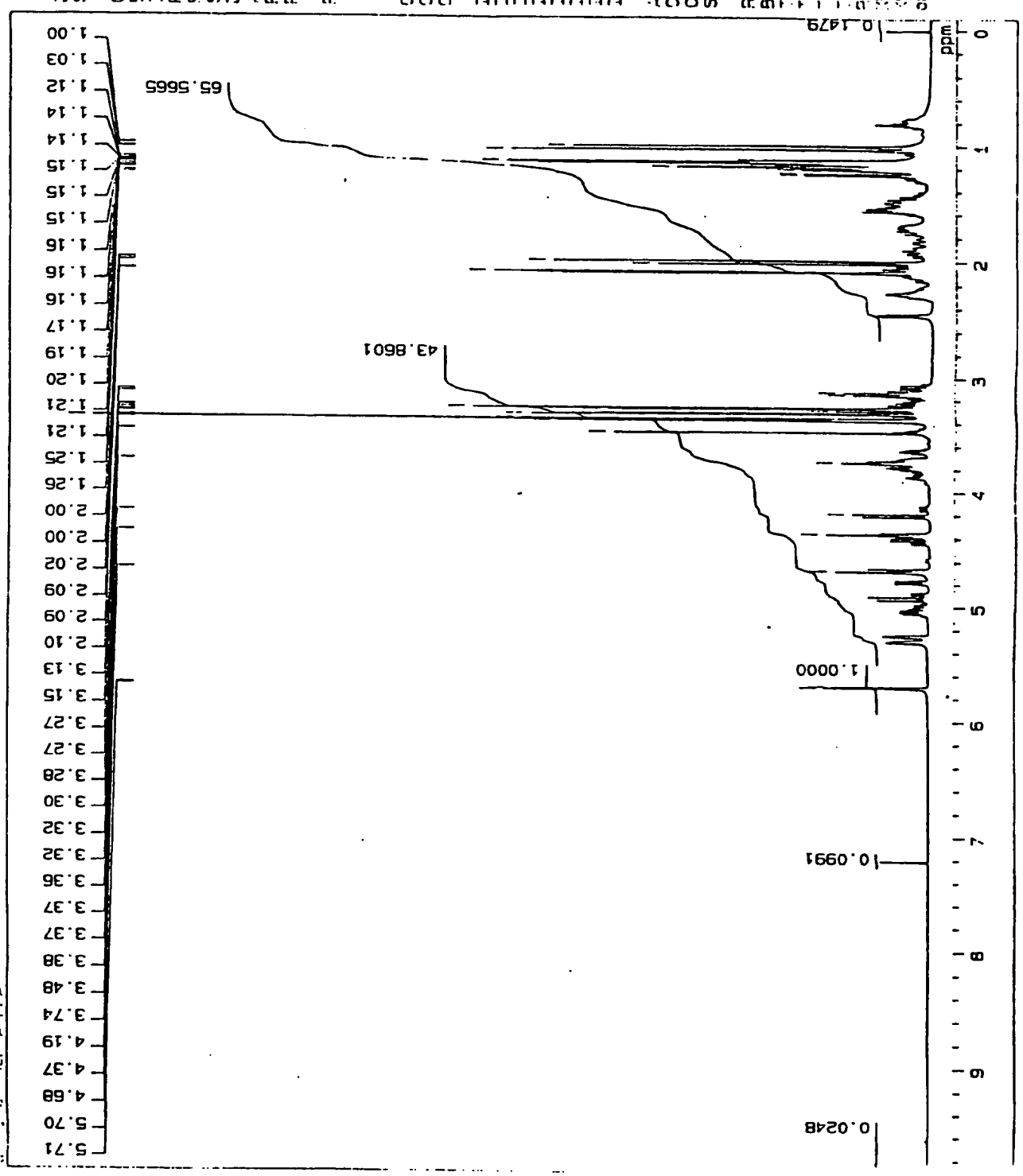

Fig 25A ^{13}CNMR of compound MV-8612 isolated from Mandevilla velutina

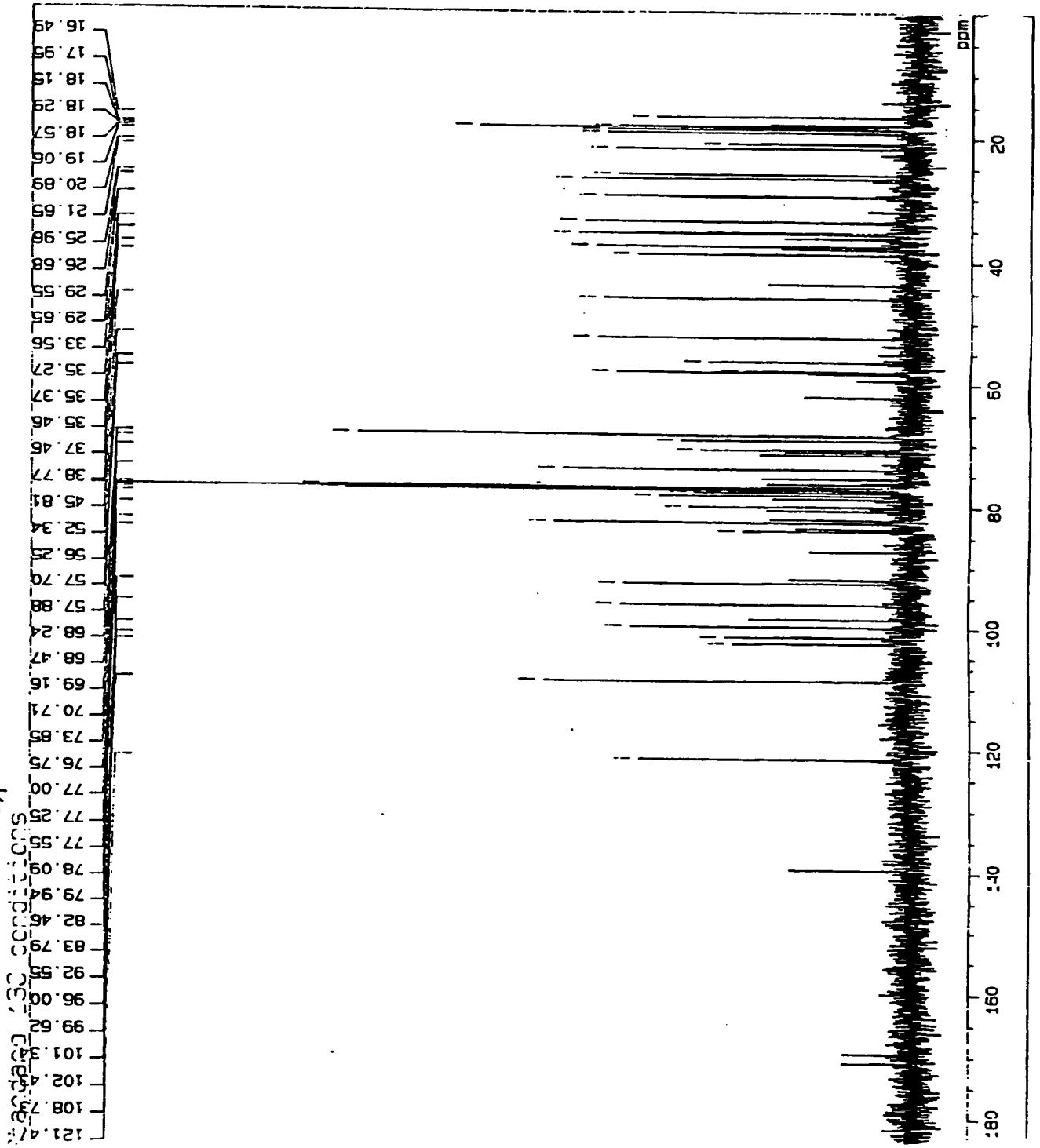

Fig 25-4 COSY of compound MV-8612 isolated from M. velutina

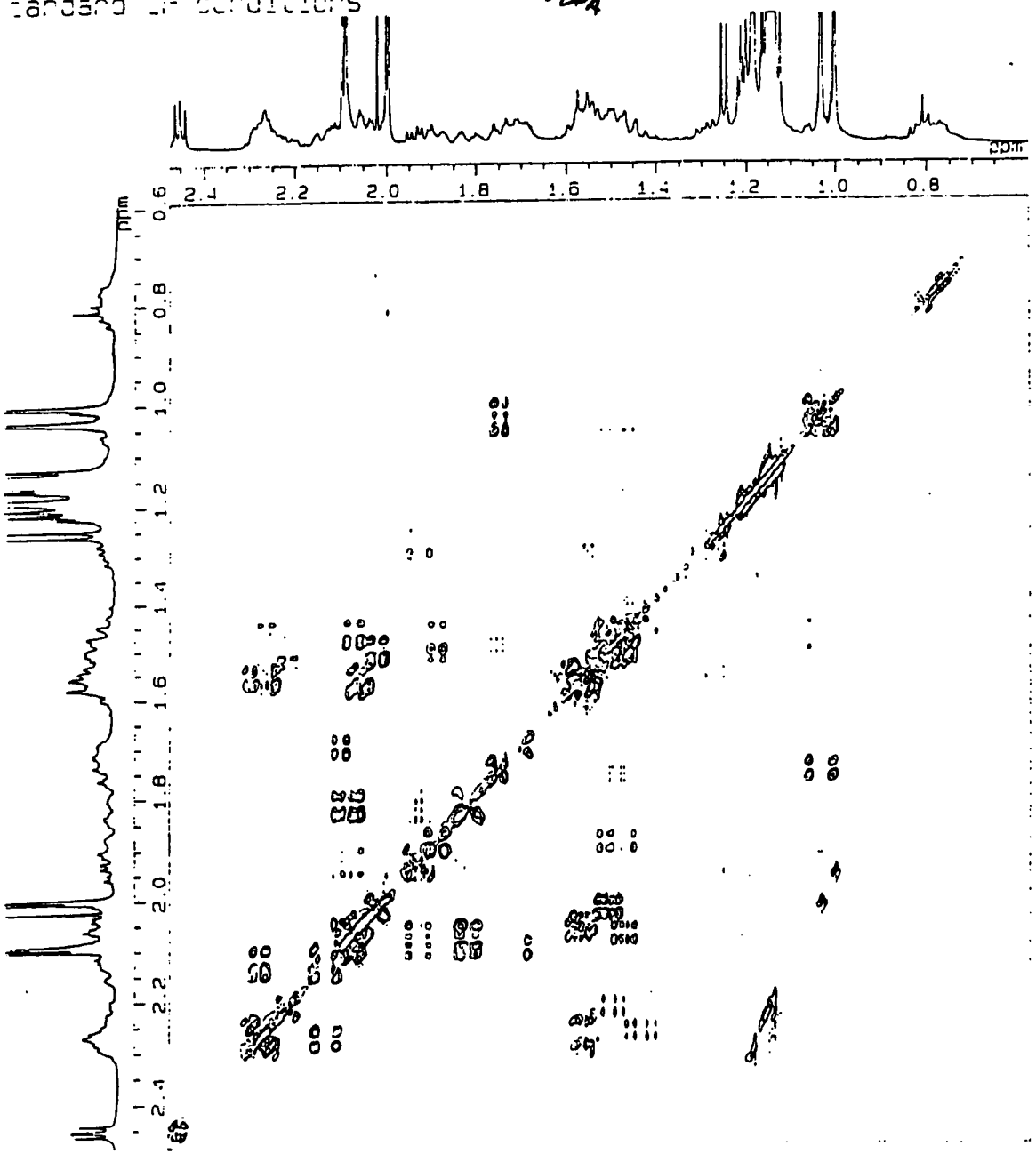

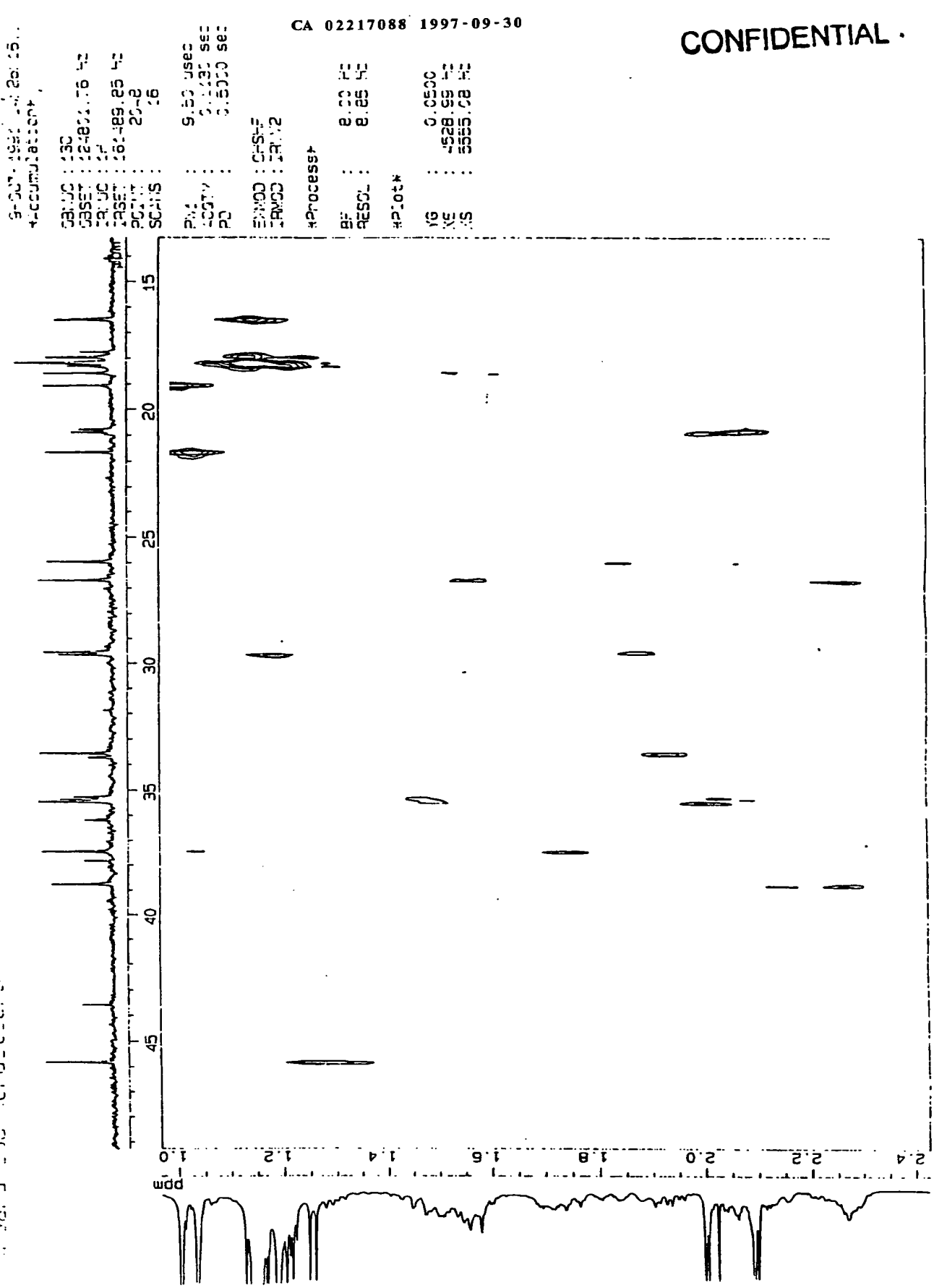

Fig. 4A HETCOR of compound Mv-8612 isoated from M. velutina

obtained using conditions

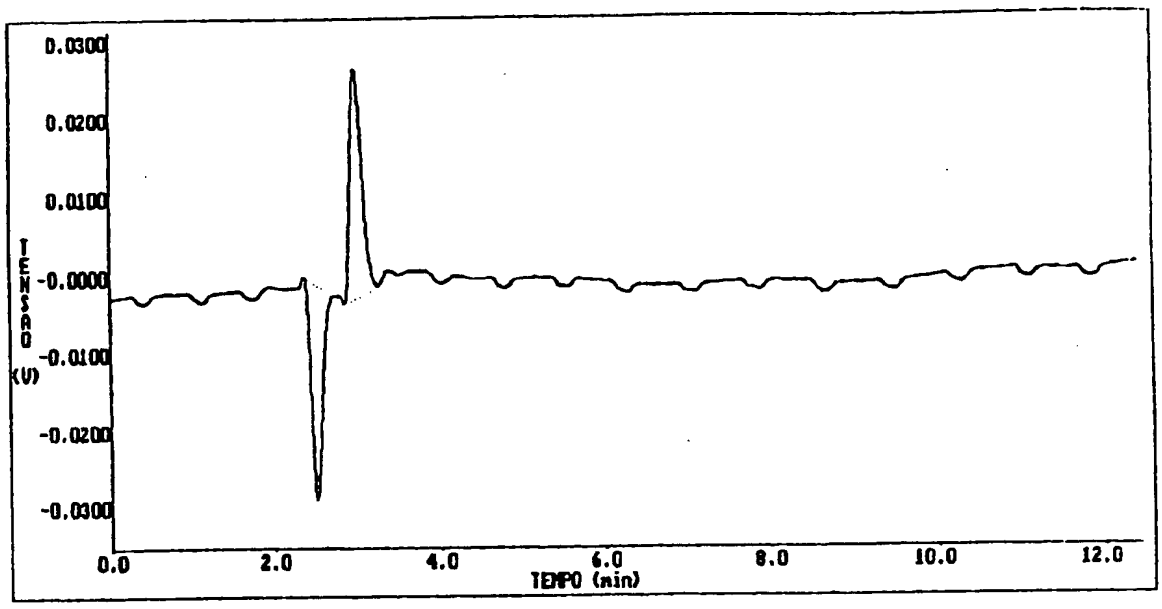

Peak 1. Solvent
Peak 2. MV - 8608
Column Temperature 25°C
Chromatogram in HPLC (Beckmann)
Refractive Index Detector
Stationary phase —> água/metanol

Fig. 7A HPLC chromatogram of compound MV-8608 isolated from Mandevilla velutina

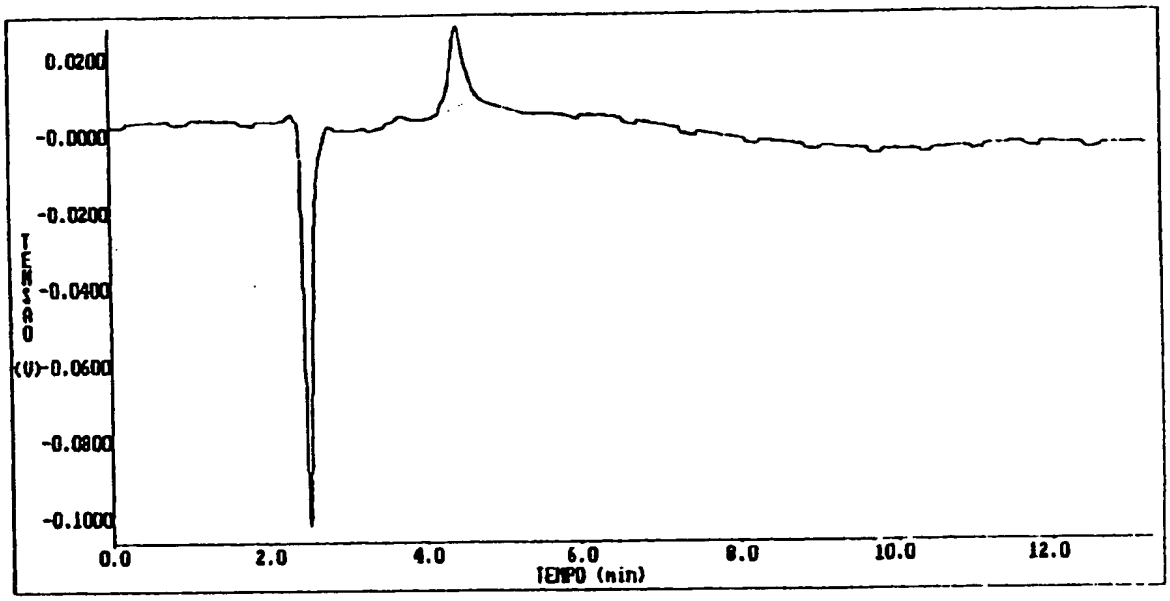

Peak 1. Solvent
Peak 2. MV - 8612
Column Temperature 25°C
Chromatogram in HPLC (Beckmann)
Refractive Index Detector
Stationary phase —> água/metanol

Fig. 8A HPLC chromatogram of compound MV-8612 isolated from Mandevilla velutina

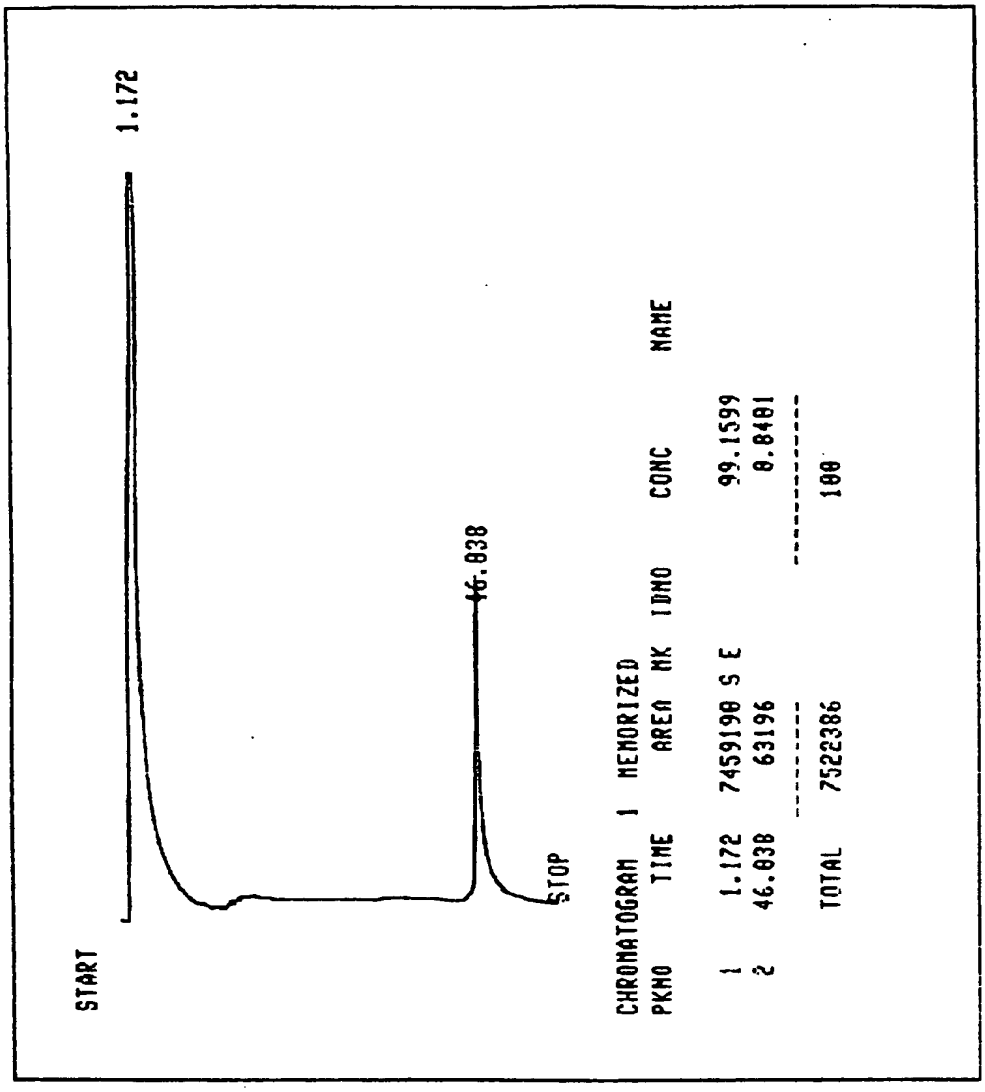

Chromatography → Shimadzu CG - 14 A
Sample → MV 8608
Colunm temperature → 80°C →250°C
Detector temperature → 290°C
Injector temperature → 250°C
Gradient temperature → 10°C / min
Colunm LM - 1
Solvent → acetone
Peak 1 → solvent
Peak 2 → MV 8608

Fig. 30A GC chromatogram of compound MV 8608 isolated from *Mandevilla velutina*

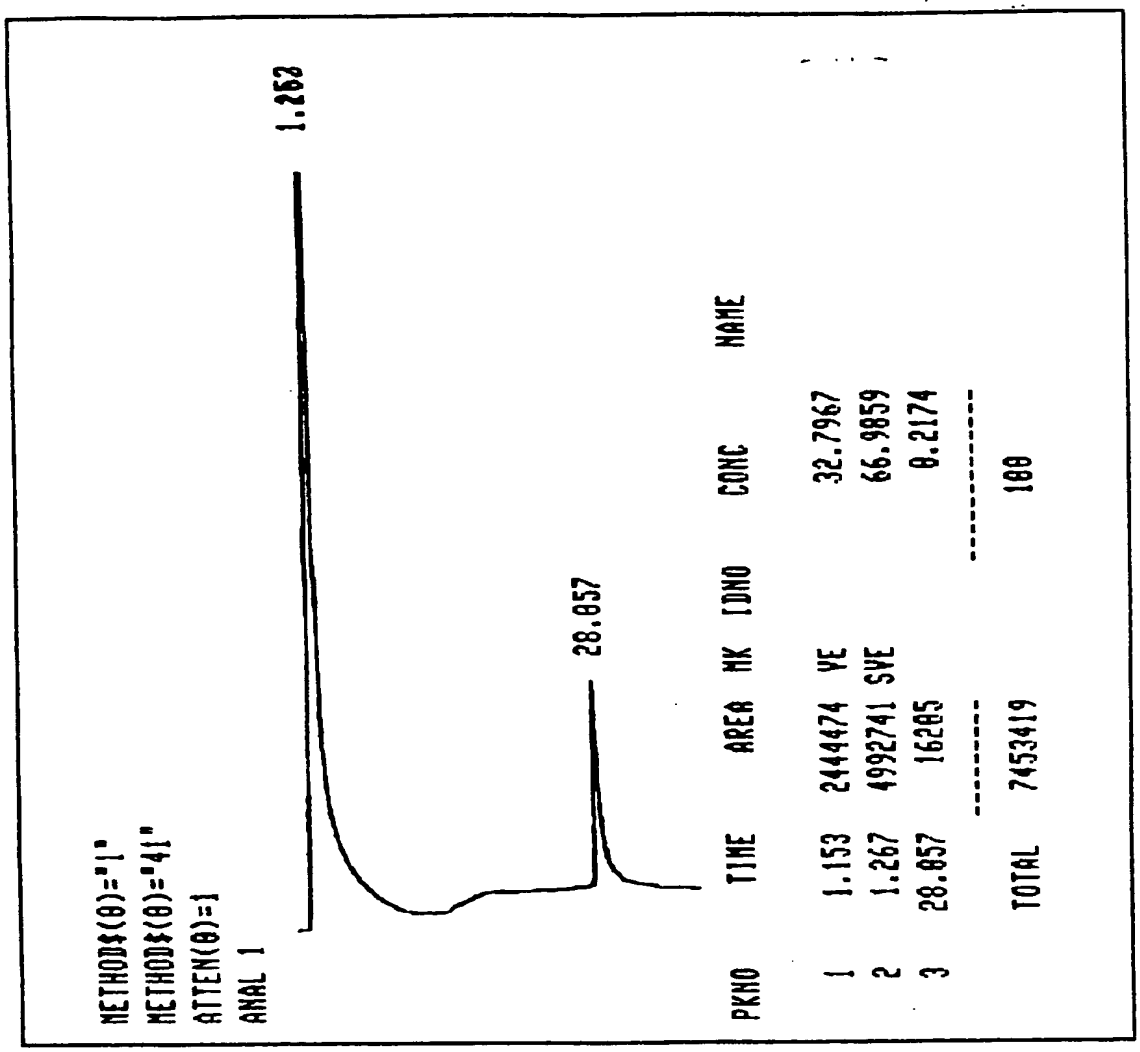

Chromatography → Shimadzu CG - 14 A
Sample → illustrol
Column temperature → 80°C → 250°C
Detector temperature → 290°C
Injector temperature → 250°C
Gradient temperature → 10°C / mim
Column LM-1
Solvent → acetone/$CHCl_3$
Peak 1 → solvent
Peak 2 → solvent
Peak 3 → illustrol

Fig 30/1 - GC chromatogram of compound illustrol isolated from *Mandevilla illustris*